UNIVERSITÀ
DEGLI STUDI
DI PADOVA

Head Office: Università degli Studi di Padova

Department of Cardiac, Thoracic, Vascular Sciences and Public Health

Ph.D. COURSE IN: Traslational Specialistic Medicine "G.B. Morgagni"

CURRICULUM: Endocrine and Metabolic Sciences

SERIES XXXII

CIRCULATING SMALL NON CODING RNAS AND MICROPARTICLES AS POTENTIAL MARKERS OF ATHEROSCLEROTIC PLAQUE COMPOSITION IN TYPE 1 DIABETES

Coordinator: Prof. Annalisa Angelini

Supervisor: Prof. Angelo Avogaro

Ph.D. student : Alessandra Giannella

A mio padre
per avermi insegnato a sognare
e per aver creduto sempre in me

A mia madre
per avermi insegnato ad avere pazienza
e a saper tenere i piedi per terra
ma con il sorriso

Alle mie sorelle
per avermi dato lo stimolo a crescere
e a impegnarmi

Perché quello che fai per noi prescinde
da qualsiasi legame di sangue,
perché sei una guida,
perché la tua grinta è fonte di ispirazione
ed ammirazione,
perché non riuscirò mai a ringraziarti abbastanza,
ti dedico ogni mio piccolo passo

....again and again, forever

INDEX

ABSTRACT

Background: Small non coding RNAs (sncRNAs) are endogenous short non coding molecules that regulate gene expression at post-translational level and are involved in several physiopathological processes. Circulating sncRNAs could be found free in biological fluids or loaded into extracellular vesicles, such as microparticles (MPs) in order to reach other tissues and amplify their signal. Next-generation sequencing (NGS) has become the main platform for biological research and biomarker discovery in the profiling of sncRNAs.

Aim: The aim of this study was: 1) to set up a protocol using NGS technology for the identification and quantification of circulating sncRNAs involved in atherosclerotic plaque composition in type 1 diabetic patients (T1DM); 2) to characterize the phenotypes of circulating MPs derived from T1DM, associated with the plaque composition to evaluate the impact of these extracellular vesicles as carrier of specific small non coding RNAs, involved in these pathways.

Material and Methods: Total RNA of 61 T1DM patients with fibrous (CFP; n 30) or calcified (CCP; n 31) carotid plaques was extracted from plasma samples, using a kit for biological fluids. For NGS sequencing, 25 CFP and 26 CCP were evaluated. The preparation of libraries was assessed using the Qiagen system. The sncRNA libraries pool was sequenced through the NGS sequencer MiSeq (Illumina), and the analysis performed by two bioinformatics tools (Partek Flow and CLC Genomics Workbench software). MPs derived from plasma of 40 T1DM patients with fibrous (CFP; n 20) or calcified (CCP; n 20) carotid plaques was assessed by centrifugation (40min x 14,000 rpm a 4°C) and characterized using flow cytometry (CytoFLEX, Beckman Coulter).

Results: An unbiased and accurate sncRNome-wide quantification was obtained, detecting already known circulating sncRNAs (miRNAs, n 2632; piRNAs, n 3286; and tsRNAs, n 640). The bioinformatic analysis using two software on the already known 2632 miRNAs showed a different profile in T1DM with CCP compared to T1DM with CFP. Circulating level of several miRNA implicated in vascular remodeling and glucose metabolism were upregulated in patients with CCP, compared to CFP (miR-503-5p, miR-93-5p, miR-106b-5p and let-7d-5p) and downregulated (miR-451a, miR-10a-5p and miR-29b-3p) in patients with CCP, compared to CFP.

We found that MPs released from endothelial cells and Platelets are enhanced in T1DM with vascular calcification (CCP) compare with T1DM with fibrous plaque (CFP); interestingly, a population of MPs derived from a niche of cells positive for CD34 and α-smooth muscle actin (αSMA) is also increased in CCP. Furthermore, the subgroup of MPs positive for calcification marker was significantly enhanced in patients with CCP in comparison to CFP patients with the main contribution given by CD34+ cells, suggesting a key role of these cells in the development of this vascular complication.

Conclusions: In conclusion, our results demonstrate the power of NGS technology to identify a huge amount of circulating sncRNAs and to discover RNA molecules present in human plasma. The identification of new molecular biomarkers with this ultra-high throughput and sensitive technique (NGS) will help to go further insight specific pathophysiological processes, such as atherosclerotic plaque composition in diabetes, allowing a potentially more targeted therapeutic approach. Furthermore, we demonstrate that microparticles exhibit differential markers in the presence of vascular calcification suggesting a potential role as carrier of small molecules to amplify their signal.

INTRODUCTION

1. Type 1 diabetes mellitus

Type 1 diabetes mellitus (T1DM) is a chronic disease characterized by increased blood glucose levels (hyperglycaemia). It is generally thought to be due to an immune-associated or directly immune-mediated, destruction of insulin-producing pancreatic β cells (1).

Although type 1 diabetes was largely considered a disorder that typically affects children and adolescents, this opinion has changed over the past decade. Polydipsia, polyphagia, and polyuria along with hyperglycaemia (symptoms associated with disease onset) remain diagnostic hallmarks in children and adolescents, and to a lesser extent in adults (2). In fact, in adults diagnosis of type 1 versus type 2 diabetes, characterized by insulin resistance as the main cause of hyperglycaemia, can be challenging. Around 5–15% of adults diagnosed with type 2 diabetes might actually have islet autoantibodies, therefore T1DM is underestimated (3).

In order to take in to account the heterogeneity of T1DM, a novel classifications was proposed: type 1A (autoimmune) diabetes that affects the majority of patients (70–90%) along with the loss of β cells due to autoimmunity response and self-reactive autoantibodies production, and type 1B (idiopathic) diabetes, whose specific pathogenesis remains unclear with often no immune response detectable(4). A subset of individuals within this latter group have monogenic forms of diabetes, such as maturity onset diabetes of the young (MODY); However, latent autoimmune disease of adults (LADA) and ketosis-prone diabetes attempt to distinguish adult cases of type 1 diabetes from those with type 2. However, the presence of a chronic inflammatory infiltration that affects pancreatic islets at the symptomatic onset of type 1 diabetes is the basis of this observation.

Despite any classification, T1DM patients need for exogenous insulin replacement for lifetime treatment. The discovery of insulin in 1921 was

clearly the most significant therapeutic event in the history of type 1 diabetes although in modern countries the management of T1DM is improved by insulin analogues and mechanical technologies such as insulin pumps and continuous glucose monitoring in order to emulate the physiological role of the endocrine pancreas and to prevent complications.

In fact, insulin therapy diminishes the risk of ketoacidosis and alleviates T1DM-associated metabolic abnormalities. However, patients with T1DM still experience substantial morbidity and mortality owing to chronic complications. T1DM patients have a reduction of life expectancy of 12 years and fourfold increased risk of death manly due to cardiovascular causes compared to subjects without diabetes (5).

1. 1 Long-term complications of T1DM

HbA1c (glycated haemoglobin) is considered a marker of long term glycaemic control and a predictor of complications, mainly caused by hyperglycaemia(6). The DCCT and EDIC studies showed that tight glycaemic control and consequently normal level of HbA1c result in reduced long term complications: these results support the hypothesis that a good glycaemic control may induce metabolic memory for many years (7),(8).

First of all, high blood levels of glucose lead to change in the cellular metabolism: the exacerbate glucose uptake into the cells induces overproduction of reactive oxygen species (ROS) by the mitochondrial electron transport chain resulting in oxidative stress and consequently DNA damage. It has been reported that DNA strand breaks activate a specific pathway that interferes with glycolysis and activates pathogenic signals producing glycolytic intermediates. These products block two enzymes, endothelial nitric oxide synthase, and prostacyclin synthase and their anti-atherosclerotic effects (fig.1) (9).

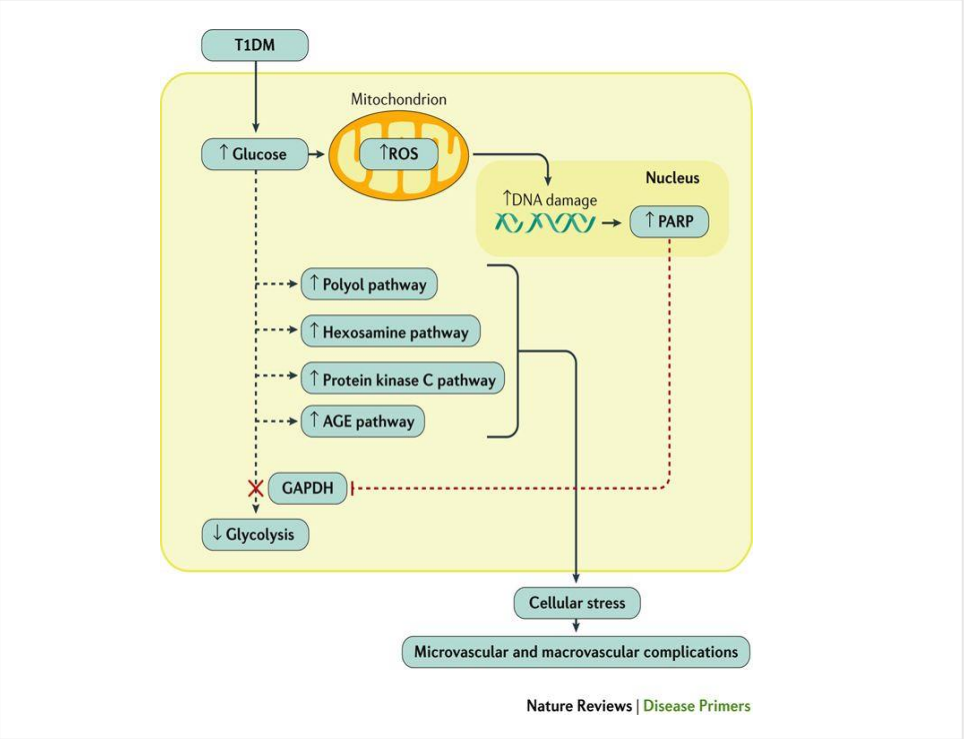

Figure 1: Intracellular effects of high glucose level. *Oxidative stress and the increased production of reactive oxygen species (ROS) are induced by increased intracellular glucose levels resulting in DNA strand breaks. DNA damage activates the production of polymers of ADP-ribose by PARP which block the activity of glyceraldehyde-3-dehydrogenase (GAPDH). As consequence, glycolytic intermediates are diverted into pathogenetic signaling pathways. AGE, advanced glycation end product; T1DM, type 1 diabetes mellitus*.

These pathologic mechanisms result in different outcomes depending on tissues and compartments involved. In fact, the complications of chronic diabetes are mainly subdivided into microvascular and macrovascular complications.

1.1.1 Microvascular complications

Microvascular complications include several conditions typical of diabetes such as nephropathy, retinopathy, and neuropathy as result of the inability of cells that arrange retina, renal glomeruli, and peripheral nerves to manage the increased level of extracellular glucose. However, concomitant risk factors as smoking and hypertension or genetic susceptibility increase the hazard of developing vascular complications.

Diabetic Retinopathy could lead to vision loss and the prevalence in T1DM is >80%(10). It is characterized by impaired blood flow and early aneurysmatic changes in the retinal vessels within their compensatory increased proliferation. These new vessels are more fragile and permeable leading to haemorrhages and decrease retinal perfusion until blindness. Moreover, T1DM patients show an increased risk of developing macular oedema, cataracts, and glaucoma, therefore they should be routinely screened (11).

Diabetic nephropathy causes chronic kidney disease (CKD) in the 20-40% of T1DM typically after 10 years from the diagnosis of diabetes (12).
In general, the diagnosis of nephropathy is based on the increased of urinary albumin excretion (from microalbuminuria 30-299 mg/24h to macroalbuminuria > 300mg/24h) and a reduction of estimated glomerular filtration rate (eGFR), in absence of other signals of renal damage. The role of hyperglycaemia in this microvascular complication is reported to be crucial, in fact, several studies show levels of glycosylated haemoglobin below 8.0 percent are associated with the regression of microalbuminuria. The microalbuminuria could be stabilized or even prevented in patients treated with antihypertensive drugs (ACE inhibitors) and statins (13).

Diabetic neuropathy includes several disorders which are grouped in diabetic peripheral sensorimotor neuropathy (DPN) and autonomic neuropathy (DAN).
DPN affects 21% of T1DM subjects and these patients should be monitored every 5 years since the diagnosis of diabetes. This disorder involved

peripheral nerves, therefore, depending on that, symptoms may be very different. The early stage of DPN for sensitive nerves included pain, dysaesthesia, and loss of protective sensation (LOPS) know as sensorial deficit (14).

DAN involves vegetative nervous system and affects cardiovascular, genitourinary and gastrointestinal nerves. In particular, cardiac autonomy neuropathy (CAN) is an independent risk factor for cardiovascular mortality and comes over 40% of T1DM. At early stage it could be asymptomatic or induce only a reduction in the heart rate variability which occurs in exercise intolerance, orthostatic hypotension, and resting tachycardia. Patients with CAN with deficient autonomic responses may be at particular risk of severe hypoglycaemia (15).

1.1.2 Macrovascular complications

Cardiovascular disease is becoming a more common macrovascular complication as type 1 diabetes live longer. They mostly manifest in T1DM as coronary artery disease (CAD), heart failure, cerebrovascular disease and peripheral artery disease (PAD). These conditions are not specific to diabetes but T1DM show a two-eightfold increased risk of developing these conditions which are more aggressive in these patients. Even if several studies show that it takes many years to notice the effect of glucose levels on macrovascular outcomes, tight glycaemic control in T1DM may reduce by 42% the incidence of cardiovascular disease (8).

The pathophysiology underlying this phenomenon has been attributed to vascular alteration and reflects an accelerated atherosclerotic process, that appears to be different in diabetic patients compared to non-diabetic subjects. Vascular lesions exhibit a larger content of lipid-rich atheroma, macrophage infiltration, and subsequent thrombosis in patients with diabetes than in patients without diabetes. These differences suggest an increased vulnerability for coronary thrombosis in patients with diabetes mellitus. (16). The inflammatory process represents a crucial mechanism in atherosclerosis

and many pieces of evidence show that it is exacerbated in diabetes, especially in T1DM. Obesity, an abnormal distribution of fat in the body, thrombosis, hyperglycaemia, and even hypoglycemia lead to an inflammatory state. In particular, acute hypoglycaemia seems to be involved in complex mechanisms that activate pro-inflammatory, prothrombotic and pro-atherogenic pathways (17).

Coronary Artery Disease (CAD) or ischemic heart disease is a cardiac disorder characterized by impaired fluid load within oxygen that affects myocardial tissue. Clinically, CAD could be asymptomatic, detectable through the presence of coronary plaque by coronagraphy, and symptomatic in turn distinguished in two categories: chronical coronary disease with stable angina, and Acute Coronary Syndrome (SCA) which includes unstable angina (AI), acute myocardial infarct (IMA) and sudden death. Type 1 diabetes represents a risk factor, especially for symptomatic CAD (16).

Heart failure is a syndrome characterized by several clinical symptoms and signs such as dyspnea, asthenia, and oedema within frequent hospitalizations and loss of life expectancy. In many cases of diabetes, it could be owed to CAD as a consequence of premature ageing affecting these patients.

Cerebrovascular diseases include many common and disabling disorders such as ischaemic or haemorrhagic stroke, aneurysms, and arteriovenous malformations. Stroke appears as a sudden localized neurologic deficiency due to a reduction of blood flow, for a few seconds until reperfusion of the area named Transient Ischemic Attack (TIA), or it persists for several minutes within cerebral tissue death with permanent damage. Diabetes is a well-known risk factor for stroke trigging pathological changes into the main vessels involved in endothelial dysfunction, increased arteriolar stiffness and chronic inflammation.

Peripheral Artery Disease (PAD) is a syndrome characterized by stenosis and occlusion that involves aorta or lower limb arteries leading to no pulse in the lower extremities and muscular atrophy. The first cause of PAD is

atherosclerosis although there are several predictors in T1DM: age, sex, foot ulcers, diastolic pressure, HbA1c, and microvascular complications. It could be asymptomatic therefore, it is important to monitor these patients to avoid negative outcomes.

1.1.3 Atherosclerosis and vascular calcification in T1DM

Long term complications in diabetes are driven by inflammation and by slowing blood flow accelerating atherosclerosis. The initial event in the development of atherosclerosis is endothelial damage and the accumulation of low-density lipoprotein (LDL) in the sub-intimal space of the arteries due to increased endothelial permeability. Endothelial dysfunction is followed by the adhesion and migration of monocytes and T cells in the intima in response to the expression of adhesion molecules on the endothelial surface. Then, the recruitment of proliferative smooth muscle cells (SMCs) from the tunica media to the tunica intima, provides the formation of atheroma in the neo-intima. SMCs produce extracellular matrix molecules, such as collagen and elastin, thus forming a fibrous cap covering the plaque mostly composed by apoptotic macrophage-derived foam cells, enriched in oxidized LDL (18). Platelet adhesion to the intima markedly contributes to the rapid growth of the atherosclerotic lesion.

During the progression of atherosclerosis, endothelial cells, macrophages, and smooth muscle cells undergo cell death by apoptosis or necrosis. The destruction of foam cells and the loss of smooth muscle cells can cause the destabilization of the atheroma core and the fibrous cap ruptures, owing to the release of metalloproteases. However, the collagen matrix produced by muscle cells within the fibrous cap maintains the plaque stable and protects it from rupture and thrombosis (19). In this context, microvascular and macrovascular calcifications are considered well-known markers of subclinical atherosclerosis burden, especially in diabetes.

Vascular calcification (VC) is a complication that occurs during aging, in particular in association with diabetes and it is associated with inflammatory

status. VC can be morphologically classified into 2 distinct forms depending on the location, within the intima or the media. Although medial calcification is the most common form in diabetes and affects peripheral arteries where smooth muscle cells (SMCs) and elastic membrane loss elasticity, we are focused on intima calcification that is the predominant type of calcification seen in coronary and carotid atherosclerotic diseases.

The earliest lesion morphology exhibits pathological intima thickening caused by SMCs apoptosis and by the release of matrix vesicles contained cholesterol-enriched lipids that occur on the formation of microcalcification. The extent of plaque calcification within lesion progression is exacerbated by macrophages infiltration of the lipid pool along with necrosis. Area of confluent calcification involved cellular matrix and necrotic core as fragments or diffuse areas.

It is well recognized that calcification has a dual function, which either promotes plaque progression towards an unstable, rupture-prone phenotype and favors stabilization, depending on the type of pattern of calcium deposition. In general, the pattern of vascular calcification could be recognized as spotty or granular microcalcification that is associated with a proinflammatory process and lesion instability, while sheet-like or laminated macrocalcification, often observed in fibrotic lesions and supports plaque stabilization. However, sheet-like matrix calcification forming nodular calcification, eventually erupts into the luminal space causing a potentially fatal thrombosis.

Several studies suggest that diabetic patients have differential mechanisms of plaque growth in comparison to non-diabetic subjects due to the main role of hyperglycaemia ad inflammation. This leads to a different core size of atherosclerotic plaque in these patients. Diabetic patients exhibit a larger percentage of lipid-reach atheroma and greater area occupied by macrophages and T cell components in the lesions which is comprehensible considering the autoimmune nature and genetic susceptibility of T1DM.

Factors, such as blood osmolarity, caused by hyperglycaemia, the activation of protein kinase C and increased expression of glycoproteins have been implicated in the effect of diabetes on platelet function.

Since vascular calcification significantly impacts morbidity and mortality in diabetes, a better understanding of its induction and development will open the way to develop new therapeutic strategies.

Furthermore, since there is no current specific treatment for vascular calcification we hope that identifying specific predictive risk factors may point the way towards a remedy that could help prevent or even slow the process of calcification.(20)

1.2 Risk factors of cardiovascular diseases in T1DM

Several epidemiologic studies recognize many elements that affect the incidence and the prevalence of CVD in T1DM. Besides risk factors in common with T2DM such as obesity, insulin resistance, reduce physical activities, traditional factors of risk for CVD like hyperglycaemia, dyslipidemia, hypertension, and smoking represent targets during therapy and prevention in T1DM.

Hyperglycemia and level of HbA1c are strongly associated with CAD, in diabetic patients within an increasing risk of death for cardiovascular complications. Therefore, promoting tight glycaemic control, also at the onset of disease represents the good practice in order to induce metabolic memory, as soon as possible (21).

Obesity is becoming a risk factor for T1DM as a consequence of the increasing prevalence of this condition in the general population as well as in type 1 diabetes. A possible explanation of this tendency in T1DM could be a higher intake of calories in order to avoid hypoglycaemia (17).

Dyslipidemia is an abnormal amount of lipids in the blood which is associated with T1DM compared to the normal population. However, not balanced glycemia, increased weight and insulin resistance induce more atherogenic cholesterol production in T1DM. Therefore, during the therapy, a concomitant condition of dyslipidemia should be carefully considered, particularly in presence of other risk factors for CVD as hypertension, CKD and familiarity, prescribing statins along with other hypolipidemic drugs as necessary (22).

Diabetic Nephropathy is a complication strongly associated with CVD showing common risk factors. In fact, the activation of the renin-angiotensin-aldosterone system along with fluid retention contributes to increased blood pressure in these patients. Consequently, diet modification and insulin treatment represent the first line in primary prevention (23).

Hypertension is an independent risk factor for CVD and affects 43% of T1DM. The main cause of this tendency is due to hyperglycemia, therefore,

medical recommendations include a hypotensive diet with reduced intake of sodium and increased physical activities together with tight glycaemic control (24).

Accordingly, in the clinical practice, duration of diabetes along with blood pressure, LDL cholesterol level, HbA1c, albuminuria, eGFR, BMI (body mass index), and physical activities should be constantly monitored as primary prevention for CVD in T1DM.

The recognition of disease heterogeneity may be a way to better personalize the treatment of T1DM in order to avoid vascular complications. In terms of scientific progress, one of the main goals of researchers is discovering new molecular markers that could be potentially useful for early diagnosis of these conditions and as new more focused therapeutic targets to avoid them.

1.3 Challenging discover of Molecular biomarkers of vascular calcification in T1DM

Vascular calcification (VC) has been considered for a long time a passive process related to ageing rather than an actively regulated and complex process. Many dynamic changes can trigger or promote VC, therefore, several potential biomarkers, risk factors and therapeutics have been proposed to be taken in to account for better handling and prevention of this condition.

Fibroblast growth factor-23 (Fgf-23) is a small protein that promotes phosphate excretion by reducing its proximal readsorption and the gastrointestinal absorption of calcium and phosphate trought the inhibition of Vitamin D conversion in its active form. (25)

Several studies show that Fgf-23 null mice develop VC and poor phosphate diet plays a major role in calcification abnormalities. These findings suggest that it could be a hall marker of VC, corroborating the hypothesis that it contributes to VC as subclinical cardiovascular injury, as shown in CKD patients with elevating serum level of Fgf-23. In fact, several studies confirmed the correlation between higher serum Fgf-23 levels and mortality and VC, regardless serum phosphatase levels(26).

Fetuin-A (fet-A) is a potential inhibitor of calcification produced by the liver that seems to be related to chronic inflammation state. The formation of fetuin-A calciprotein particles (CPP) induces the clearance of hydroxyl apatite crystals, binding early calcium phosphate deposits and inhibiting their growth along with the amount of mineral deposition in the vessels during VC process(27). Furthermore, many studies support the evidence that lower serum Fet-A levels are associated with vascular calcification. These findings corroborate the hypothesis of Fet-A as a new biomarker for this disease, although the exact role of Fet-A in vascular calcification needs to be further evaluated (25).

Matrix Gla Protein (MGP) is a vitamin K dependent carboxylated protein expressed by chondrocytes, vascular SMCs, endothelial cells and

fibroblasts ables to inhibit arterial calcifications. As Fet-A, MGP binds calcium crystals and plays a role in the maintaining of VSMCs phenotype preventing osteoblastic differentiation, a phenomenon that occurs during vascular calcification. MGP could protect mineral nucleation sites on elastin preventing spontaneous calcification of the elastic laminae. The activation of MPG depends by vitamin K carboxylation, therefore, vit K deficiency induces magnificient of VC phenomenon in experimental models (28). This finding explains the observation that warfarin leads to extensive VC also in human studies and that Vit K therapy partially reverses warfarin effects in VC in rats. Since warfarin is commonly used as anticoagulant drug in therapy, the effects on VC process should be considered and further studied are needed, as long term consequences, especially in diabetic and CKD patients(25).

Bone Morphogenic Protein- 2 (BMP2), a TGFβ like growth factor family member, is a key factor involved in many processes from the tissue remodeling in adults to the development in the embryo. BMP2 regulates the bone formation promoting osteoblast differentiation and mineralization, while its inhibition protects against atherosclerosis and against VC, in vivo and in vitro studies. BMP2 expression is increased in calcified VSMC which suggests its key role in the trans-differentiation osteogenic phenotype during VC(25).

Osteoprotegerin (OPG) is a regulatory factor derived by stromal cells in the bone marrow which guides the bone turnover, inhibiting osteoclast differentiation as a decoy receptor for NF-KB ligand (RANKL system). OPG also inhibits alkaline phosphatise (ALP) activity and its levels were found to be significantly higher in CKD patients (25). This molecule is considered a protective factor against VC by blocking bone remodeling process in vessels, since it neutralizes the pro-apoptotic action of TRAIL (TNF-related apoptosis-inducing ligand) responsible for vascular cell apoptosis strongly contributing to mineralization(29). According to several studies, OPG seems to be a marker of VC onset rather than a progression predictor, in fact OPG levels were significantly increased in patients with moderate calcification but

not in several VC. Although there are some evidence of correlation between OGP levels and calcification, its role as marker rather than a protector or as an active player in this process should be elucidated. Recombinant OGP treatments were proposed to decrease or even inhibit VC with promising results in mice model, nevertheless, they are not in clinical study.

Osteopontin (OPN) is a phosphoprotein that inhibits mineralization and it is expressed in mineral tissues. OPN blocks hydroxyapatite formation and activates osteoclast function. OPN is active as inhibitor of mineralization in VSMC when phosphorylated, binding mineralized crystal surface. On the contrary, in its cleaved form facilitates vascular mineralization acting as a proinflammatory cytokine and proangiogenic factor(30). For these reasons, its potential role as serum biomarker for calcification is still debated. On the contrary, OPN plays a key role in inflammatory process and its relation with diseases related to inflammation such as atherosclerosis, diabetes and other autoimmune disorders has already been shown.

Osteocalcin (OCN) is a vitamin K dependent matrix protein with a strong affinity for hydroxyapatite. It is expressed in calcified atherosclerosis plaques and its role in VC is still controversial. In fact, even if OC inhibits crystal growth, on the contrary, it seems to promote differentiation and mineralization, upregulating sox9, ALP and mineral content in VSMC and chondrocytes, in vitro. Several studies also demonstrated its metabolic role stimulating insulin secretion and glucose uptake in responsive cells, arguably involving hypoxia- inducible factor 1 alfa (HIF-1α) that triggers a gene expression modulation of glucose metabolism factors (25). Furthermore, a subpopulation of circulating endothelial progenitors cells expressing OCN shows procalcific polarization in diabetic patients affected by CAD. However, OCN role as potential serum marker of VC is still discussing for controversial findings in several studies, therefore in order to use it as a diagnostic or screening tool, its place in VC pathogenesis must be clarified.

Pyrophosphate (Ppi) is a small molecule acts as a calcification inhibitor blocking hydroxyapatite crystal formation. It has been shown that a

decrease of PPi along with high phosphate levels and type 1 collagen could accelerate the calcification process(31).

For each one of these potential biomarkers, there is a downside as involved in many pathways and diseases: their direct effects on the vasculature could lead at the same time to indirect effects in other tissue and pathways, such as bone turnover. Therefore, these actions are not so easy to discriminate. In fact, there is also a substantial overlap between VC regulatory mechanisms and those that regulate bone mineralization in the skeleton, or CKD and other complications of diabetes. Therefore a good biomarker should be achieved clinical goal ,for instance, selecting high-risk patients, providing a prognostic value that should be as specific as possible for the targeted long term complications.

For this reason, in the last two decades it is catching on new classes of molecules detectable in biological fluid that could regulate specific pathways, such as small non-coding RNAs.

2. Non-coding RNAs

Over the last years, the rapid development of high –throughput sequencing technologies has revealed a regulatory function of RNA in protein synthesis leading researchers to re-examine the roles of RNA in physiological and pathological processes. It is well known that only 3% of the transcripts encode for proteins, while at least 80% of the genome is actively transcribed. Since the discover of ribosomal RNA (rRNA) and transfer-RNA (tRNA), has been raised the question of whether the remaining non-protein coding transcripts are considered transcriptional noise or actual molecules contain genetic information, recently named non-coding RNAs (sncRNAs) (Fig.2)

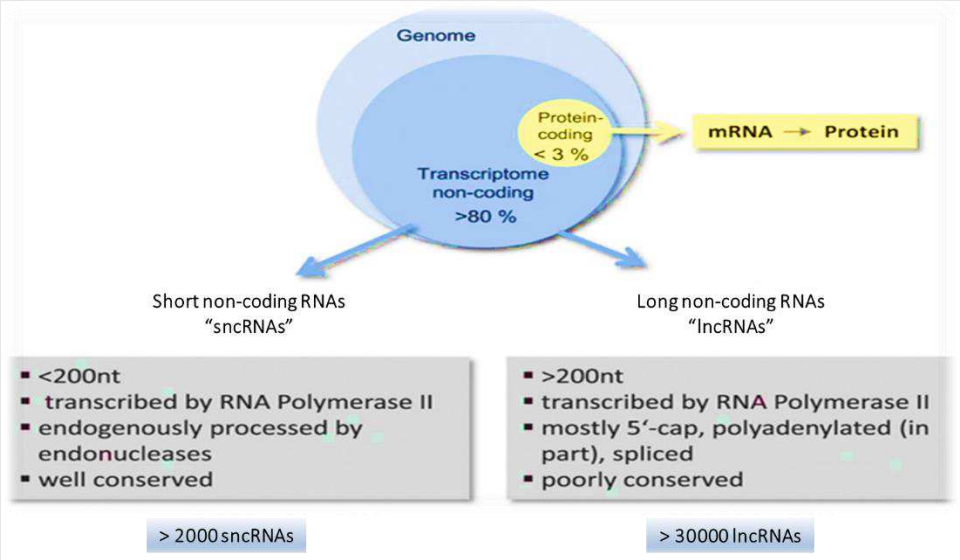

Figure 2: The main classes of non coding RNAs.

sncRNAs could be divided into two main classes according to their size, biogenesis, and conservation during evolution.: Long non-coding RNAs (lncRNAs) and small non-coding RNAs (sncRNAs). It has been estimated that the transcriptome contains about 100000 lncRNAs and more than 10000 sncRNAs that have been studied to date and new classes are constantly discovered such as circular RNAs (circRNAs) (32).

2.1 Long non-coding RNAs

Long non coding RNAs are a type of non-coding RNAs longer than 200 nucleotides that can regulate gene expression acting as epigenetic regulator, transcriptional and post-transcriptional factors.

lncRNAs have different roles in the regulation of protein synthesis binding proteins that regulated mRNA splicing or interacting with transcription factors and coordinating the localization of RNA-protein complex on promoter sequences. lncRNAs can also drive the recruitment of methyltransferases to specific genetic loci in order to regulate chromatin remodeling and gene expression. Furthermore, some lncRNAs may maintain a low coding potential, encoding small peptides or micro peptides (less than 100 amino acids) involved in various biological processes. It is a heterogeneous class of molecules hard to detect and manipulate because of their instability in biological fluid and their short lifespan (33).

2.2 Small non-coding RNAs

Small non-coding RNAs are a huge class of small molecules no longer than 200 nucleotides which include several categories of molecules with different size, structure, and function. sncRNAs are divided in two main classes: housekeeping or structural sncRNAs such as tRNA or rRNA, and regulatory sncRNAs that including *microRNAs* (miRNAs), *small-interference RNAs* (siRNAs), *piwi-associated RNAs* (piRNAs), *tRNA-derived small RNA* (tsRNAs), *small nuclear RNAs* (snRNAs) and *small nucleolar RNAs* (snoRNAs). However, additional new classes of small RNAs are emerging through the next-generation sequencing (NGS) analysis, which markedly expanded our knowledge of small RNAs.

2.2.1 microRNAs (miRNAs)

microRNAs represent the most widely studied class of ncRNAs. miRNAs are small RNA molecules of about 22 nucleotides that mediate post-transcriptional gene silencing, regulating gene expression and protein synthesis. They are involved in many processes including proliferation, differentiation, apoptosis, and development and several studies demonstrated that they are implicated in different diseases.

miRNAs can regulate the expression level of hundreds of genes simultaneously and many of them cooperate to modulate a specific target.

miRNA biogenesis

miRNA genes are transcribed by RNA polymerase II (Pol II) as a long primary transcript with a local hairpin structure (pri-miRNA) (fig.3a).

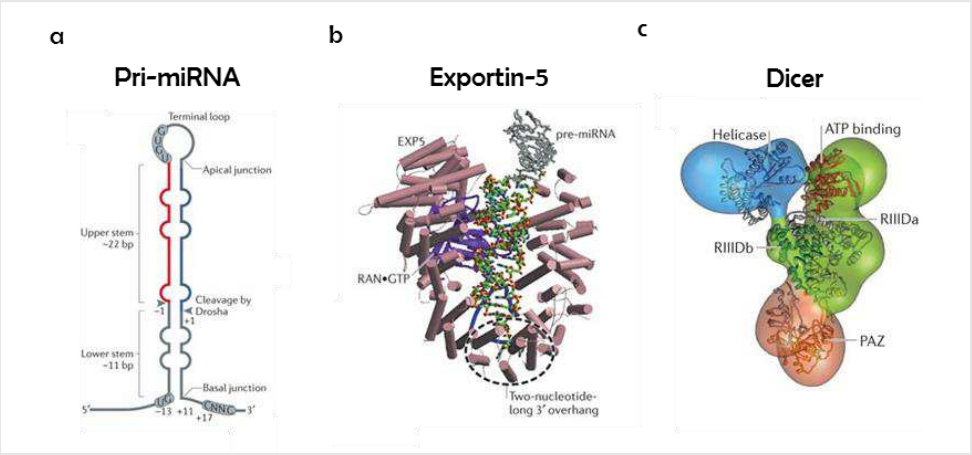

Figure 3 The main actors of miRNAs Biogenesis. *a) A typical pri-miRNA; Exportin-5 structure; c) Dicer structure*

miRNA transcription is controlled by RNA Pol II-associated transcription factors and by epigenetic regulators adding modifications such as DNA methylation and histone acetylation or methylation(34). miRNA sequences are dislocated in all the genome, however, in human genome, the majority of canonical miRNAs are encoded by introns of non-coding or coding transcripts, whereas rarely could be encoded by exonic regions. Often, several miRNA loci constitute a polycistronic transcription unit distributed in close proximity to each other. The miRNAs in the same cluster are generally

co-transcribed, even though each miRNA can be additionally regulated at the post-transcriptional level. Generally, miRNA genes that reside in the introns of protein-coding genes share the promoter of the host gene, but it is not unusual that they have multiple transcription start sites with promoters distinct from those of their host genes.

Following transcription, the pri-miRNA undergoes several steps of maturation: the nuclear RNase III Drosha cleavages specifically on double-stranded RNA, the stem-loop, to release a small hairpin-shaped RNA of ~65 nucleotides in length (pre-miRNA)(35). Drosha works with its essential cofactor DGCR8 with RNA-binding activity, formed a complex called Microprocessor (fig 4).

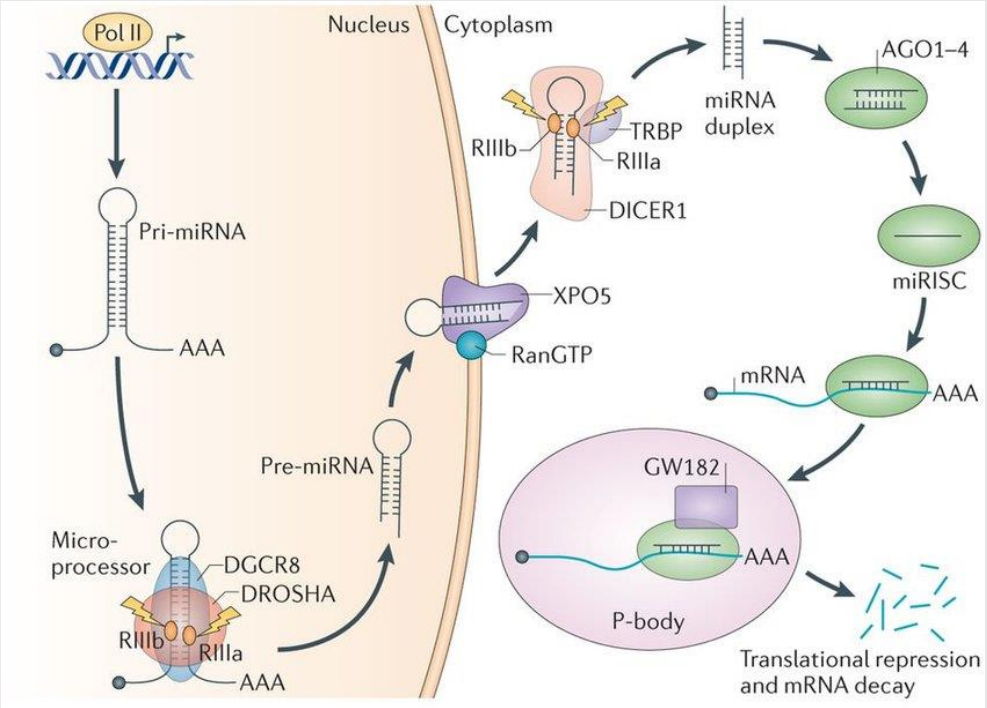

Figure 4: miRNA biogenesis. *Pri-miRNA transcript is cleaveged by the microprocessor to generate pre-miRNA; pre-miRNA is exported to cytoplasm by Exportin5 (XPO5) and then processed by Dicer along with AGO proteins. The forming complex (miRISC) allows to start the silencing process with the generation of a mature miRNA. Mature miRNA binds its gene target to induce its translation repression.*

Drosha-mediated processing of intronic miRNA does not affect splicing of the host pre-mRNA thought it occurs co-transcriptionally before splicing catalysis, whereas when it is located in the exonic region, Drosha-mediated cleavage leads to destabilization of the host mRNA.

Then, pre-miRNA is exported into the cytoplasm, through the interaction with protein exportin 5 (EXP5) forming a transport complex along with RAN·GTP, a GTP-binding nuclear protein (Fig.3b). The crystal structure of this complex forms a 'baseball mitt'-like structure into which the pre-miRNA stem is placed, avoiding the interaction between the pre-miRNA and positively charged inner surface. There is a basic tunnel-like structure at the bottom of the mitt-like structure, which strongly interacts with the two-nucleotide-long 3′ overhang of the pre-miRNA(36).

Following translocation, GTP is hydrolyzed and the complex is disassembly at the release of the pre-miRNA into the cytosol, where pre-miRNA is cleaved by Dicer near the terminal loop, liberating a small RNA duplex. Dicer is an RNase III-type endonuclease of ∼200 kDa (Fig. 3c) and pre-miRNA is recognized by its N-terminal helicase domain by interacting with the terminal loop, whereas the PAZ (PIWI–AGO–ZWILLE) domain binds to the termini of pre-miRNA(37). Dicer binds to pre-miRNA with a preference for a two-nucleotide-long 3′ overhang that was initially generated by Drosha. In mammals and flies, Dicer binds to the 5′ phosphorylated end of the pre-miRNA and cleaves it 22 nucleotides away from the 5′ end.

Human Dicer activity is mediated by the interaction with TAR RNA-binding protein (TRBP; encoded by TARBP2) and with dsRBD cofactor PACT (also known as PRKRA)(38).

When a small RNA duplex is generated by Dicer, it is loaded onto an Argonaute (AGO) proteins forming a complex called RNA-induced silencing complex (RISC) in two steps: the loading of the RNA duplex and its subsequent unwinding. AGO proteins play a critical role in miRNA biogenesis by forming the catalytic engine of the silencing complex.

The mature miRNA functions within an AGO protein complex (Figure XX), which comprises a single polypeptide chain composed of four characteristic domains: the amino (N)-terminal domain, the Piwi–Argonaute–Zwille (PAZ) domain, the middle (MID) domain and the P-element induced wimpy testes (PIWI) domain(39). All four human AGO proteins can incorporate siRNA and miRNA duplexes, but only one of the two single-stranded RNA will be utilized to base pair with target mRNA (RNA messenger) for gene silencing, commonly the guide strand. The guide strand is determined during the AGO loading step, mainly on the basis of the relative thermodynamic stability of the two ends of the small RNA duplex, whereas the released passenger strand is degraded quickly. The less abundant passenger strand (miRNA*) is also less potently active in silencing (40).

microRNA functions

miRNA target sites are generally located in the 3′ UTR of mRNAs (RNA messengers); they possess strong complementarity to the seed region, which is the main criterion for target-site prediction. The strongest canonical (seed-matching) target sites are those that complement miRNA nucleotides 2–8 and have an adenine opposite miRNA nucleotide 1 (known as 't1A'), followed by those complementing nucleotides 2–8 without a t1A and nucleotides 2–7 with a t1A. t1A is not recognized by the miRNA guide strand, but by a binding pocket within AGO. Target sites with complementarity to nucleotides 2–7 or 3–8 of the miRNA are much weaker but still considered canonical(41).

MicroRNAs (miRNAs) mediate gene silencing by guiding Argonaute (AGO) proteins to target sites in the 3′ untranslated region (UTR) of mRNAs. The miRNA-loaded AGO forms the targeting module of the miRNA-induced silencing complex (miRISC), which promotes translation repression and degradation of targeted mRNAs. AGO–miRNA binding to the 3′ UTR leads to gene silencing through translation repression and mRNA decay (42). The latter involves recruitment by AGO of a member of the glycine-tryptophan

protein of 182 kDa , (GW182). GW182 interacts with polyadenylate-binding protein (PABPC), thereby promoting mRNA deadenylation. It leads to decapping and makes the mRNA susceptible to rapid degradation by 5′–3′ exoribonuclease 1 (XRN1)(43).

Inhibition of translation initiation is also caused by interfering with the function of eukaryotic initiation factor 4 A-I (eIF4A-I) and eIF4A-II (44). the miRISC induces their dissociation from target mRNAs and thereby inhibits ribosome scanning and assembly of the eIF4F translation initiation complex. A recent investigation in human and D. melanogaster cells reported that the AGO Trp-binding pockets that mediate GW182 binding are required for translation inhibition (41). Thus, miRISC-mediated translation inhibition is still incompletely understood.

Both modes of miRISC-mediated gene silencing are thought to be interconnected, and ribosome profiling assays revealed that inhibition of transcription of mRNA is a reversible process responsible for 66–90% of protein silencing, while the degradation of mRNA is an irreversible process(45,46).

Each miRNA can silence hundreds of genes, although the effect on gene is generally mild, and multiple miRNAs can regulate the same gene. miRNA binding of neighboring target sites on a target mRNA can result in cooperative repression. Furthermore, entire cellular pathways can be regulated by individual miRNAs or miRNA clusters. (47).

microRNA nomenclature

New knowledge of miRNA origins, biogenesis, and function requires a revision of nomenclature guidelines to provide an unbiased naming protocol. Classification rules have not yet been unified, but it is generally considered that miRNAs with the same sequences at nucleotides 2–8 of the mature miRNA belong to the same 'miRNA family'. For instance, the human genome contains 14 paralogous loci (encoding 'miRNA sisters') that belong to the let-7 family. Thirty-four miRNA families are phylogenetically

conserved from C. elegans to humans, and 196 miRNA families are conserved among mammals. miRNA sisters generally act redundantly on target mRNAs, but distinct roles have also been suggested.

Genes encoding miRNA sisters are indicated with lettered suffixes (for example, mir-30a and mir-30b). The same mature miRNA is generated from multiple separate loci, thereby numeric suffixes are added at the end of the names of the miRNA loci (for example, mir-29b-1 and mir-29b-2). Each locus produces two mature miRNAs: one from the 5′ strand and one from the 3′ strand of the precursor (for example, miR-30c-5p and miR-30c-3p)(48).

2.2.2 Small-interference RNAs (siRNAs)

siRNAs are short ncRNA molecules comprising 20-25 nucleotides derived from longer double-strand precursor RNA molecules that are cleaved by DICER to induced degradation of perfectly complementary target mRNAs. siRNAs protect genome integrity in response to foreign or invasive nucleic acids such as transposons, transgenes, and viruses (49).

In general, the double strands RNA (dsRNA), transcripted by cellular genes, by infecting pathogens or artificially introduced into the cells, are processed by Dicer in the cytoplasm into a smaller dsRNA molecules (fig.5)

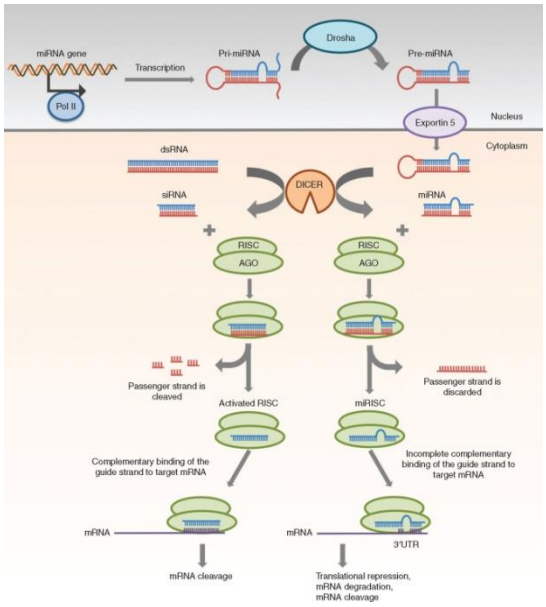

Figure 5: Gene silencing mechanisms of siRNA*. dsRNA is processed by Dicer into siRNA which is loaded into the RISC. AGO2 cleaves the passenger strand of siRNA. The guide strand then guides the active RISC to the target mRNA. The full complementary binding between the guide strand of siRNA and the target mRNA leads to the cleavage of mRNA.*

This short dsRNA molecule (siRNA) has 3′ two-nucleotide overhangs and interacts with RNA-induced silencing complex (RISC), activating the endonuclease argonaute 2 (AGO2) component of the RISC. It cleaves the passenger strand (forward strand) of the siRNA while the guide strand (reverse strand) remains associated with the RISC. Subsequently, the guide strand into the active RISC interacts with its target mRNA inducing specific gene silencing(50).

2.2.3 Piwi-interacting RNAs (piRNAs)

piRNAs are a class of small non coding RNAs of 24-30 nucleotides Dicer-independent that binds the PIWI protein, a sub-family of Argonaute proteins. Piwi was originally discovered in *Drosophila*, in which it functions in germline stem-cell maintenance and self-renewal (*P*-element-*I*nduced *Wi*mpy Testes or Piwi). piRNAs are transcribed from specific genomic loci known as *piRNA clusters* that give rise to long non coding RNAs (lncRNAs) then processed into piRNAs (51).

One of the main functions of piRNA in mammalians is to control transposon mobilization in the germline genome. Transposons are repetitive sequences spread in large proportion of mammalian genomes, and a fraction of these repeats are mobile elements, also termed transposable elements (TEs)(52). TEs play crucial roles in driving genome evolution by rising the development of new genes and novel immune strategies. Active retrotransposition which requires active cell divisions, is more frequent in germ cells to allow the imprinting and epigenetic reprogramming in these cells. However, this plasticity could results in deleterious effects by uncontrolled retrotransposition and therefore, requires tight handling of TEs action. In order to preserve the integrity of the genome that is transmitted to the next generation, an additional retrotransposon control has evolved in germline through the piRNA pathway(53).

Primary Biogenesis

piRNAs are mainly distinguished based on their biogenesis (fig.6). Primary piRNAs are transcribed as single-stranded in somatic cells or as a piRNA precursor double-stranded in germinal cells, by RNA polymerase II, from piRNA clusters(54).

In mammalian, the piRNA precursors are exported into the cytoplasm, facilitated by Maelstrom (MAEL), a conserved HMG-box domain protein with RNA-binding activity(54). In the cytoplasm, piRNA precursors

associate with the RNA helicase MOV10L1, en anzyme essential for piRNA biogenesis. This complex interacts with PLD6 (MITOPLD), an endonuclease that generates the 5′ uridine end (1U) of primary piRNAs. Intermediate fragments with a 5′ uridine (1U) are preferentially bound by PIWI proteins and thereby stabilized. PIWI-bound piRNA intermediates then undergo 3′ end processing, which most likely involves exonucleolytic shortening by a 3′–5′ trimmer that has not been identified in mammals yet. The process is facilitated by Tdrkh, a Tudor and KH domain-containing protein, whose absence causes the accumulation of 31–37 nucleotide (nt) long intermediates(55).

Double strands piRNA originated from piRNA clusters are processed directly by PIWI proteins to undergo 3′ end processing. In particular, in *Drosophila* germline cells, dual-stranded piRNA clusters are loaded onto both Piwi (following the same process) and Aubergine (Aub) to form piwi-piRISCs (fig.6) (56).

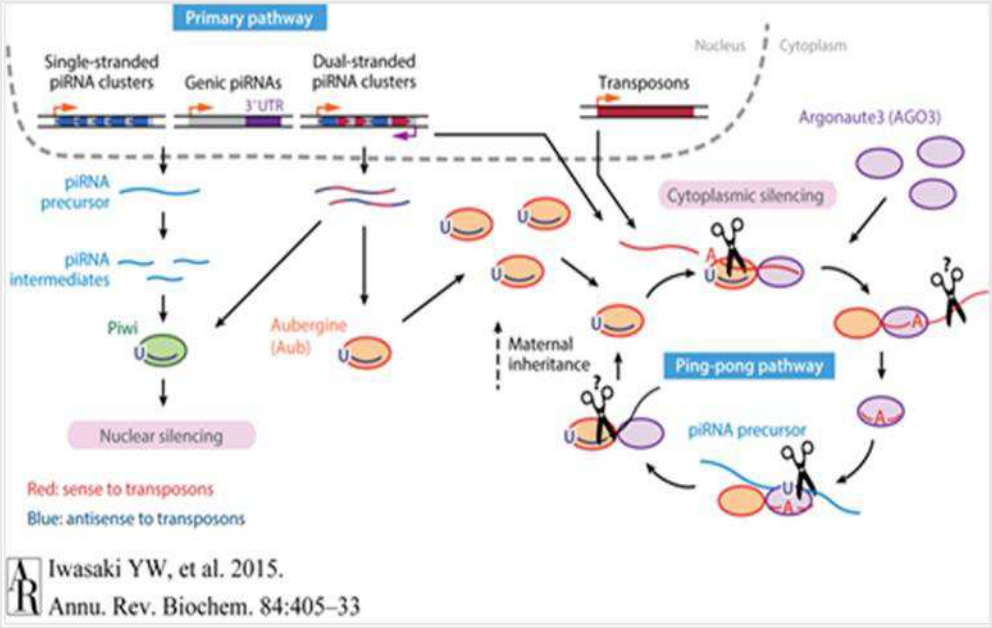

Figure 6: piRNA biogenesis. *piRNA are generated starting from two processes. The primary pathway or primary biogenesis generates primary piRNA which can drive the production of secondary piRNA in the ping-pong pathway or secondary biogenesis.*

Secondary Biogenesis

piwi-piRISC initiate a process known as the 'ping-pong' amplification cycle in the cytoplasm to produce secondary piRNAs and repress transposon transcript derived from the same piRNA cluster. In the ping-pong pathway, argonaute and Piwi act in a complementary fashion to cleave sense and antisense of transposon transcripts and piRNA.(57) Secondary piRNAs derived from the cleavage of transposon transcripts overlap with the primary piRNA generated during primary biogenesis, for 10 nt in 5′ and often have adenine at their tenth position. Secondary piRNAs generation in a feed-forward mechanism results in the consumption of transposon transcripts, thereby silencing transposons. Furthermore, they could be recognized by another piRNA precursor that in turn enhance the generation of new mature primary piRNAs and eventually start a new cycle.(58)

piRNA functions

The primary function of piwiRNAs is transposon silencing. Transposon are mobile genetic elements which promotes DNA recombination, such as replication and insertion in new sites, generating double-stranded DNA breaks or disrupt coding sequences (54). As consequence, transposons can drive aberrant expression of neighboring genes. Therby the main role of PIWI proteins is protect germ cells from the expression of transposons through the complex piRNAs and PIWI proteins, called the PIWI ribonucleoprotein (piRNP). piRNP is involved in transposon repression and transposable element expression and mobilization suppression, by two different mechanisms: at level of transcri ption and post-transcription.

PIWI proteins and piRNAs can trigger the establishment of repressive epigenetic DNA or chromatin modifications, thus inducing efficient transposon silencing on the transcriptional level. Besides transcriptional transposon control, nuclear PIWI proteins are guided by piRNAs towards nascent

transposon transcripts and activate endonuclease to facilitate the degradation of the transposons.

Post –transcriptionally, piRNAs induce target degradation of trasposoms elements (TE) splicing the transposable element transcripts through PIWI proteins by a base-pairing recognition between piRNAs and transposon transcripts, as previously described in the ping pong cycle (59).

Recent studies have investigated another potential role of piRNAs in the cellular division. For instance, the mammalian piRNAs can be divided into two classes, pre-pachytene, and pachytene piRNAs, depending on the stage of meiosis at which they are expressed in developing spermatocytes (60), In mammals, fetal piRNAs silence transposons in male germ cells. By contrast, the most abundant piRNA population in mammals, the pachytene piRNAs, is depleted of transposon sequences (54).

Interestingly, antiviral defense in somatic tissues is typically ascribed to siRNAs. However, some species use piRNAs against viral infection. A possible explanation for the use of two classes of small silencing RNAs to fight viruses may reflect the difference between RNA interference (iRNA) and piRNA pathways: iRNA is triggered by double-stranded RNA, whereas mature piRNAs are single-stranded RNA. The two pathways may target RNA from different types of viruses or stages of viral infection, boosting the overall antiviral response.

piRNA nomenclature

The complexity of nomenclature of piRNAs depends on the various genome versions used by different non-coding RNA databases in reference studies. piRNA-disease association studies incorporated data from various reference piRNA databases, and each of them has unique ID. For example, piRNABank and piRNAQuest use have _piR_000001 and piRBase follows piR_hsa_000001, which makes piRNA search quite challenging. However, piRBase is the first database that systematically integrates various types of

data to support piRNA functional analysis: the total numbers of unique piRNAs and species have been increased. As piRNA studies expanded rapidly, Databases are constantly updated with more related information supporting iRNA functional analysis (61).

2.2.4 tRNA derived Small RNA (tsRNAs)

tRNA-derived small RNA (tsRNA) are ubiquitous molecules of 28-36 nucleotides that belong to the small non-coding RNA. tsRNA are generated by the cleavage of transfer RNA (tRNA) which are the fundamental components of the translation machinery in that they deliver amino acids to the ribosome. The discovery of tsRNAs can be dated back to the late 1970s, when they were considered as product of tRNA random degradation and attracted only minimal interest. The wide application of high-throughput next generation sequencing technology has unveiled various tsRNAs from bacteria to humans and their production is conserved throughout evolution (62).

Biogenesis of tRNAs

The biogenesis of mature tRNA begins with the transcription of precursor tRNA (pre-tRNA) by RNA polymerase III. The 5′ leader sequence and a 3′ polyuracil (poly-U) tail of a newly transcribed pre-tRNA can be cleaved by endonucleolytic ribonuclease P (RNase P) and ribonuclease Z (RNase Z), respectively, followed by the addition of a 3′ CCA tail with the help of the tRNA nucleotidyl transferase. The mature tRNAs have a length of 73–90 nts and adopt a clover-leaf shaped secondary structure, composing a D-loop, an anticodon loop, a T-loop), a variable loop, and an amino acid acceptor stem.

tsRNA biogenesis

tsRNAs are produced through the activity of various endonucleases attacking single-stranded of mature tRNA in open loop structures. It has been supposed that extent chemical modifications could modulate endonucleolytic cleavage of mature tRNAs thereby influencing tsRNA biogenesis. On the other hand, many tRNA modifications support various ‘proofreading’ steps during tRNA maturation into a functional structure, therefore loss of particular tRNA modifications might impact efficient folding thereby allowing stress-induced endonucleases to better access single stranded of mature tRNA regions. Specific tRNA modifications likely change the structural context of

tRNAs thereby modulating access for endonuclease activities or serving as platforms for specific enzymes. These modified nucleotides could limit the extent of exonuclease activity and thus increase the stability of produced tsRNAs. tsRNAs can be extremely stable with half-lives measured in days and this stability is connected to numerous nucleotide modifications as well as to correct tertiary structure (63).

Based on the length and cleavage sites of mature tRNAs, tsRNAs can be divided into two main types: *stress-induced tRNA fragments (tsRNA^S*) produced by specific cleavage in the anticodon loop of mature tRNAs with 28–36 nts length; and *tRNA-derived fragment* (tRF) constitutively expressed with about 14–30 nts length and derived from the mature or primary tRNAs (fig.7).

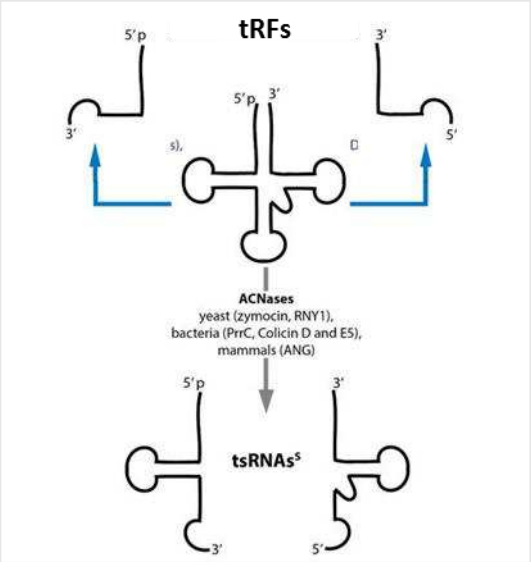

Figure 7: tsRNA are distinguished in two main classes. (up) constitutive tRNA fragments (tRFs);(down) Stress- induced tRNA fragments (tsRNAs^S)

Both types of tsRNA can accumulate during different biological processes in several species and have very different biogenesis pathways that are slowly being uncovered. Moreover, the naming conventions of tsRNAs are inconsistent, as researchers generally named the identified tsRNAs in their systems primarily based on their own preferences (64).

Stress-induced tRNA fragments (tsRNA^{stress})

tsRNAs^{stress} are produced by cleavage of tRNAs in response to stress, such as starvation, oxidative stress, nutritional deficiency, hypoxia and hypothermia, heat and cold shock or ultraviolet irradiation (63). In addition, tsRNAs^{Stress} appeared to increase during aging. Two subtypes of tsRNAs^{Stress} have been discovered, 5′-tiRNAs and 3′-tiRNAs, which are generated by the cleavage in or near the anticodon loop of a tRNA. During stress tRNA cleavage in humans is carried out by ribonuclease as RNase angiogenin (ANG) which is a member of the RNase A superfamily. ANG was discovered and characterized by its ability to promote new blood vessel growth, making it a potential anticancer therapeutic target. In human cells, tRNA is protected by several ribosomial proteins and only ~ 1% of tRNA is cleaved by ANG during a stress response. However, it is surprising that some tRNAs are more susceptible than others to stress-induced cleavage by ANG and which tRNA are targeted for cleavage can change in response to different stresses, further indicating selectivity(65) .

tsRNAs^{Stress} are mainly located in the cytoplasm, with a small amount in the nucleus and mitochondria, and can also be detected in the circulation system of human. Interestingly, specific tsRNAs^{Stress} were also detected in human breast milk and in mature mouse sperm indicating tsRNAs^{Stress} production for directed transmission into the next generation(66). Some high-throughput experiments indicated that 5′-tiRNA is more abundant than 3′tiRNA.

Constitutive tRNA fragments (tRFs)

tRFs are produced by the cleavage of mature tRNAs in the absence of cellular stress exposure. These stress independent- tsRNAs are constitutively produced throughout the lifespan of an organism,in specific cell types or at specific developmental stages. Some of these represent the same molecule as a stress-induced fragment and even share a biogenesis pathway, but are exemplified by their stable noninduced production.

High levels of constitutive tsRNAs were detected in both hematopoietic and lymphoid systems as well as in cell and vesicle-free blood fractions, suggesting that these tsRNAs can be secreted and exist as stable entities outside of membranous organelles (67).

These small RNAs, referred to as tRFs, are 19–21 nucleotides and are generated as a result of cleavage in any of the tRNA loops. One of the more intriguing tRNA-derived small RNA implicated in cancer biology, termed tRF-1001, is derived from the 3′ trailer of tRNASer. Select tRFs have been identified in various healthy tissues including heart, colon, lung, and small intestine (68).

tsRNA functions

tiRNA and tRF have been recognized as small non coding RNAs with a relevant biological role. These framments hold similar functions with microRNAs regulating mRNA stability. For example, 3-tRFs derived from $tRNA^{Gly\text{-}GCC}$ in mature B lymphocytes or from $tRNA^{Leu\text{-}CAG}$ in non-small cell lung cancer cells have miRNA-like structure and function, inhibiting protein translation or cleaving partially complementary target site.

It has been well characterized that stress-induced tRNA cleavage results in reduction in protein synthesis. Specific stress-induced tsRNAs displaced various eukaryotic initiation factors from both capped and uncapped mRNA causing translational repression such as tsRNA-Ala^{UGC} and tsRNA-$Cys^{GCA)}$. In another mode of action, $tsRNAs^{Stress}$ indirectly interfered with protein synthesis, in particular through binding to ribosomal components. Interestingly, these $tsRNAs^{Stress}$ competed with mRNA for ribosomal binding in response to alkaline stress conditions.

Some $tsRNAs^{Stress}$ are involved in the regulation of osmotic stress, ANG-cleaved tsRNAs associate with cytochrome c to promote survival. At the onset of apoptosis, cytochrome c is released from the mitochondria to form a large protein structure called the apoptosome.(69) Various tsRNA interact

with cytochrome c upon release from the mitochondria to block apoptosome formation and promote survival.

Emerging data shows that tsRNAs^{Stress} play vital roles in regulating stem cell fate. In hematopoietic stem/progenitor cells (HSPCs), the ribonuclease ANG cleaves mature tRNA and the tRNA fragments are able to repress translation which is required for maintaining the stemness of these cells. Recent work has revealed that some tsRNAs can regulate epigenetic inheritance. In sperm from mice fed a high-fat diet (HFD), there was a marked increase in tsRNA (70).

Changes in tsRNAs^{Stress} abundance have been observed in many stress-exposed or virus-infected cell types or tissues. Some evidence suggest that they promote viral replication through an increase of transcription and protein synthesis. Profiling of small RNAs in liver from human subjects with advanced hepatitis B or C revealed that tsRNAs^{Stress} were significantly increased in humans with chronic viral hepatitis.

Furthermore, since tsRNAs originate from pre-tRNAs and from mature tRNAs, they could bind to tRNA interacting proteins thereby competing with their parental molecules and resulting in the modulation of specific molecular pathways and thereby cellular physiology (71).

Interestingly, small RNA pathway components can associate with tsRNAs under specific conditions in fact also a human Piwi-like protein (Hiwi2), preferentially interacted with tsRNAs, which the authors named tRNA-derived piRNAs (63).

tsRNA nomenclature

The naming of tsRNAs, both in literature and public databases, is still largely inconsistent. Starvation-induced tsRNAs in eukaryotic cells were first reported in *Tetrahymena* and simply named tRNA fragments. However, other authors labelled the products of stress-induced tRNA fragmentation in different organisms with different names such as stress-induced tRNA-derived

RNAs (sitRNAs) or tRNA-derived, stress-induced RNAs (tiRNAs). In addition, tsRNAs existing under steady-state conditions were either called tRNA-derived fragments (tRFs) or tRNA-derived small RNAs (tsRNAs,). Others have called these RNAs, tRNA-derived RNAs (tDRs) or even tRNA-derived small non-coding RNA (tsncRNAs) (72).

Although various authors attempted to introduce some order into the nomenclature, the net result was only a distinction between tRNA halves (28–36 nucleotides) that are largely stress-induced (often also called tiRNAs) and tRFs (14–30 nucleotides) that are produced under steady-state conditions. Therefore, attempts to systematically name tsRNAs and assign recognizable nomenclature is necessary.

2.2.5 Small nuclear RNAs (snRNAs)

Small nuclear RNAs comprise a small group of highly abundant, non-polyadenylated, non-coding transcripts with an average size of 150 nt localized in the nucleus with important functions in intron splicing and other RNA processing.

The snRNAs can be divided into two main classes on the basis of common sequence features and protein cofactors: *Sm-class RNAs* are characterized by a 5′-trimethylguanosine cap, a 3′ stem-loop and a binding site for a group of seven Sm proteins (the Sm site) that form a heteroheptameric ring structure. *Lsm-class RNAs* contain a monomethyl phosphate cap and a 3′ stem-loop, terminating in a stretch of uridines that form the binding site for a distinct heteroheptameric ring of Lsm proteins (32).Generally, in transcript splicing, snRNA presents as a ribonucleoprotein particles (snRNPs) along with additional proteins that form a large particulate complex (spliceosome) bound to the unspliced primary RNA transcripts in order to mediate the process. For instance, U1 snRNA is a component of the spliceosome and recognizes splice donor sites (or 5′ splice sites) through direct base-paring. Selection of a 5′ splice site is influenced by several factors, including sequence complementarity between the splice site and U1 snRNA, local secondary structure of pre-mRNA, trans-acting proteins bound to adjacent regions, and competition with other 5′ splice sites.

Besides splicing, additional evidence indicate snRNPs function in nuclear maturation of primary transcripts in mRNAs, gene expression regulation, splice donor in non-canonical systems and in 3′-end processing of replication-dependent histone mRNAs.(73) For instance, U7 snRNA is involved in the 3′ processing of histone mRNA and is not inherently involved in pre-mRNA splicing. However, by changing the sequence bound by like-Sm (LSm) proteins, U7 snRNA can be converted into an artificial splicing factor that induces either inclusion or skipping of an exon, depending on the location of the target site on the transcript and presence of any additional modifications in the U7 snRNAs(74)

2.2.6 Small nucleolar RNAs (snoRNAs)

snoRNAs are intermediate-sized ncRNAs (60–300 bp). The term small nucleolar RNA was originally coined to reflect the nucleolar localization of the first members of this group relative to their nucleoplasmic cousins, the snRNAs They are components of small nucleolar ribonucleoproteins (snoRNPs), which are complexes that are responsible for sequence-specific 2′-O-methylation and pseudouridylation of ribosomal RNA (rRNA). Post-transcriptional modifications of rRNAs take place in the nucleolus and facilitate rRNA folding and stability.

snoRNAs are responsible for targeting the assembled snoRNPs to a specific target (59). The RNAs commonly referred to as snoRNAs comprise two families, the *C/D* and *H/ACA* RNAs. Most C/D and H/ACA RNAs function in ribosomal (r)RNA modification and processing in the nucleolus. However, the C/D and H/ACA RNAs have evolved many functions and targets as well as a corresponding range of cellular localization that includes sites outside of the nucleolus to gain access to different substrates (32).

2.2.7 Other classes of sncRNAs. Many classes of ncRNA have been described that are associated with the transcriptional start sites (TSSs) of genes: for example, *promoter-associated small RNAs* (PASRs), *TSS-associated RNAs* (TSSa-RNAs), *promoter upstream transcripts* (PROMPTs) and *transcription initiation RNAs* (tiRNAs) - responsible for misunderstanding with tsRNAs. For all of these classes, their biological functions are poorly defined, although they are probably involved in transcription regulation (59).

2.3 Circulating sncRNAs and their potential as biomarkers

Molecules generated locally could be released by cells and tissues and distributed through biological fluids. Their altered concentrations have been linked to various diseases, becoming proper biomarkers that provide useful biological and clinical information. These molecules provide useful information to identify and categorize patients toward an individual risk profile, to diagnose and monitor disease conditions, and to effectively draw prognoses of patients and to adapt treatments. Therefore, noninvasive and highly sensitive biomarkers can provide a detailed and more accurate fingerprint of the patient's disease state.

Recently, interest in small noncoding RNAs (sncRNAs) has begun increasing not only because they represent the vast majority of the human transcriptome but also because they have been associated with several pathological conditions, such as cancer, cardiovascular disease and diabetes mellitus.

SncRNAs have been demonstrated to cross the membrane barrier, propagating their information between adjacent and distant cells. Indeed, circulating sncRNAs have been described in different human body fluids, including blood, serum/plasma, urine, and breast milk. Circulating sncRNAs are found to be stable and detectable in body fluids, even though these environments contain high amounts of RNases. Furthermore, some plasma sncRNAs are also stable at different range of pH, at room temperature, or after freezing and thawing cycles. These features make circulating sncRNAs suitable as biomarkers for for diagnostic and prognostic applications or therapeutics (75).

Several sncRNAs have been proposed as potential biomarkers in diabetes and its long-term complications. In particular, microRNAs have been proposed as biomarkers that discriminate for type 1 diabetes mellitus. For istance, some studies demonstrated that the expression of *miR-25-3p* and *miR-320c* are increased in the serum of new-onset T1DM subjects, while the expression of *miR-375* correlates with the level of beta-cell death in new-

onset patients. Furthermore, the level of *miR-574* correlated with autoantibodies in T1DM subjects, although decreased plasma *miR-574* expression has been linked to diabetic nephropathy and T2DM. Indeed, several microRNAs are well known to be related to many common risk factors of diabetes (76).

miR-126 is one of the most frequently investigated miRNAs in diabetes mellitus and its complication. It is highly enriched in endothelial cells and in platelets and plays a key role in endothelial homeostasis, in maintaining vascular integrity, in angiogenesis and in wound repair. Since endothelial activation and inflammation are hallmarks of micro- and macrovascular complications in diabetes, loss of miR-126 was considered predictor as well as risk estimation/classification marker not only for early diabetes but also for endothelial dysfunctions due to diabetes. Our previous study also contributed to these foundings (77). Furthermore, this miRNA concentration negatively correlated with HbA1c levels, suggesting a damaging effect driven by long-term high plasma glucose. Decreased levels of miR-126 are also associated with reduced response to VEGF (vascular endothelial growth factor) and endothelial dysfunction: when released by EC, miR-126 modulates VEGF responsiveness, thus contributing to vascular protection in a paracrine manner. It was demonstrated that miR-126 targets SPRED1 (Sprouty-related, EVH1 domain-containing protein) and PIK3R2 (phosphoinositol-3 kinase regulatory subunit 2), negative repressor of VEGF pathway. In particular, as VEGF is a crucial mediator in diabetic nephropathy, miR-126 could be helpful also in predicting this type of complication. Furthermore, several studies showed and confirmed that reduced circulating levels of miR-126 were observed, and correlated to peripheral artery disease in T2D. Jansen et al. found that loss of miR-126 is related to CAD risk (78). Unlike T2D, the role of miR-126 in T1D is not yet fully clarified although the analysis of blood and urine samples of T1D patients confirmed lower miR-126 levels in urine T1D compared to controls

Other microRNAs are also related to several vascular complications of diabetes.

MiR-21 was initially recognized as a profibrotic miRNA in cardiovascular diseases. Its upregulation was proposed as useful biomarker for already existent fibrotic remodeling known to induce fibrosis in many organs including heart and kidney, since involved in endothelial-to-mesenchymal transition. Recent studies showed that MiR-21 was upregulated both in plasma and urine samples of pediatric T1D patients. Furthermore, the positive correlation emerged in urine samples between miR-21 and the inflammatory C-reactive protein (CRP) suggesting the presence of ongoing inflammatory events in the kidney of T1D patients. Olivieri et al. confirmed higher plasma levels of miR-21 also in T2DM patients with cardiovascular complications (79).

MiR-29 is another relevant miRNA involved in diabetes and its complications. MiR-29 family is composed by miR-29a, miR-29b, and miR-29c, sharing the same seed sequence. The most important function of miR-29 consists of its protective role in fibrotic disease, although an increase in miR-29 levels is found in the serum of T1D children and adult patients with T2DM. Both hyperglycemia and pro-inflammatory cytokines, the hallmarks of DM, upregulated the expression of miR-29 family miRNAs. Furthermore, focused studies on miR-29 family proposed miR-29 as biomarker for atherosclerosis in T2D patients. Furthermore, urinary miR-29a was significantly increased in patients with high albuminuria than in normo-albuminuria suggesting that it is also involved in nephropathy (80).

This miRNA also appears to play an important role in vascular calcification regulating the activity of both osteoblasts and osteoclasts. Disruption of the fine-tuning of these miRNA family members is not only associated with vascular calcification but also with arterial stiffening, in fact, miR-29b correlated with carotid intima-media thickness in T2D patients. In contrast, the main target of miR-29 is a disintegrin and metalloproteinase with thrombospondin motifs-7 (ADAMTS-7). ADAMTS-7 is downregulated by

miR-29 and this results in reduced activity of BMP-2. The end result is protection against vascular calcification and preservation of arterial elasticity.(81) However, others reported that miR-29 promotes vascular calcification through the downregulation of elastin production in turn associated with the transition of VSMCs to an osteogenic phenotype and with augmented calcium deposition in the vascular wall (82). Further studies are necessary to clarify the established role of this miRNA in CV pathway (81).

Other miRNAs have been identified to be dysregulated in patients with calcification-related diseases. *miR-223*, a microRNA physiologically involved in the bone formation process, have been positively associated with Elevated inorganic phosphate concentrations in turn associated with increased risk for vascular calcification, suggesting a role of this miRNA in vascular calcification (83).

On the other hand, many miRNAs have been identified as protecting against vascular calcification. For instance, the *miR-30 family* has a protecting role not only against vascular calcification but more in general against cardiovascular diseases. In fact, in our previous study, we investigate the protective role of circulating *miR-30c-5p* in particular in the progression of atherosclerosis showing that it is associated with incidence and prevalence of this condition and could be a predictive marker since its downregulation is already present 11 years before the development of carotid plaque. We also demonstrate that it is involved in apoptotic pathway modulating the expression of Caspase 3. Other studies demonstrated that miR 30b and miR-30c target RUNX2, a transcriptor factor that regulates osteocalcin, receptor activator of nuclear factor κ-B ligand (RANKL) and osteopontin, which in turn modulate bone matrix formation and are considered themselves VC biomarkers (84).

Considering the canonical biological markers of CV previously described, it is interesting to note that *miR-297a* may regulate the calcification process via suppression of fibroblast growth factor 23 (FGF23) or the reduced bioavailability of *miR-143* in cells undergoing inorganic phosphate-

induced calcification results in increased expression of *platelet-derived growth factor* (PDGF), which is associated with the propagation of vascular calcification. This miRNA also targets mediators intensively secreted during calcification as osterix and Smad1, higher level of miR-32 was detected in the plasma of patients with coronary artery calcification (85).

Regarding other sncRNA, only a few studies have been reported about the role of circulating piRNAs in metabolic diseases. For instance, the over-expression of two piRNAs (DQ732700 and DQ746748) interferes with the generation of metabolic factors coupling glucose sensing to insulin release providing initial evidence for an involvement of piRNAs in the control of beta-cell functions under both physiological and pathological conditions(63,86).

On the other hand, specific tsRNAs were also found in biological fluids such as saliva, tears, urine and breast milk. Although connections between tsRNA function and human health remain largely descriptive, several studies described the interaction of tRNA derivatives under various environmental stresses. For instance, during acute inflammation, increased levels of tsRNAs could be detected in the circulatory system suggesting that these molecules may act as information carriers and signaling messengers. For istance, mature mouse sperm contain high levels of tsRNAs influencing epigenetic mechanisms in the fertilized zygote (86). Specifically, in vivo, in mouse model the modulation of tsRNA in response to diet manipulation leading to metabolic changes including insulin resistance and glucose intolerance in the offsprings. Interestingly, offspring born from mice fertilized by sperm with high concentrations of tRNA fragments displayed a higher incidence of glucose metabolism disorders Futhermore, the 5'-tRNA^{Gln} fragments could mediate TRMT10A deficiency-induced oxidative stress and beta-cell apoptosis. In addition, paternal physical exercise appeared to influence the abundance of small RNAs in sperm and their transmission of 'metabolic memory' into the next generation (87).

However, most of these conclusions regarding piRNAs and tsRNAs have been made through association, using classical genetic animal knockout models for processing and modification systems. Therefore, solid functional proof using actual patient-derived material, which would allow connecting the observed changes in sncRNAs abundance and identity with human syndromes is still largely lacking.

2.3.1 Transport mechanisms of circulating sncRNAs

Circulating sncRNAs are present in most biological fluids, relatively stable, and hold great potential for disease biomarkers and novel therapeutics. Circulating miRNAs are transported by extracellular vescicles (EV) which are membrane-derived vesicles such as exosomes and microparticles, apoptoticc bodies, and by the association to RNA-binding proteins, such as nucleophosmin, Ago2 (Argonaute protein 2), or lipoprotein complexes like high-density lipoprotein.

Protected from ribonucleases by their carriers, sncRNAs are delivered to recipient cells modulating the expression of genes and altering cellular phenotype (88),(75).

2.3.2 Extracellular vescicles (EV) as carrier of sncRNAs

EVs are highly heterogeneous structures that differ in size, biochemical content, and by their biogenesis and secretory mechanisms.

Current nomenclature distinguishes different populations of EVs: *exosomes* which are small vesicles (30–100 nm) that originate from intracellular endosomes and are released by fusion of multivesicular bodies with the plasma membrane; *microvesicles/ectosomes* which are generally larger (100–1000 nm) and originate from budding and blebbing of the plasma membrane; *apoptotic bodies* which are the largest class of extracellular vesicles (500–2000 nm) released from cells during apoptosis; and *lipoproteins,* namely high-density lipoproteins (HDL) and low-density lipoproteins (LDL), which

are both highly abundant in plasma. Whereas exosomes and MPs are composed of a bilayer-phospholipid shell and hydrophilic core, lipoproteins consist of a single layer of lipids, a hydrophobic core, and are defined by specific structure-function apolipoproteins. Futhermore, biophysical studies suggest that miRNAs could be also associated with protein complexes 50-300 kDa in size, which includes AGO2 as well as other ribonucleoprotein in and out of membrane-derived vesicles.

All these extracellular vesicles serve as carriers for sncRNAs and seem to be the main source of plasma sncRNAs (88).

scnRNA-based intercellular communication is composed of three critical processes. First, scnRNAs must be selectively and actively secreted from cells and packaged into appropriate carriers. Second, scnRNAs must be protected from circulating RNAses and transferred to targeted or receptor-specific recipient cells. Third and most importantly, miRNAs must retain the ability to recognize and repress mRNA targets within recipient cells.

This specific sorting and packing mechanisms is not completely understood, although several studies suggest that it is regulated by specific sequence motifs, posttranscriptional modifications, or subcellular localization.

Extracellular vesicles and their sncRNA content can be taken up by recipient cells, enabling cell-to-cell communication. To propagate their RNAderived information, vesicle fuse with the membrane of target cells, enter the cell by endocytosis or remain attached to the plasma membrane activating specific signaling pathways.

Recently it has been investigated the role of the EV- miRNA signature in physiophatological processes. For example, and some evidences demonstrate that isolated EV from the plasma of T1DM subjects could serve as a potential source of biomarkers to early diagnose, disease progression, and reaction of the autoimmune process in T1DM. Several other miRNAs were highlighted to be predictive of diabetic complications. Jansen et al. showed that endothelial cells were the major cell sources of MPs containing miR-126

and miR-26a, and hyperglycemia reduces the packaging of these miRNAs into EV. Furthermore, endothelial apoptotic bodies can convey miR-126 to atherosclerotic lesions, demonstrating unique paracrine-signaling function for miRNA, during atherosclerosis, through EVs(76).

A recent report provided evidence that miRNA-containing vesicles regulate intercellular communication between endothelial cells and SMCs by selective packaging of regulators of SMC phenotype: miR-143/145 in endothelial cell-derived vesicles are transported to SMCs, in the vessel wall.

Other miRNAs (miRNAs 30, 125-b, 143, 145 and 155) released by EV into recipient cells regulate the expression of a specific set of osteogenic genes such as Smad1, RUNX-2, ALP and osterix(89). In addition to these findings, un abnormal concentration of these miRNAs released by EVs induce a shift in calcium and MAPK signaling pathways implicated in SMC-mediated calcification (89).

Even through the major part of the studies concerning EV is focused on their content in miRNAs, recently evidence confirmed the presence of other classes of sncRNAs in circulating EV. For instance, the comparison of cellular and vesicle-borne tsRNAs in the immune system showed that immune cells contained exclusively 30–35 nt-long tsRNAs while extracellular vesicles carried 40–50 nt-long tsRNAs. These combined observations suggested that specific tsRNAs could serve as signaling molecules in the blood and lymphatic circulatory systems. Furthermore, metabolic labeling revealed that tsRNAs entered maturing sperm through micro-vesicles (called epididymosomes), which are secreted from somatic cells lining the epididymis (63).

Summarizing, these foundings suggest that an easily available non-invasive analysis of sncRNAs contained in EV from biological samples such as plasma or urine represents a interesting source of peculiar information related to human diseases.

3. Extracellular Vescicles

3.1 Extracellular vesicles in cell to cell communication

EV release is stimulated via multiple physiological and pathological conditions, making themselves potential diagnostic biomarkers for monitoring various diseases, regardless of their content in sncRNAs. Physiological conditions, such as shear stress, cellular activation or apoptosis normally induce ther release of EV. In fact, EV are detected in a number of biological fluids, including peripheral blood, urine, saliva, synovial fluid, seminal fluid, nasal secretions, tears, vitreous humor, cerebrospinal fluid and breast milk. Circulating EV levels per se has been shown to be associated with various cardiovascular and metabolic disorders, including atherosclerosis and diabetes mellitus(76) .

EVs are structures consisting of fluid surrounded by a phospholipidic bilayer, originated by mother cell membranes and contain a large variety of lipids and proteins. In addition, EVs contain a soluble interior cargo composed by proteins and genetic material (mRNAs and micro RNAs. During EVs generation, specific proteins may be included or excluded from the cell membrane, thus surface protein expression can be not identical to their parental cells.

EVs were initially precipitated from platelet-free plasma although for many years they were considered inert cellular debris. EVs are nowadays recognized as a heterogeneous population of circulating small vesicles originating from almost all cell types.

EVs classification is based on their different sizes and biogenesis in “Microparticles” (MPs), “exosomes” and “apoptotic bodies”. Most exosomes express proteins such as tetraspanins (CD9, CD63, and CD81), Alix, flotillin, TSG101 and Rab5. The enrichment in cholesterol, ceramide, sphingolipids and raft-associated phosphoglycerides, provides an additional tracking opportunity for exosomes characterization. EVs shedding is highly influenced by intracellular elements such as calcium, that affects membrane

phospholipid distribution through specific enzymes such as flippase, floppase, and scramblase.

Cell activation and apoptosis, along with an increase in cytosolic calcium, alter the normal distribution of phospholipids in the plasma membrane, due to inhibition of *flippase* activity, with a consequently increased phosphatidylserine (PS) exposure on the outer membrane. EVs represent a novel mechanism through which cells exchange genetic information and are able to induce epigenetic changes of neighboring cells by horizontal transfer of RNA (88).

3.1.1 Microparticles and their singular features

Microparticles (MPs) were first described as "platelet dust" in the early 1960s[1], and were assumed to be biologically nonsignificant shortly after their discovery. In the recent years, MPs are now receiving great attention for their biological role and as potential biomarkers of several diseases.

Membrane glycoproteins, distinctive of the parental cells, allow a fine identification of their origin. The establishment of a set of EVs markers, indicative of their cell or tissue origin, could be useful for the quantification of specific vesicle subsets in biological samples and their potential disease correlation.

This issue has been especially unraveled for microparticles, which among extracellular vesicles is the only class that maintains this characteristic feature: besides the membrane glycoproteins externalization which allows microparticles identification, additionally, they express specific protein markers that define the cell origin (88).

To characterize the cellular origin of MPs in peripheral blood, the most common approach is to stain MPs with fluorescently-labeled antibody directed against antigens of parental cells: glycophorin A (CD235a) for blood cells and erythrocyte-derived MPs; CD45 and CD8 label lymphocytes-derived MPs (LMP); CD62E, CD144 and CD146 for endothelial-derived MPs (EMP); CD62P, CD41 and CD42 for platelets -derived MPs (PMP);

3.2 Microparticles in Diabetes and Its vascular complications

Pathological remodeling of the vasculature involves an intricate and dynamic interaction between vascular cells (endothelial cells, smooth muscle cells, and adventitial cells), blood cells (platelets, leukocytes), and their direct microenvironment. In the next paragraphs, the contribution of each type of cell and their EV in diabetes and its long term complication such as atherosclerosis and VC is further described.

3.2.1 Endothelial cell-derived MPs (EMP)

The endothelium acts as a selective barrier in the continuous exchange of molecules between blood and tissues. Vascular endothelial cells (ECs) are largely involved in the regulation of normal vascular tone and permeability, homeostasis maintenance, coagulation/fibrinolysis balance, the composition of subendothelial matrix, leukocytic diapedesis and thrombogenesis prevention. A pathological event such as dyslipidemia, hyperglycemia or inflammation occurring cell activation thus endothelial dysfunction. Dysfunctional EC release MPs, vasoactive substances and chemotactic factors altogether contribute to the initiation of inflammatory response and to eventual atherogenic development. Besides activated EC, apoptotic EC may also release EMPs with a different surface immunophenotype. In detail, activated cell-derived MPs express a high amount of CD62E, while apoptotic EMPs are mainly Annexin V+. An elevated ratio of annexinV+ EMPs to CD62E+ EMPs reflects an impaired immune phenotype of EMPs and allows to diagnose through a specific pattern of EMPs, the origin and degree of endothelial dysfunction in dysmetabolic disorders (76).

EMPs play a remarkable role in coagulation, inflammation, endothelial function, and angiogenesis and thus disturb the vascular homeostasis, contributing to the progression of vascular diseases. In fact, elevated levels of circulating EMPs were found in plasma from patients with vascular diseases and atherosclerosis.

3.2.2 Platelets derived MPs (PMP)

EVs from platelets are released when platelets attach to the vessel wall and are involved in several processes in the human body, such as coagulation and atherosclerosis. PMP are distinguished through the detection of surface molecules such as CD62P, LAMP-1, CLEC-2, and GPVI. Since EVs express phospholipids on their surface, they are capable of binding (activated) coagulation factors. Interestingly, their coagulation activity is 50–100 times higher compared to activated platelets. In fact, a genetic disorder that is associated with deficient EV formation by platelets leads to bleeding. This suggests that the promotion of coagulation by EVs is an important physiological mechanism (90).

Besides the involvement of platelet-derived EVs in the coagulation process, PMP have crucial roles in different biological functions: hemostasis, host defense, response to injury, and immune response. In fact, they retain many properties of their parent cells, such as the presence of surface-specific antigens, the ability to deposit chemokines to the vessel wall and to confer inflammatory signals to distal sites.

PMP have been shown to influence vascular cells (endothelial cells and smooth muscle cells) and leukocytes, thereby changing their phenotype and function. When isolated PMP are incubated with monocytes, they bind to monocytes and since PMP are rich in inflammatory molecules (e.g., CD40L) they can adhere to leukocytes by CD62P – PSGL-1 interactions and transport pro-inflammatory signals (91).

Although platelets do not make contact with VSMCs under healthy conditions, it might occur after vascular damage leading to changes in proliferation, migration, marker expression and phenotype of VSMCs, and so PMP might alter the behavior of surrounding cells. Taken together, PMP influence both phenotype and behavior of leukocytes and vascular cells, thus are important initiators and propagators in vascular remodeling and downstream processes, such as calcification.

3.2.3 Macrophage-Derived Vesicles

Atherosclerosis creates moderate hypoxia (2% oxygen) for local cells and leads to activation of pro-inflammatory responses. Pro-inflammatory macrophages secrete elastolytic cathepsins and collagen-degrading MMPs (e.g., MMP-2 and -9). This process lead to proteolytic extracellular matrix degradation and remodeling which cause atherosclerotic plaque instability and rupture, the leading cause of cardiovascular morbidity. Inflammation precedes and may serve as a requisite step for the onset of both atherosclerotic and calcification.

Macrophages can directly contribute to cardiovascular calcification through release of calcifying EVs in a hyperphosphatemic milieu. In EVs released by macrophages, calcium mineral nucleates on complexes containing S100A9, a pro-inflammatory and pro-thrombotic factor , PS, and annexin V on the EV membrane. Accumulation and aggregation of these EVs results in mineral growth within atherosclerotic plaques (92).

3.2.4 Matrix Vesicles and calcified Vesicles derived from vascular smooth muscle cells

SMC-derived EVs are the most studied type of calcifying EVs in cardiovascular tissues. Vascular smooth muscle cells (VSMCs) are the most abundant cell source of the vasculature. Their role is central to vessel dilation and constriction as well as vessel remodeling. VSMCs produce components of the vascular extracellular matrix (ECM), therefore altering the composition of connective tissue and can increase the number of VSMCs present in the vasculature by proliferating. VSMCs are commonly considered to be heterogeneous, having either *contractile* or *non-contractile* (*synthetic*) phenotype.

In *contractile* phenotype VSMCs contract and relax to enable blood flow around the body. in this state, they express highly VSMC-specific markers for contractility such as SM-αA, calponin, and SM22α. These cells have low motility, hence decreased cellular migration is observed, as well as

decreased levels of proliferation. Under physiological conditions, most VSMCS showed contractile phenotype actively secreting Matrix Vesicles (MVs) to regulate microenvironment. MVs are a subgroup of EVs, which are coated in double membranes and consist of phosphatidylserine and annexin but also contain endogenous calcification inhibitors such as vitamin K - dependent matrix GLA protein (MGP) and circulating fetuin-A (93).

When *synthetic*, VSMCs exhibit a marked decrease in expression for VSMC-specific contractility markers, but express more highly markers for matrix metalloproteinase, collagenase, osteopontin and an increase in production of EVs (90).

Phenotype switching enables VSMCs to maintain blood flow as well as support the vascular niche. During vessel repair, migration and proliferation of VSMCs are necessary. Terminal differentiation of VSMCs is not a definitive end and it is possible to switch between phenotypes depending on the demand of the vascular niche. Contractile VSMCs are generally referred to as quiescent differentiated cells, whereas the synthetic state is associated with plasticity and a sort of dedifferentiated state of VSMCs.

Smooth muscle cells and osteoblasts share similar mesenchymal origins and under pathological stresses, SMCs can exhibit an osteoblast-like phenotype. In a hyperphosphatemic environment or inflammation-driven atherosclerosis, vascular SMCs upregulate expression of osteogenic differentiation genes and release EVs enriched with pro-calcific factors.

The role of EVs released by VSMCs is significant in VSMC phenotype switching and calcification. VSMCs have been found to release a variety of EVs when in either synthetic or osteogenic phenotype. Furthermore, EVs share similarity to osteoblast EVs, having calcium-binding capacity and osteoblast-like ECM production. However, under pathological conditions, certain vesicles acquire calcification potential. In fact under Long-term stress and mineral imbalance, VSMCs in synthetic phenotype, promote the release of MVs and switch into a calcified state.

Calcified EVs released by VSMCs are the smallest molecules to form microcalcification. It is revealed that SMC-derived calcifying EVs tend to aggregate and form microcalcifications in areas with sparse collagen when released into the extracellular matrix (ECM). Large calcification formed by the accumulation of microcalcification gradually create mature minerals.(90) These observations indicate a role for EVs in the formation and progression of cardiovascular calcification.

One major challenge in EV research is to distinguish between different EV populations, such as calcifying EVs, and MVs. Annexins present on calcifying EVs play a dual role of Ca2+ uptake and counteracting the calcification inhibitory activity of fetuin-A during ectopic mineralization. calcifying EVs express high level of annexin A5 .The precise function of annexins in calcification has not been fully unraveled. Increases of annexin A2, annexin A5, and alkaline phosphatase co-localisation are proportional to decreases in fetuin-A expression within in vitro VSMC calcification models.

Interestly, prothrombin (PT) contains a Gla domain. It has been recently demonstrated that production of calcifying VSMC-derived EVs can be inhibited by PT interaction. The Gla domain of PT interacts with the surface of EVs, preventing nucleation sites for calcification. Furthermore, circulating levels of PT are reduced in patients with vascular calcification. Accordingly, in the absence of MGP, VSMC-derived EVs act to induce calcification, suggesting a potentially novel role for inhibition of calcification via PT-EV interactions.

3.2.5 Mesenchymal Stem Cells as Perivascular Progenitors

During vascular damage, loss of VSMCs attracts perivascular Mesenchymal Stem Cells (MSCs) from the adventitia, which are a source of VSMCs and contribute to repair after vascular injury. Indeed, the presence of a specialized progenitor population of VSMCs localized in the adventitia of muscular arteries has been suggested by several groups.

\The perivascular niche or *pericytes* are present at intervals along microcapillaries, and pericyte-like cells are also located in the adventitia of large arteries. A pericyte is defined as mesenchymal stem cell (MSC) that is completely or partially embedded in the endothelial basement membrane.

It was first described many years ago that pericytes have an osteogenic potential and subsequently pericyte-like cells with osteogenic capacity were isolated from VSMCs nodules of human aorta. A decade ago it has been reported that Sca1+/CD34+/PDGFRβ+ cells that reside in the adventitia of arteries possess a differentiation capacity towards smooth muscle cells and osteoblasts in vitro (90). Thus, the presence of adventitial MSC-like cells with osteogenic and myogenic potential until recently the involvement of these MSC-like pericytes in cardiovascular disease development was discussed.

Adventitial progenitors have been found to differentiate into osteoblasts, chondrocytes, adipocytes, macrophages as well as VSMCs. This has led to the hypothesis that adventitial progenitor cells are master regulators of the vascular niche. When progenitor dysfunction occurs, differentiation of VSMCs to an osteoblastic, chondrogenic or macrophage-like arise.

It was recently revealed that the Hedgehog transcriptional activator Gli1 specifically labels perivascular MSC-like cells. Gli1+ cells reside in the pericyte niche with direct contact with endothelial cells of the microvasculature and in the adventitia of large arteries (94). Gli1+ cells possess all criteria that have been used to define a MSCs, including surface marker expression, tri-lineage differentiation and plastic adherence.

Futhermore, Gli1+ cells are a major cellular source of myofibroblast in fibrosis of all major organs such as lung, kidney, liver, heart and bone marrow and could be differentiated into calponin+, αSMA+, smoothelin+ VSMCs in vitro. This data indicates that adventitial Gli1+ MSC are indeed progenitors of VSMCs. These studies indicate a great migration of Gli1+ cells into the media and neointima during chronic injury and atherosclerosis.

Multiple co-staining experiments indicated that adventitial Gli1+ cells first differentiated into contractile VSMCs (α-SMA+, calponin+) and then

underwent a phenotypic switching with loss of contractile VSMC markers and acquisition of synthetic VSMC state. Importantly, during vascular calcification, a high percentage of Gli1+-derived cells acquired nuclear expression of the transcription factor Runx2 indicating differentiation into osteoblast-like cells thus, adventitial Gli1+ cells are important progenitors of synthetic VSMCs and osteoblast-like cells in the vascular wall. Adventitial Gli1+ cells can be considered an important therapeutic target in vascular calcification (90).

Thereby, we speculate that these niche of MSCs may also secrete EVs and contribute to vascular calcification.

.

AIM OF THE STUDY

The aim of this study was:

1) to set up a protocol using NGS technology for the identification and quantification of circulating sncRNAs involved in atherosclerotic plaque composition in type 1 diabetic patients (T1DM);

2) Characterize the phenotypes of circulating MPs derived from T1DM, associated with the plaque composition to evaluate the impact of these extracellular vesicles as carrier of specific small non coding RNAs, involved in these pathways.

MATERIAL AND METHODS

Workflow of the study

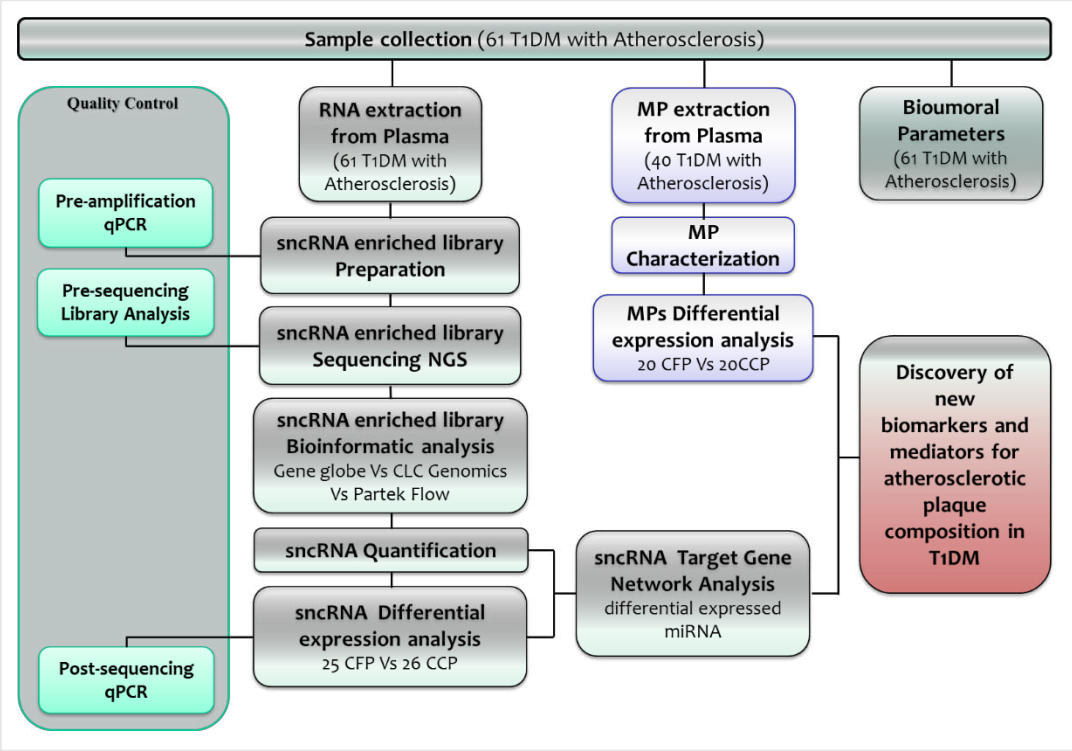

Figure 8: Workflow of the study. *T1DM (Type 1 Diabetes Mellitus); MP (Microparticle); CFP (Carotid Fibrous Plaque); CCP (Carotid Calcified Plaque);*

1. Subjects

This study was performed with the collaboration of the Unit of Metabolic Disease, Department of Medicine-University of Padova and the Center of Center for Biomedical Research on Diabetes and Associated Metabolic Diseases, Department of Endocrinology and Nutrition, University Hospital de la Santa Creu i Sant. 61 subjects with type 1 diabetes were recruited from the diabetic outpatient clinics at University Hospital Germans Trias i Pujol and at University Hospital Arnau de Vilanova in the North-Western region of Spain (Catalonia).

Inclusion criteria were as follows: age >18 years; type 1 diabetes for at least 1 year; normal renal function (estimated glomerular filtration rate (eGFR) >60 mL/1.73mq.min).

Exclusion criteria were: previous cardiovascular diseases, defined as any form of clinical coronary heart disease, stroke or peripheral vascular disease (including any form of diabetic foot disease); and a urine albumin/creatinine excretion ratio >300 mg/g.

This study was carried out in accordance with the International Ethical Guidelines and the principles of the Declaration of Helsinki; Local Ethics Committee of both participating centers approved the protocol (PI11/11 and PI-13-095); all participants signed informed consent forms. Patients filled out a complete lifestyle questionnaire regarding medical history, current therapy, smoking habits, and physical activity.

For each subject, age, sex, body mass index and waist circumference were obtained by standardized methods. Plasma glucose, serum total cholesterol, triglyceride, HDL cholesterol were measured using routine enzymatic methods (95).

For Next generation Sequencing and for microparticles analysis, fasting blood samples were collected into EDTA-containing tubes and centrifuged at 3000g for 10 min. Plasma was stored at -80°C until use.

1.1 Carotid Ultrasound Imaging

The detailed protocol to evaluate the presence of carotid plaques by ultrasound has been previously described (95). Briefly, carotid ultrasonography imaging was performed using a LOGIQ® E9 (General Electric, Wauwatosa, WI, USA) equipped with a 15-MHz linear array probe or a Sequoia 512 (Siemens, North Rhine, Westphalia, Germany) equipped with a 15-MHz linear array probe.

Plaques were identified using B-mode and color Doppler examination in both the longitudinal and transverse planes, to consider circumferential asymmetry. They were defined as a "focal structure that encroaches into the arterial lumen of at least 0.5 mm or 50% of the surrounding carotid intima media thickness value or demonstrates a thickness of 1.5 mm, as measured from the media-adventitia interference to the intima-lumen surface" according to the Mannheim consensus (96).

Further, the LOGIQ E9 ultrasound system had a 3D image acquisition system with a low depth sweep box with a 45◦ angle and a slow acquisition time to scan the volume. Volume acquisition used 3 orthogonal sectional plans (A, B, C) and started with the sectional image (A), which gave a 2D image showing the longitudinal view of the carotid arteries and bulb. Images B and C showed the transverse and horizontal axes, respectively.

The volume sweep was recorded as raw data and used for volume calculations. Volume calculation was made by delineating the plaque contours and with the transverse plane (B) as described previously(97). Atherosclerotic plaques were classified using the well-known five-type classification system based on visual assessment of echogenicity with vessel lumen and adventitia as reference structures: uniformly echolucent, predominantly echolucent, uniformly echogenic, predominantly echogenic and extensively calcified plaques (95).

For the aim of this study, we additionally reclassified individuals into two clinical categories: fibrous (hypoechoic) and calcified (hyperechoic) plaques. The arterial territories explored included the common and internal carotid territories and the bifurcation from the left and right carotid arteries.

All participants in this study underwent the same carotid ultrasound examination, and all measures and ultrasound studies were assessed at each participating hospital by the same researcher.

2. NGS pre-sequencing analysis

2.1 sncRNA Extraction

SncRNAs from plasma samples was extracted using the miRNeasy Serum/plasma" kit (Qiagen, Germany), according to the manufacturer's protocol. This kit combines phenol/guanidine-based lysis of samples and silica-membrane–based purification of sncRNA. Briefly, 200 µl of plasma was lysed with 5 volumes of lysis buffer Qiazol, a monophasic solution of phenol and guanidine thiocyanateand, then incubated with chloroform to separated lysate into aqueous and organic phases by centrifugation. The upper, aqueous phase represents RNA partition then extracted, and ethanol is added to provide appropriate binding conditions for all RNA molecules from approximately 18 nucleotides (nt) upwards. The sample is then loaded into the RNeasy MinEluite spin column, where sncRNAs bind to the membrane and phenol and other contaminants are efficiently washed away. High-quality RNA is then eluted in 40 µl of RNase-free water and stored at -80 ˚C.

2.2 Pre-library amplification Quality Control: house keeping miRNA profiling by qPCR

Before starting the preparation of sncRNA libraries, the quality of blood samples and RNA extraction were tested in order to guarantee the high level of efficiency of NGS. In particular, the presence of retro transcriptase enzyme inhibitors, contaminants or haemolysis were determined using a protocol previously described (84).

Briefly reverse transcription was performed using the miRCURY LNA™ Universal RT (Exiqon, Denmark). Individual miRNAs were detected by CFX500 (Biorad, California, USA) using ExiLENT SYBR® Green master mix and LNA™ primers (Exiqon, Denmark), for hsa-miR-103a-3p as miRNA reference for plasma samples, and hsa-miR-451 as haemolysis control. Then, we used the values of Cq to determine the quality a of the RNA isolation, the cDNA synthesis reaction and the PCR efficiency.

We did not use spike-ins for normalization in biofluid samples (plasma, serum) because this approach does not correct for many aspects of

technical variation (e.g. variation in endogenous RNA content), as reported previously (84).

2.3 sncRNA NGS libraries preparation

Universal cDNA synthesis and library preparation of sncRNAs from plasma samples was obtained using QIAseq® miRNA Library kit (Qiagen, Germany), according to the manufacturer's protocol. The QIAseq miRNA Library Kit has been optimized to prepare sequencing libraries of miRNA and other similarly sized RNAs such as piRNAs and tsRNAs with a 3' hydroxyl group and a 5' phosphate group.

Briefly, in an unbiased reaction, adapters are ligated sequentially to the 3' and 5' ends of sncRNAs. Subsequently, universal cDNA synthesis with UMI assignment, cDNA cleanup, library amplification and library cleanup are performed (fig.9). Each step is futher described below.

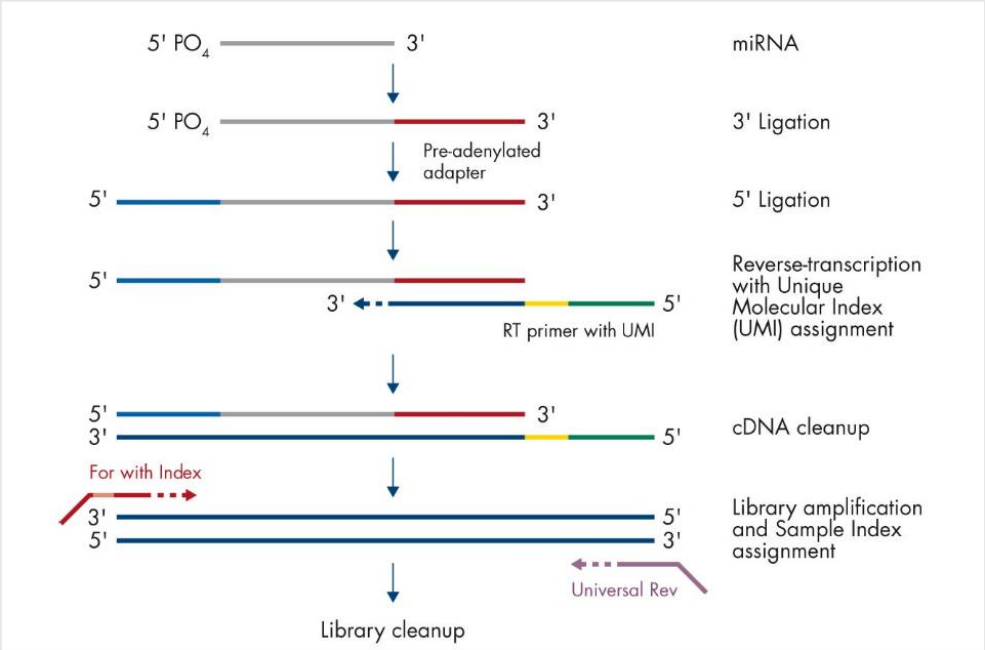

Figure 9: miRNA sequencing library preparation using the QIAseq miRNA Library Kit*. 3' and 5' adapters were ligated to mature miRNAs. The product was reverse-transcribed to cDNA using a reverse transcription (RT) primer with a Unique Molecular Index (UMI). Then, cDNA cleanup was performed and library amplification occurred with indexing forward primers and a universal reverse primer. After final library cleanup, the sncRNA library is then ready for QC and subsequent NGS.*

2.3.1 Adapter ligation

A pre-adenylated DNA adapter was ligated to the 3' ends an RNA adapter was ligated to the 5' end of all sncRNAs. These adapters are highly optimized for efficient ligation as well as prevention of undesired side products.

The manufacturer's protocol does not recommend assessing the concentration of total RNA derived from plasma samples but rather starting with 5 µl of the eluate total RNA. The reaction mix content a specific buffer Ligation Activator and specific enzymes to allow the ligation of the adapters. At first, the 3' pre-adenylated DNA adapter was added incubating the reaction mix for 1 hour at 28°C and for 20 minutes at 68°C. Immediately after chilling, the 5'RNA adapter and their specific reagents were added to the reaction product and incubate at the same temperatures, to allow the ligation.

At the end of this step we obtained fragments with known terminal sequences.

2.3.2 cDNA synthesis and cDNA cleanup

The RT primer binds to a region of the 3' adapter and facilitates conversion of the 3'/5' ligated sncRNAs into cDNA. The reverse transcription (RT) primer contains an integrated Unique Molecular Index (UMI) to assign a UMI to every sncRNA molecule. During reverse transcription, a universal sequence is also added that is recognized by the sample indexing primers during library amplification. The UMIs into the reverse transcription process enable unbiased and accurate sncRNome-wide quantification by NGS.

NGS analysis is traditionally based on the number of reads, but reads can be misleading and sequencing bias can result in an overestimation of sncRNA expression. At low input, this effect is amplified, which is why biofluid experiments or other experiments with low input can be so difficult to execute successfully. UMI technology adds molecular tags to each sncRNA molecule to eliminate this bias. For example, there are three copies of miRNA 1 and two copies of miRNA 2 in the sample X, and the total

number of unique tags is five in the ratio 3:2 for these miRNAs. The raw reads following sequencing may not reflect a 3:2 ratio due to sequencing bias or PCR error, but the UMI count ensures that the data reflects the reality in the sample (fig. 10).

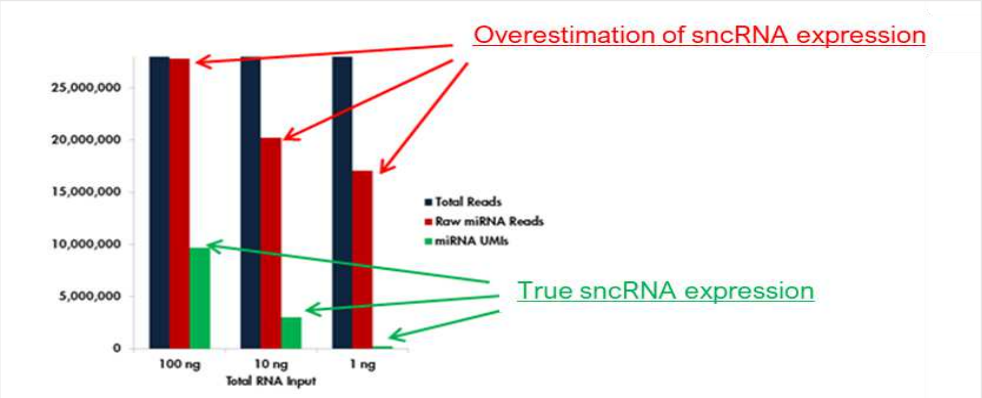

Figure 10: Effect of Unique Molecular Index (UMI) count on sncRNA expression by NGS analysis .

After reverse transcription, a cleanup of the cDNA was performed using a streamlined magnetic bead-based method, in order to enrich the samples with cDNA fragments that contain the adapter and remove the exceeded reagents.

2.3.3 Libraries amplification and cleanup

The library amplification step provides for the use a universal reverse primer and a specific forward primer that contains a barcode to assign each sample a unique index. This Barcode is then recognize during the sequencing step to collect the sequences derived from the same sample. The un-biased amplification of all sncRNAs in a single reaction ensures that sufficient target is present for next-generation sequencing. A HotStartTaq DNA polymerase drives the amplification of the libraries and is activated by this heating step (95°C for 15 minutes) following by 22 cycles of denaturation, annealing and estimation steps . After library amplification, a cleanup of the sncRNA library is performed using a streamlined magnetic bead-based method. This step allows to enrich the library with specific size RNA and to remove eventually contaminants, aqdapter dimers and inhibitors. This important and delicate procedure could strongly influence the efficiency and the results.

2.4 NGS Library pre-sequencing Quality Control (QC)

2.4.1 sncRNA library QC by High Sensitivity DNA electrophoresis

sncRNA Libraries were analized by LabChip GX Touch Nucleic Acid Analyzer (PerkinElmer, Massachusetts, USA) using HT DNA 5K/RNA LABCHIP kit (D-MARK Biosciences, Canada, USA) according to the manufacturer's instructions. A typical electropherogram obtained from sncRNA library shows a peak between 170-180 bp corresponding to miRNA-sized library and a smaller peak approximately of 188 bp corresponding to a piRNA-sized library.

2.4.2 sncRNA library QC by qPCR.

The analysis of quality sncRNA libraries was also performed by qPCR using three different primers: the first, called NGS 3C Primer, for assessing the performance of 3' adapter ligation; the second, NGS 5C Primer, for assessing the performance of 5' adapter ligation and the third, NGS RTC Primer, for the performance of reverse transcription reaction. The analysis of amplification curve of all the three different qPCR reactions should give a threshold cycle (Cq) less than 28, indicating a correct library preparation, Cq values for some of all the PCR controls greater than 28 suggest a poor library preparation.

2.5 sncRNA Library quantification by fluorimetric spectroscopy

The Qubit dsDNA HS assay is a fluorometric assay that uses dsDNA-binding dyes in order to determine accurately NGS library concentration. 2 µl of sncRNA Library were loaded in a Qubit® 3.0 Fluorimeter (Termo Fisher scientific, Massachusetts, USA). Briefly, Qubit working solution was prepared mixing Qubit dsDNA reagent with Qubit Buffer in 1:200 ratio. After calibration with Qubit standard 1 and 2 incubating 10 µl with Qubit working solution, 2 µl of each sncRNA Focused Library were incubated with Qubit working solution to obtain the concentration of the samples in ng/µl. The

molarity of each sncRNA Focused Library (in nM) was determined using the following equation:

(X ng/µl)(106)/(112450) = Y nM

A pool of libraries to sequence in multiplexing was generated in equimolar amounts (4 nM) by dilution with RNAase free water of each sample to reach the final concentration as recommended by Illumina. (https://support.illumina.com/help/pooling-calculator/pooling-calculator.htm) Finally, pool of libraries was measured by Qubit® 3.0 Fluorimeter to verify the correct final concentration

3. Next Generation Sequencing on sncRNA libraries:

SncRNA libraries were sequenced using MiSeq Illumina Platform following manufacturer's instructions. Miseq is a Next Generation Sequencing system with a sequencing by synthesis technology (SBS).

SBS uses four fluorescently labelled nucleotides to sequence on a flow cell surface in parallel, the tens of millions of clusters obtained from bridge amplification: fragments in each cluster are linearized by cleavage within one adaptor sequence and denatured, generating single-stranded template for sequencing. During each sequencing cycle, a single labelled deoxynucleoside triphosphate (dNTP) is added to the nucleic acid chain. The nucleotide label serves as a terminator for polymerization and after each dNTP incorporation; the fluorescent dye is imaged to identify the base and then enzymatically cleaved to allow incorporation of the next nucleotide.

Sequencing fragments are immobilized on a flow cell surface designed to facilitate access to enzymes ensuring high stability of surface bound template and low non-specific binding of fluorescently labelled nucleotides.

Flow cell with v3 chemistry and 150 cycles (Mi Seq reagent kit v3) was used to performed the sequencing in single reads of 75 pb fragments for sncRNA library. Since this flow cell allows to generate around 30 million reads per run, 9 samples per run were loaded to guarantee almost 3 million reads per sample. Furthermore, to verify the accuracy and reproducibility of the results some replicates were included in the study.

DNA fragments from the pool of 9 libraries at 4nM were denatured with 0.2N NaOH into single strands and then further diluted to reach a final concentration of 20 pM. This concentration is estimate to generate an optimum cluster density of 1200-1400 k/mm2, to avoid the phenomenon called "*overclustering*" in which the instrument is unable to discriminate the brightness of the reads due to their exceeded abundant.

An excessive cluster density (overclustering) or a low cluster density (underclustering) do not enable the instrument to properly recognize and count the reads obtained with precise estimate. Overclustering increases signal brightness, which makes finding the focal plane difficult and causes

poor template generation, poor cluster registration, and other image analysis issues. These issues negatively affect sequencing data. In fact when overclustering is extreme, image focusing can fail and terminate the run at any cycle (Run failure).

3.1 NGS quality control

Illumina Platforms provide several internal quality control during the sequencing run such as the Phred Q scores. Q score reveal how much of the data from a given run is usable in a resequencing or assembly experiment. Low Q scores can lead to increased false-positive variant calls, resulting in inaccurate conclusions. The process of generating a Phred quality scoring scheme is largely the same of Sanger sequencing.

Q scores are defined as a property that is logarithmically related to the base calling error probabilities (P):

$$Q = -10 \log10 P$$

For example, if Phred scale assigns a Q score of 30 (Q30) to a base, this is equivalent to the probability of an incorrect base call 1 in 1000 times. This means that the base call accuracy (i.e., the probability of a correct base call) is 99.9%. When sequencing quality reaches Q30, virtually all of the reads will be perfect, having zero errors and ambiguities. This is why Q30 is considered a benchmark for quality in next-generation sequencing (98).

Finally, the data obtained from the sequencer are collected as FastQ files, one for each samples and loaded into bioinformatics tool for the analysis.

4. NGS post sequencing analysis

4.1 sncRNA analysis by Bioinformatic tools.

Expression analysis is crucial for the understanding of small RNA regulation and it is a starting point for genetic functional studies. High-throughput small non-coding RNA sequencing (sncRNA-seq) offers advantages compared to the other methods, specifically by distinguishing very similar small RNA sequences. Its unbiased nature also allows detection of novel sncRNAs. Despite these advantages, there are many bioinformatics challenges in the processing of high-throughput small RNA sequence. The short sequence length makes these sncRNAs difficult to map in large, complex, and repetitive reference genomes, as human genome, and many small RNAs are composed of near-identical family members. In recent years, several bioinformatics tools have been developed to manage the mounting flow of sncRNA-related data, with different method of normalization, such as scaling normalization, Trimmed Mean Method (TMM) in edge R (99), global normalization and DEseq that uses a negative binomial model (100).

In this study, two different bioinformatics tools were compared for evaluating their sensitivity and accuracy in detecting and quantifying sncRNA: Partek Flow (Partek,Missouri, USA) and CLC genomics workbench 12.0.3 (Qiagen, Germany).

These bioinformatics tools provide different specific pipelines for sncRNAs analysis characterized by a first part that includes adapter trimming and alignment of the sequences for the quantification of sncRNAs, and a second part, which includes normalization and differential expression analysis.

4.1.1 sncRNA quantification analysis

The first part is similar for both tools which steps are the following:

- **Upload of data:** Fragment sequences from each sample with a length of 75 bp from NGS were loaded as FastQ files into bioinformatics tool. FASTQ file is a text file that contains the sequence data and each

entry in a FASTQ files consists of 4 lines: a sequence identifier with information about the sequencing run and the cluster; the sequence (the base calls; A, C, T, G and N); and the base call quality scores.

- **Trimming Adapter Sequences:** Adapter sequences should be removed from reads because they interfere with downstream analyses, such as alignment of reads to a reference. The adapters on the 3' ends contain the sites that allow library fragments to attach to the flow cell. Cut-adapt is the tool that searches for the adapter in all reads and removes it.
- **UMI sequences count:** As previously described, the aligned sequences were counted considering the presence of UMI to optimize the quantification.
- **Aligning reads with reference genome:** The goal of read alignment is to map comparatively short sequencing reads efficiently to a large reference genome to identify the 'correct' genomic loci from which the read originated. The Bowtie package enables ultrafast and memory-efficient alignment of large sets of sequencing reads to a reference sequence, such as the human genome (101). In our study, a sequential alignment strategy was used to map on several databases: reference human genome hg38 was used and miRBase v.22.1 was considered as first annotation model. All the sequences recognized in miRBase were collected as mature miRNAs, while sequences do not have a match with miRBase annotated sequences were collected as unmapped and were used for further alignment with databases for other classes of sncRNAs.

4.1.2 Annotation Models

The choice of a correct annotation model as sncRNA database is an important and critical issue since there are several options that are not quality-assured.

- ***miRNA annotation model (miRBase)***

The miRBase database is a searchable database of published miRNA sequences and annotation. Each entry in the miRBase sequence database represents a predicted hairpin portion of a miRNA transcript with the information on the location and sequence of the mature miRNA. Both hairpin and mature sequences are retrieved by name, keyword, references and annotation and all the sequences are also available for download (102).

The latest release of the miRNA database (miRBase Release 22.1, October 2018) downloaded in Partek and CLC Genomics bioinformatics tools, has catalogued 1917 annotated hairpin precursors, and 2654 mature sequences in humans, although the functional importance of many of these miRNA annotations remains to be determined.

After a systematic effort to validate experimentally miRNAs from miRBase version 14, it is estimated that nearly one-third of the tested loci (173 of 564) lacked convincing evidence that they produce authentic miRNAs. Although some of the misannotated miRNAs have been removed from the database during the years, many more have since been added without validation, suggesting that current miRNA database might be substantially inflated. For this reason, the users can now send feedback to report authentic miRNAs from false annotations.

The main criteria to validate authentic miRNAs are: the 5′ homogeneity (although one should be cautious, because some authentic miRNA loci naturally produce alternatively processed isoforms); sequencing reads abundance; phylogenetic conservation; evidence for RNase III-mediated processing such as the loss of miRNA following Drosha or Dicer knockdown; and evidence of Argonaute proteins association.

- ***piRNA annotation model (piRBase)***

In light of the rapidly increasing studies on piRNA, several piRNA related databases, such as piRNABank, piRNAQuest, piRNA cluster database and IsopiRBank, have been generated. However, all these databases are limited for piRNAs sequences and from the number of species. piRBase v1.0

implemented the number of unique piRNA sequences to 173 million, including 21 species (61).

- ***tsRNA annotation model (MINTbase)***

  MINTbase is a repository database that comprises nuclear and mitochondrial tRNA-derived fragments ('tRFs') found in multiple human tissues. MINTbase contains information about 26 531 distinct human tRFs from 11 719 human datasets(103).

4.1.2 sncRNA normalization and Differential Expression Analysis

After the enrichment of aligned sequences with sncRNAs database, read count numbers for sncRNA across samples have to be normalized and several option could be considered for the analysis of the data to compare two or more groups of samples.

- **Filter Reads feature:** Low expression miRNAs (low reads) may be indistinguishable from noise and will decrease the sensitivity of differential expression analysis. For this reason, an option could be considered to filter the data, considering the sncRNAs with a minimum number of reads count by setting a cutoff.
- **Normalization:** All RNA-seq experiments are subject to sources of systematic variation such as library size, transcript length, and G-C content Small RNA-seq experiments are further impacted by the highly non-normal distribution of expression of different small RNAs, particularly miRNAs (104). Often a few miRNAs account for a very large fraction of total reads while the vast majority of miRNAs each contribute a small percentage of reads. Moreover, sample input amounts of extracellular RNA are often extremely limited, increasing the potential for both sampling error and experimental bias. To address these issues, a number of normalization methods have been developed. Although, there is no consensus regarding the optimal normalization method, but it is known that different methods can

result in different results in downstream analysis, particularly differential expression analysis (DE).

Trimmed mean of M-values (TMM) is a scaling method that involves application of a standard linear mathematical operation to each sample. TMM determines a scaling factor, which is the weighted trimmed mean of log expression.

Another general approach to normalization is to preserve the distribution of the data among different data sets such as *DESeq*. In DESeq, a scaling factor for each sample in the dataset is obtained by computing the median of the ratios of each sncRNA in one sample over the geometric mean of that sncRNA across all samples. The same scaling factor is then applied to the read counts for all of the genes in that sample.

For these considerations, two different methods of normalization were compared: DESeq from PArtek and TMM from CLC Genomics.

- **Differential expression analysis (DE):** Finally, there are several statistical model to perform the differential expression analysis of smallRNA seq data and each software provides different options described above

4.2 Partek Flow Software

Partek Flow is a software for analysis from next generation sequencing data of sncRNA, RNA transcriptome and whole genome, exome or targeted panel DNA sequencing. The software allowed managing tasks to customize the workflow providing quality control for alignment, for quantification, and statistical analysis. This tool enables a reserve workstation online and efficient online support. The pipeline generated from the Partek Flow for our study is designed below (fig. 11 and 13).

4.2.1 sncRNA Quantification

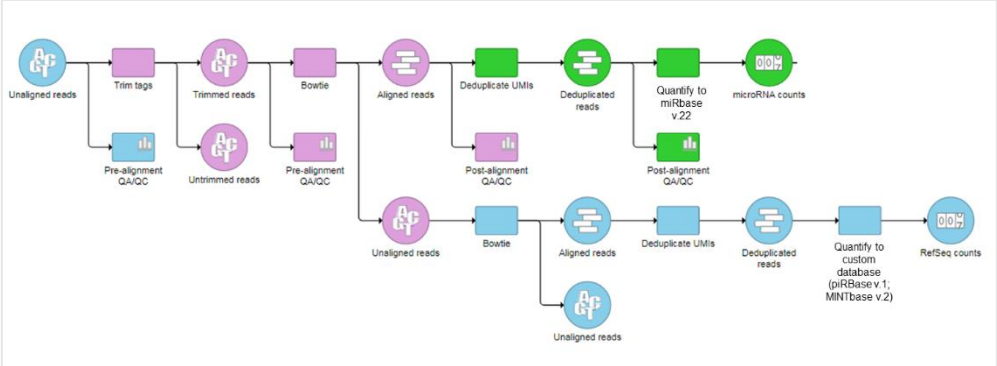

Figure 11: Pipeline of Partek flow: quantification of sncRNA libraries

- **Upload of data:** Unaligned reads from NGS were downloaded as FastQ formats.
- **Trimming Adapter Sequence**: This task (Trim tags) allows to trim the adapter with known sequence at 3' end, retaining only the fragments with the features reported in fig. 12. Sequences with less than 15 pb or without adapter or without UMI are discarded and are not used for the analysis.

Figure 12: structure of a DNA fragment in sncRNA library

- **Align insert sequences:** Bowtie was used for the alignment of the sequences with miRBase v.22.1 database considered as first annotation model, in the human genome (hg38). The sequences

unmapped were collected as unaligned reads for analysis with piRBase v.1 or with MINTbase v.2 for tsRNAs.

- **UMI sequences count:** The "Deduplicated UMIs" task enable to take in to account UMI and optimize the quantification.
- Partek flow also allows performing several optional tasks to evaluate the quality of the data.

4.2.2 sncRNA Differential Expression Analysis

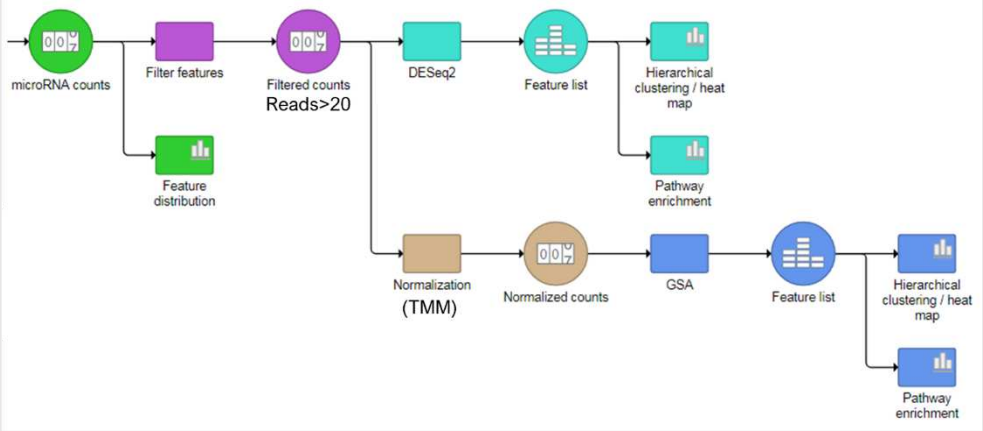

Figure 13: Pipeline of Partek flow: Differential expression Analysis of sncRNA libraries

- **Filter Reads feature.** The sncRNAs with reads count >20 were considered for the analysis while those with lower than 20 reads were discarded.
- **Normalization and differential expression analysis (DE).** Partek flow allows choosing among several normalization methods, in particular, we performed *DESeq2* and *TMM*.

  The *DESeq2* task can be invoked from data nodes directly generated by quantification tasks that contains raw read count values for each feature in each sample and cannot be run on a normalized counts data node because DESeq2 internally corrects for library size. The package DESeq2 provides methods to test for differential expression by use of negative binomial generalized linear models; the estimates of dispersion and logarithmic fold changes incorporate data-driven prior distributions (100).

TMM normalized counts were analyzed with *GSA* task. Gene-specific analysis (GSA) is a statistical model used to test the differential expression of sncRNA in Partek Flow. The goal of GSA is to identify a statistical model that is the best for a specific gene and then use the best model to test for differential expression.

- **Exploratory analysis task:** These options provide to generate a heat map and visualize a pathways enrichment in of the results.

4.3 CLC Genomics Workbench software

CLC Genomics Workbench is a comprehensive analysis package for the analysis and visualization of data from all major next-generation sequencing (NGS) platforms. It supports key next-generation sequencing features within genomics, transcriptomics, and epigenomics research fields. This tool provides quality control, alignment, quantification, statistics, and visualization tasks. The software also allowed managing each task to customize the suggested ready-to-use workflow; indeed, we performed the analysis using the following pipeline. (fig. 14 and 15)

4.3.1 sncRNA Quantification

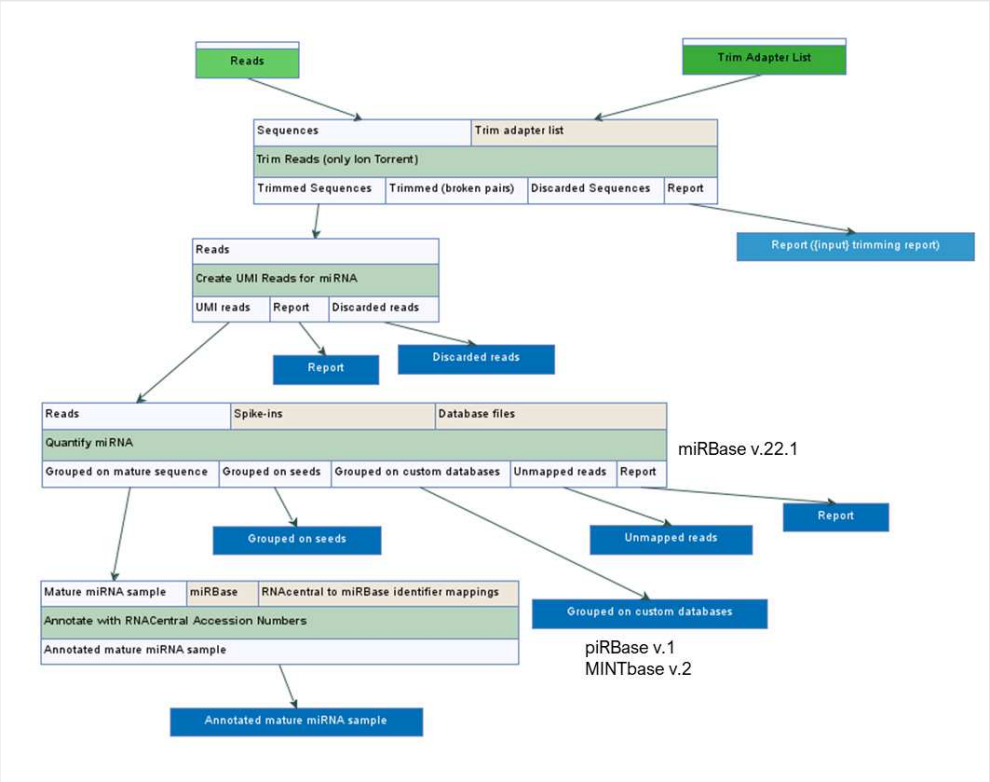

Figure 14: Pipeline of CLC Genomics Workbench-Quantification of sncRNA libraries

- **Upload of data:** Unaligned sequences derived from NGS data were downloaded as FastQ formats.
- **Trim Adapter and UMI sequences count:** Adapter sequence was trimmed and sequences with less than 15 pb or without adapter or without UMI are discarded and are not used for the analysis.

- **Align insert sequences:** The ready-to-use workflow provides the alignment with miRBase v.22.1. The unmapped sequences were aligned with piRBase v.1 and with MINTbase v.2 databases, respectively for piRNA and for tsRNAs.
- ClC Genomics also allows performing several optional tasks to evaluate the quality and the accuracy of the data.

4.3.2 sncRNA Differential Expression Analysis

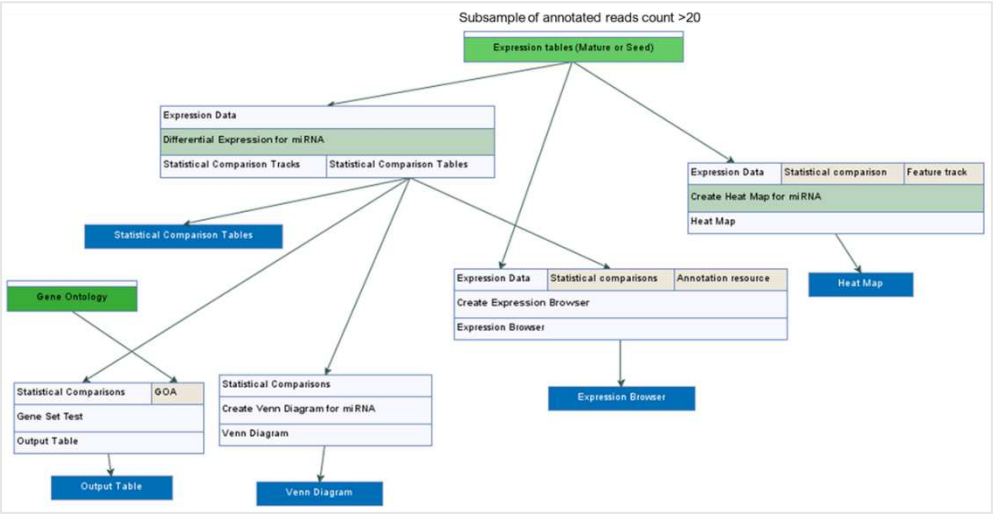

Figure 15: Pipeline of CLC Genomics Workbench- Differential expression Analysis of sncRNAs.

- **Filter Reads Feature:** The sncRNAs with reads count >20 were considered for the analysis creating a subsample collection, sncRNAs with read count lower than 20 were discarded.
- **Normalization and differential expression analysis (DE):** The software enables to choose among several normalization methods, although in the ready-to-use workflow only Trimmed Mean Method (TMM) is set. The differential expression analysis by this software provides a GLM model (Generalized Linear Model) with a negative binomial distribution, similar to EdgeR or DESeq2 (100,105)
- **Exploratory analysis task:** These options provide to generate a heat map and visualize a pathways enrichment in of the results.

4.4 Post- sequencing QC: miRNA profiling by qPCR

2 µl of purified sncRNA were retrotranscripted and PCR real time was performed with Taqman probes. (Termo Fisher scientific, Massachusetts, USA). Briefly reverse transcription was performed using the TaqMan Advanced miRNA cDNA Synthesis Kit which provides a pre-amplification step of the CDNA using universal primers and specific master mix to uniformly increase the amount of cDNA for each target. Individual miRNAs were detected by CFX500 (Biorad, California, USA) using TaqManFast Advanced Master Mix with TaqMan Advanced miRNA assays, for hsa-miR-122-5p, hsa-mir-431-5p and hsa-mir-93-5p, according to the manufacturer's protocol. Mean of Cq values of replicates obtained by qPCR were compared with the reads count result in NGS data for each sample.

4.5 Putative Target Gene for miRNAs Network Analysis

Target genes for miR-39-5p, miR-503-5p, miR-29b-3p, miR-451a, miR-10a-5p, miR-106b-5p and let7d-5p were identified and compared using a bioinformatics tool with online target prediction algorithm, miRWalk (http://zmf.umm.uniheidelberg.de/apps/zmf/ mirwalk2/ index. html). Gene targets for these miRNAs were selected through gene ontology (GO) functional analysis and through ontology biological process (GOBP). To create the visualization summary networks, Cytoscape v3.2.1 was used.

4.6 Statistical analysis

For the miRNA screening study, a sample size calculation was performed to determine the number of samples to assure a statistically significant difference between sncRNA from plasma patients with carotid fibrous or calcified plaques. We performed a power calculation to test whether our sample size could provide enough power to detect a fold change at least 1.4 for circulating miRNAs of expression level between the two groups.

For this aim we calculated that the sample size should be at least of 19 subjects per group to reach a desired power of 80%, standard deviation

estimated at 0.5 and average power with a FDR (false discovery rate) of 10%. Since our experimental design provides 25 subjects with fibrous plaque and 26 subjects with calcified plaque for NGS analysis , our sample size should be large enough to reach the required 1.4 fold change(106).

Continuous variables are expressed as mean ± standard deviation; comparisons between two groups were performed with the Student's t test. To determine the association between studied variables regression analysis were performed. Statistical significance was accepted at $p<0.05$. SPSS ver 25 (IBM_SPSS statistics, Bologna, Italy) and GraphPad Prism ver 8.0.2 (GraphPad software, San Diego , CA, USA) was used.

5. Circulating microparticles Analysis

5.1 Microparticles Characterization

Platelet-poor plasma (PPP) was prepared within 3 h of blood collection by double centrifugation (3000g for 15 min). Microparticles (MPs). MPs derived 40 T1DM patients with fibrous (CFP; n 20) or calcified (CCP; n 20) were isolated from 350 µl of PPP through centrifugation at 18000g for 40 min at 4 °C.

The resulting pellet is the enriched fraction of isolated MPs. MPs were resuspended in 350 µl of phosphate-bufered saline (PBS, Sigma, USA) and stored at −80 °C until use. Samples, analysed only after a single freeze–thaw cycle, were thawed by incubation for 5 min in a water bath at 37 °C immediately before assay.

All assays were performed on flow cytometer CytoFLEX (Beckman Coulter, Miami Florida). The MPs gate was established using a blend of mono-dispersed fluorescent beads of three diameters (0.5, 0.9, and 3 µm) (Megamix, BioCytex, DiagnosticaStago, France)(77).

Ten µl of freshly thawed MPs were directly incubated for 20 min at room temperature in the dark with 2 µl of fluorescent conjugated monoclonal antibodies against cell-type specific antigens and 2 µl of annexinV-FITC (fluorescein isothiocyanate) from Annexin V-FITC Apoptosis Detection Kit (EBIO -Termo Fisher scientific, Massachusetts, USA).

Endothelial-derived MPs were identified using CD62E-PE (phycoerythrin, EBIO -Termo Fisher scientific, Massachusetts, USA), and platelet-derived MPs using CD62P-APC (Allophycocyanin, EBIO -Termo Fisher scientific, Massachusetts, USA); leukocyte-derived MPs using CD45-PE (EBIO-Termo Fisher scientific, Massachusetts, USA); Tissue Factor-bearing (TF + MP) with CD142-PE (clone HTF-1; EBIO -Termo Fisher scientific, Massachusetts, USA); mesenchymal/stem cell-derived MPs using CD34-PE (EBIO -Termo Fisher scientific, Massachusetts, USA); Smooth Muscle cell-derived MPs with αSMA-PE, (αSmooth Muscle Actin, R&D systems, Minnesota, USA) and MPs positive for calcification marker with ALPL-Alexa Fluor-700 (Alkaline Phosphatase, R&D systems, Minnesota,

USA). MPs were also labelled with Calcein-AM 20µM (Sigma-Aldrich, Missouri, USA)

The samples were diluted in 80 µl of 0.22 µm filtered Annexin-V binding buffer or filtered PBS before analysis. MPs count was expressed as absolute numbers per microliter.

The data from CytoFLEX Platform were analysed with CytExpert Software (Beckman Coulter, Miami Florida).

5.2 Immunofluorescence of MPs

MPs labeled with fluorescent-conjugated monoclonal antibodies were fixed with 4% paraformaldehyde, and after centrifugation and resuspension in 15 µl of Elvanol mounting medium, seeded on slides. Images were captured using Leica DMI6000CS fluorescence microscope (Leica Microsystems,Germany) was used and samples were analysed with DIC and fluorescence objectives. Images were acquired at 100x/1·4 oil immersion lens (image size 1024 × 1024 pixel). Images were acquired using a DFC365FX camera and processed using the Leica Application Suite (LAS-AF) 3.1.1. Software (Leica Microsystems).

RESULTS

1. Clinical Parameters of T1DM

The main clinical parameters of the study group of type 1 diabetic patients are reported in table 1. Subjects were divided into two groups according to the presence of Carotid Fibrous Plaque (CFP, n=30) or to the presence of Carotid Calcified Plaque (n=31; CCP) determined by Carotid Ultrasound Imaging. There were no significant differences in the baseline characteristics between T1DM patients with CFP and T1DM patients with CCP, except for LDL level which are slightly higher in T1DM patients with CFP.

Variable	T1DM (n=61)	Fibrous Plaque CFP (n=30)	Calcified Plaque CCP (n=31)	P-value
Age	52,54 ± 8,25	52,10 ± 8,88	52,97 ± 7,72	0,686
Sex (F/M)	35/26	17/13	18/13	0,686
Diabetes Duration (years)	24,87 ± 11,42	25,13 ± 10,31	24,61 ± 12,58	0,860
BMI (kg/m^2)	26,72 ± 3,73	26,98 ± 3,30	26,47 ± 4,14	0,596
PAS (mm Hg)	133,31 ± 13,58	129,97 ± 13,51	136,55 ± 13,06	0,058
PAD (mm Hg)	77,21 ± 10,09	76,43 ± 10,06	77,96 ± 10,22	0,557
Glycemia (mg/dL)	160,42 ± 82,07	152,97 ± 80,86	167,64 ± 83,91	0,490
Triglycerides (mg/dL)	93,11 ± 47,39	102,06 ± 57,41	84,45 ± 33,87	0,148
Cholesterol (mg/dL)	181,39 ± 38,04	190,56 ± 40,57	172,51 ± 33,72	0,063
HDL (mg/dL)	59,87 ± 17,03	58,16 ± 17,90	61,51 ± 16,26	0,447
LDL (mg/dL)	105,24 ± 30,25	113,60 ± 32,71	97,16 ± 25,67	0,033*
HbA1c (%)	7,62 ± 0,97	7,71 ± 1,15	7,54 ± 0,77	0,488
IMT (mm)	0,74 ± 0,13	0,74 ± 0,14	0,74 ± 0,12	0,990
GFR (mL/1,73 mq.min)	94,51 ± 14,86	93 ± 13,39	95,97 ± 16,25	0,440

Table 1: Clinical parameters of the study cohort. *BMI (Body Mass Index); PAS (Systolic Artery Pressure); PAD (Diastolic Artery Pressure); HDL (High Density Lipoprotein); LDL (Low Density Lipoprotein); HbA1c (glycated haemoglobin); IMT (Intima Media Thickness); GFR (Glomerular Filtration Rate). The values are expressed as mean ± DS*

2. NGS pre-sequencing analysis

2.1 Pre-amplification Quality Control

The quality of sncRNAs isolated was determined to proceed in the NGS library preparation process, in particular to verify the presence of retrotrascriptase inhibitors or eventually contaminants and the presence of haemolysis in plasma samples.

For this goal, in a subgroup of plasma samples from T1DM randomly selected, the values of Cq (threshold cycle) of two microRNAs, has-miR-451 e has-miR-103a-3p was determined by qPCR.

The Cq values obtained show good amplification of the reaction of qPCR (15<Cq>28) and there was no significant difference in the values of Ct among the samples. The reproducibility of Ct values was around 90% with a CV <10% (fig.16).

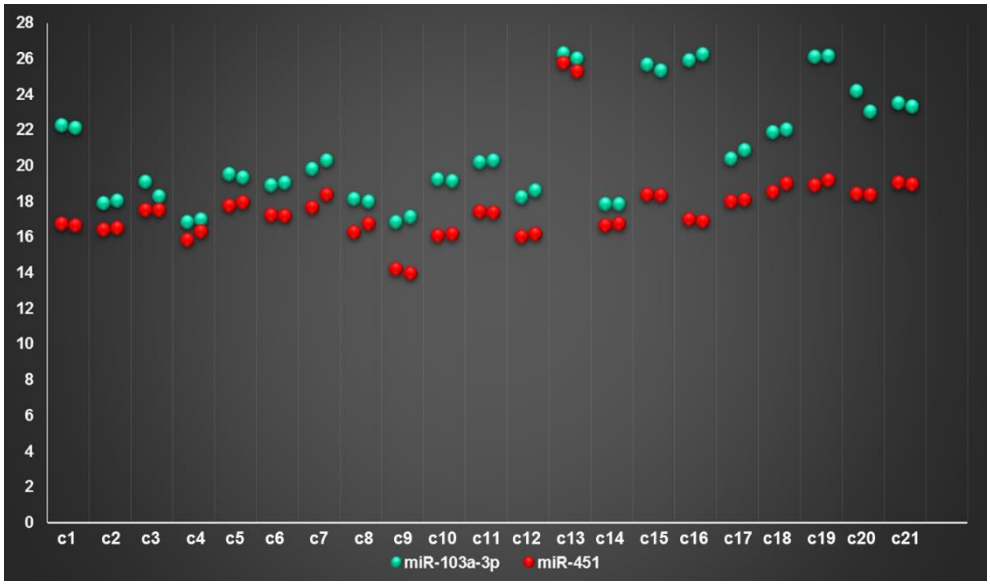

Figure 16: Pre-amplification QC by qPCR. *After reverse transcription, sncRNAs extraction products underwent amplification by qPCR. Blue dots represents Cq values obtained for miR-103a-3p and red dots for miR-451 for each samples in duplicate.*

2.2 Pre-sequencing Quality Control by High Sensitivity DNA electrophoresis

Accurate quantification and proper quality check of next-generation sequencing libraries is key to a successful sequencing run. For this goal, several quality controls (QC) of snc RNA library have been performed.

First, sncRNA libraries has been analysed by Lab Chip, before sequencing, to verify the quality of the sequences obtained and their enrichment in small non coding RNAs.

An example of a "good quality" sncRNA library electropherogram compared with a "bad quality" is shown in Figure 17. In the first case (fig. 17a) there is an evident and a net peak at approximately 180 bp (miRNA-sized library), and and a smaller at 188 bp (piRNA-sized library).

In the second electropherogram, (fig. 17b) it is not possible to discriminate any peaks for the presence of contaminants or of the lack of amplification of the sncRNA libraries.

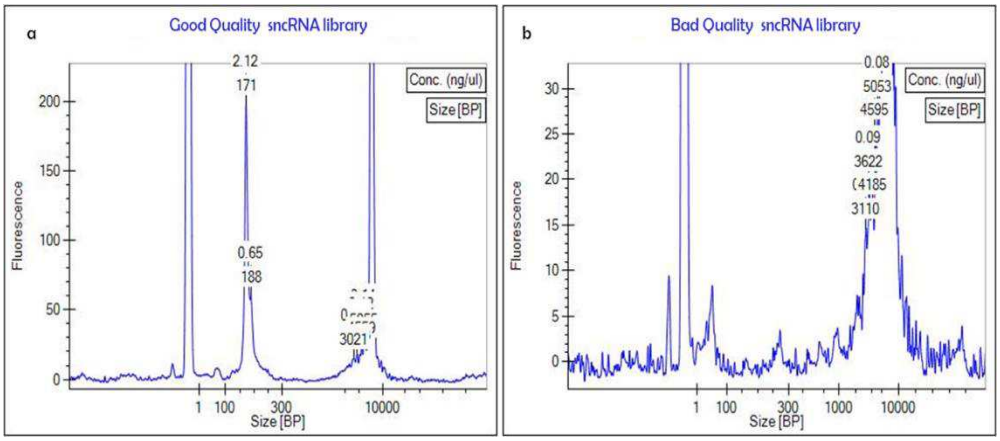

Figure 17: Pre-sequencing QC by electropherogram. *Representative electropherograms of a good quality sncRNA library (a) and a bad quality sncRNA library (b)*

A second option to verify the quality of sncRNAs library is the evaluation of gel-electrophoresis which allows to discriminate the presence of contaminants in the libraries (fig. 18).

For istance, the presence of dimers is represented by a band at 150 pb, low concentration of the libray is characterized by a weak signal, the presence of smears indicates a library of bad quality and absence of bands corresponds to the lack of amplification.

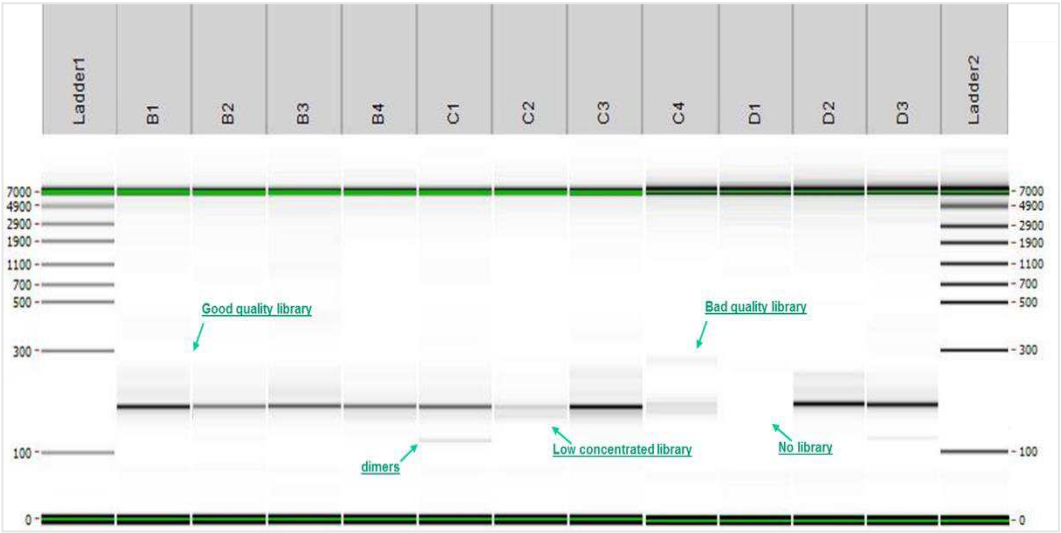

Figure 18: Pre-sequencing QC by Gel-electrophoresis. *Representative gel of sncRNAs libraries shown good quality, presence of dimers, low concentration, bad quality or absence of fragments.*

2.3 Pre-sequencing Quality Control by qPCR

A third option for library QC usually performed in case of unsuccessful library preparation and no peak was observed during Lab Chip analysis is the evaluation by qPCR, which allows to determine whether it could be due to a technical or sample issue.

As described in the methods, the quality control by qPCR enables to follow each step of library preparation by evaluation of Cq values for C3' ligation, C5' ligation and reverse transcription steps.

A value of threshold cycle (Cq) less than 28 indicates that all these steps have been performed correctly, while a value of Cq greater than 28 for one or for

all steps suggests that the library preparation has not been performed correctly or that the sample has been compromised (fig.19).

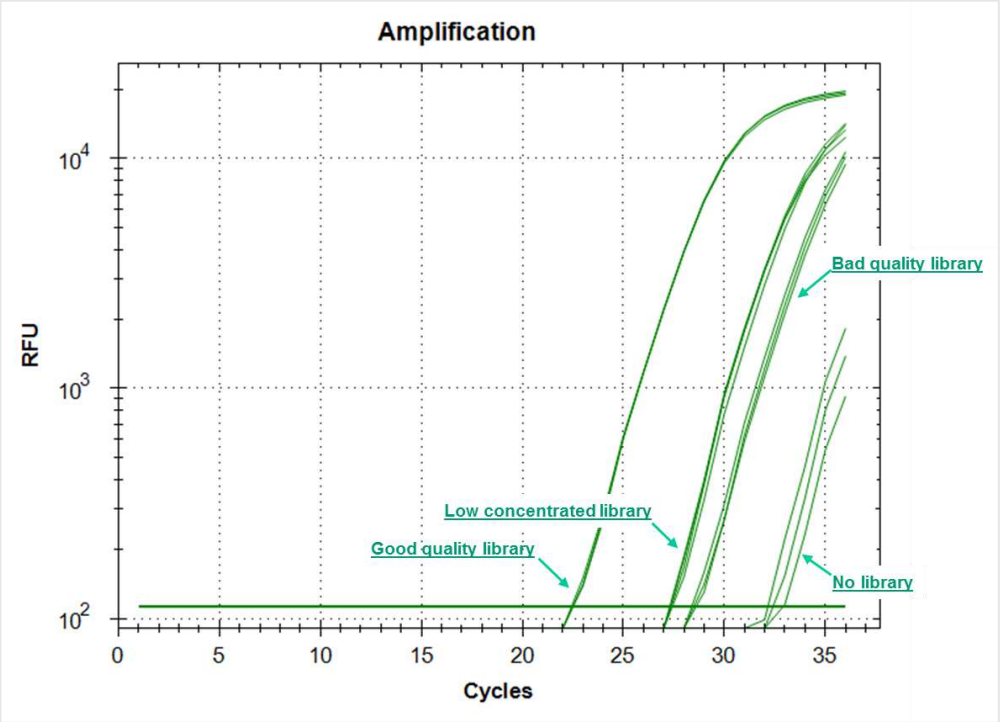

Figure 19: Pre-sequencing QC by qPCR. *Representative Cq values of C3' ligation control obtained in case of good quality library (Cq < 23), low concentrated library (Cq ≈ 27), bad quality library (Cq>28), no library (Cq>30)*

3. Next Generation Sequencing on sncRNA libraries:

Several sequencing runs were performed to obtain an accurate sncRNome-wide quantification by NGS of 26 CFP and 25 CCP type 1 diabetic patients.

The quality of the NGS runs was evaluated by several parameters such as cluster density, Passing Filter clusters and Q-score.

3.1 Cluster Density

The evaluation of the *cluster density* represents an important step of the internal quality control performed by MiSeq instrument. The density of clusters on a flow cell significantly affects data quality and yield from a run, and it is a critical metric for measuring sequencing performance.

A *cluster* is a clonal group of library fragments on a flow cell and each cluster produces one single read. During clustering, each fragment binds to the flow cell and seeds a template that is amplified until the cluster consists of hundreds or thousands of copies.

Issues with cluster registration can be diagnosed with the Imaging Metrics. For each tile (raw), a report of run metrics is generated showing the intensity values extracted from each cluster.

With optimal clustering, they reflect numeric intensity values. With overclustering, no value is reported even though clusters are visible in the thumbnail images. This is an indication that image extraction failed due to overclustering.

Figure 20 shows two representative images of clusters obtained from our runs with optimal cluster density (left) and overclustering (right) density.

In the first case, optimal cluster density maximizes total data output, while in the second case, overclustering density results in lower data output.

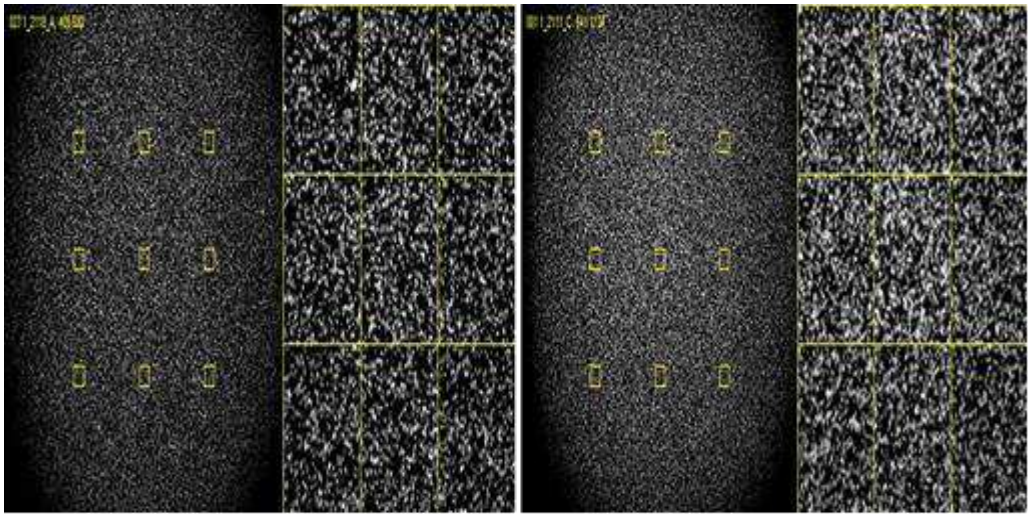

Figure 20: Representative Thumbnail images of clusters. *Picture of clusters captured during a sequencing run cycle with optimal cluster density (left) and overclustering (right).*

3.2 Base Calling and Passing Filter:

During a sequencing run, the Real-Time Analysis software extracts intensities from images to perform base calling, and then assigns a quality score to the base call. *Base calls* are made from the resulting signal (intensity) that each cluster emits.

Illumina sequencers perform an internal quality filtering procedure called *chastity filter*, and reads that pass this filter are called PF (*Passing Filter*). The *chastity* is defined as the ratio of the brightest base intensity divided by the sum of the brightest and second brightest base intensities. Clusters of reads pass the filter if no more than one base call has a chastity value below 0.6 in the first 25 cycles. This filtration process removes the least reliable clusters from the image analysis results.

Density box plots generated by the software compare tile cluster density to %PF cluster density. Cluster density indicates how many clusters are on the flow cell, while %PF cluster density indicates how many of those clusters passed filter. (fig. 21)

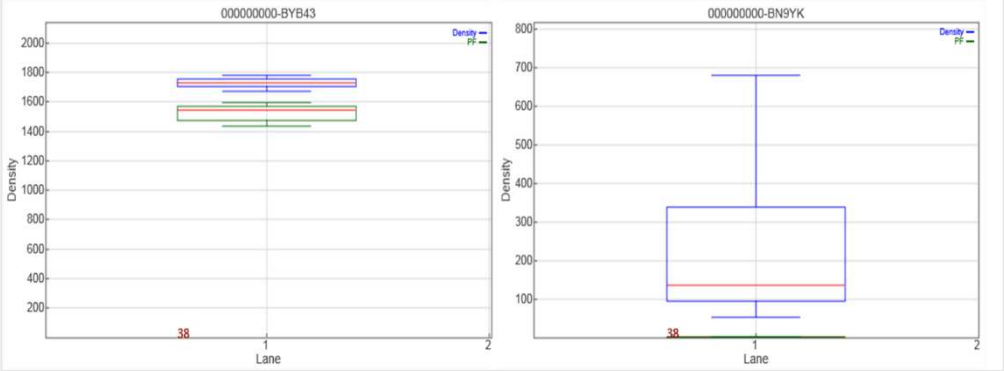

Figure 21: Cluster density and Passing Filter. *Density box plots of optimal cluster density and % passing Filter clusters (left) compared with a case of overclustering (right). blue boxes illustrate raw cluster density range, green boxes illustrate %PF cluster density range, and red lines indicate median cluster density values.*

With optimal density, the raw cluster density and %PF box plots appear close together. As density, increases beyond optimum, the %PF decreases and the box plots appear further apart. In addition, clusters might be misidentified so raw cluster density is underestimated. In our example, with severe overclustering, no clusters pass filter and the %PF plot is displayed as a horizontal green line at zero density.

In our experiments we obtained an optimal cluster density (1718,68± 117,81 K/mm^2) as expected for V3 chemistry in Illumina technology, with high %PF (83,89± 2,45) among the sequencing runs.

3.3 Q-Score

Q-Score (*Phred quality score*) is used to measure base calling accuracy, and it is one of the most common metrics for assessing sequencing data quality. It indicates the probability that the sequencer calls a given base incorrectly.

Q scores can reveal how much of the data from a given run is usable in a resequencing or assembly experiment. Low Q scores can lead to increased false-positive variant calls, resulting in inaccurate conclusions. Illumina's sequencing chemistry delivers unparalleled accuracy, is ideal for a range of sequencing applications, including clinical research.

In all our runs we obtained a Q30 (Q-Score provide by MiSeq) with an average of 95,35% ± 0.75 (fig. 22)

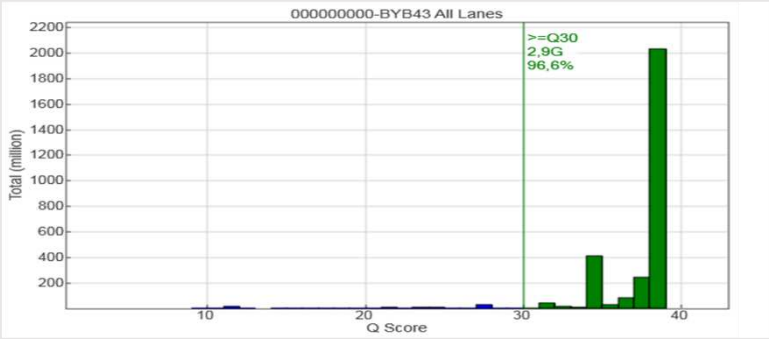

Figure 22: Q-score for Illumina sequencing. *Representative histogram with the resulting Q-score as Q30 obtained by sequencing run with Illumina platform.*

4. NGS post-sequencing and bioinformatics Analysis

The data obtained from Illumina platform are collected as FastQ files, and analysed by bioinformatics tools. Since we want to compare the results obtained from the two different software Partek flow and CLC Genomics Workbench which provide different algorithms and normalization methods for the differential expression analysis (DE), we decided to set up the same features for quantification analysis step.

4.1 Quantification analysis:

4.1.1 Adapter trimming and reads count

Removal of adapter from the fragment sequences by trimming is the first steps in analyzing NGS data. As reported in the Methods, the adapters contain the sequencing primer binding sites, the index sequences, and the sites that allow library fragments to attach to the flow cell. Figure 23 shows the sequence length distribution in relation to total reads. Al the length of 19-24 nucleotides there is a peak with the maximal amount of reads corresponding to the size of miRNAs class, at the length of about 27 nucleotides a small peak is present corresponding to the size of piRNAs class.

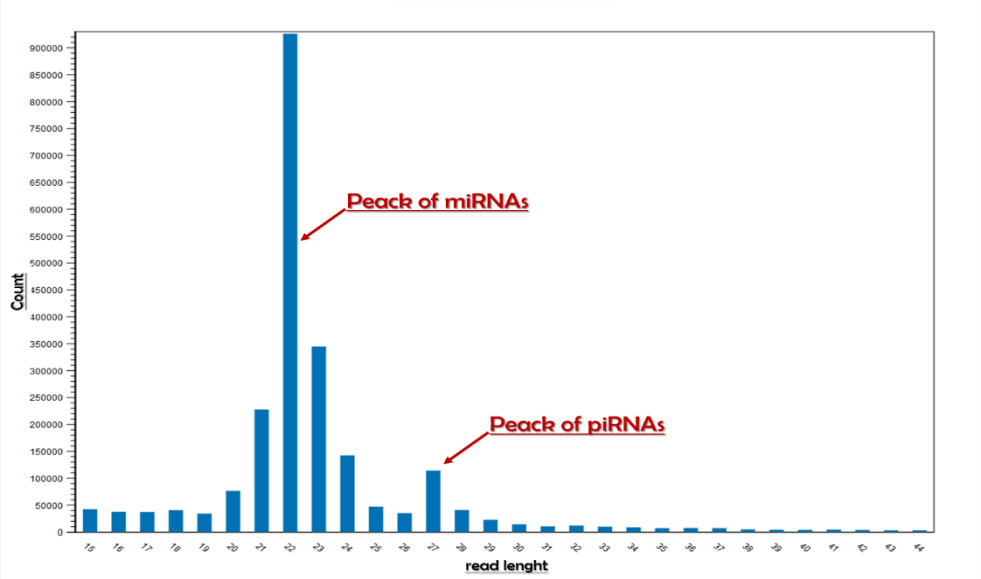

Figure 23: Representative trimmed read length distribution. *count of the trimmed reads related to the size of the fragments. The major part of them are distributed in the typical range size of miRNAs and piRNAs.*

4.1.2 Alignment to reference genome and annotation models

The second step of NGS analysis is the alignment of the trimmed fragment sequences to a reference genome (Homo Sapiens – human hg38) and to selected specific annotation models for sncRNAs, by Bowtie aligner characterized by high accuracy for short reads of <55bp. The results obtained from this analysis are summarized in Figure 24

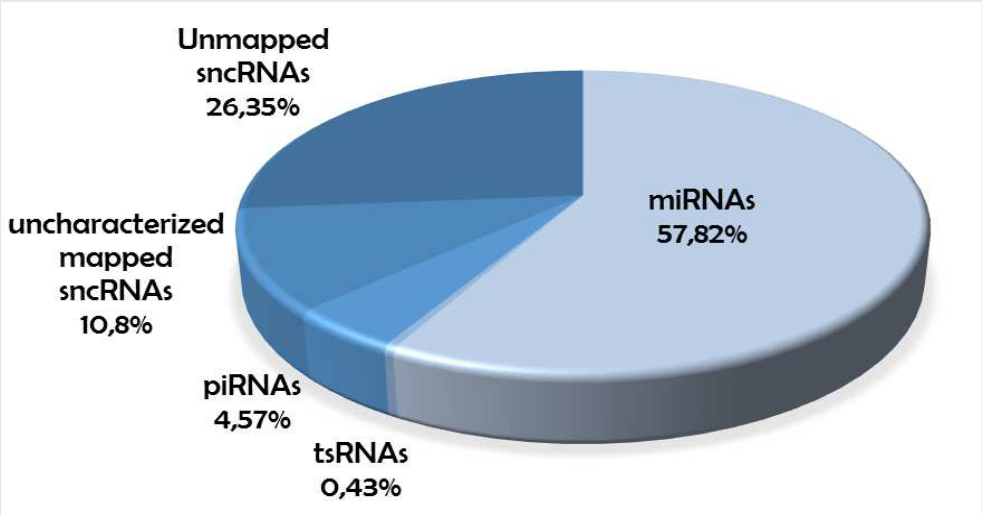

Figure 24: Distribution of the reads among the classes of sncRNAs. *miRNAs, piRNAs, tsRNAs, other sncRNAs mapped across the genome and unmapped sncRNA-size molecules are expressed as percentage of the total reads count/sample.*

Among the total number of reads obtained from our NGS data, we found that 57,82% of the reads were recognized as already known miRNAs, 4.57% corresponds to piRNAs and 0,43% to tsRNAs. Futhermore, we obtained that 10.8 % of the reads were collected as uncharacterized sncRNAs, mapped in the human genome while 26,35% of the reads were unmapped molecules with tha same size of sncRNA.

4.1.3 Quantification of miRNAs, piRNAs e tsRNAs

Quantification of count reads was performed using miRBase v.22.1 for the quantification of mature miRNAs, piRBase v.1 for piRNAs and MINTbase v.2 for tsRNAs.

- ***miRNAs quantification***

As expected, miRNAs were the most abundant class of sncRNAs in our samples. Figure 25 shows the distribution of the number of reads to each miRNA in the annotation model. More than 20% of miRNAs are high expressed among the samples collecting up to 20000 reads/sample, 23% of miRNAs count about 1000-200 reads/sample and 55% of miRNAs are low expressed (200-20 reads per sample).

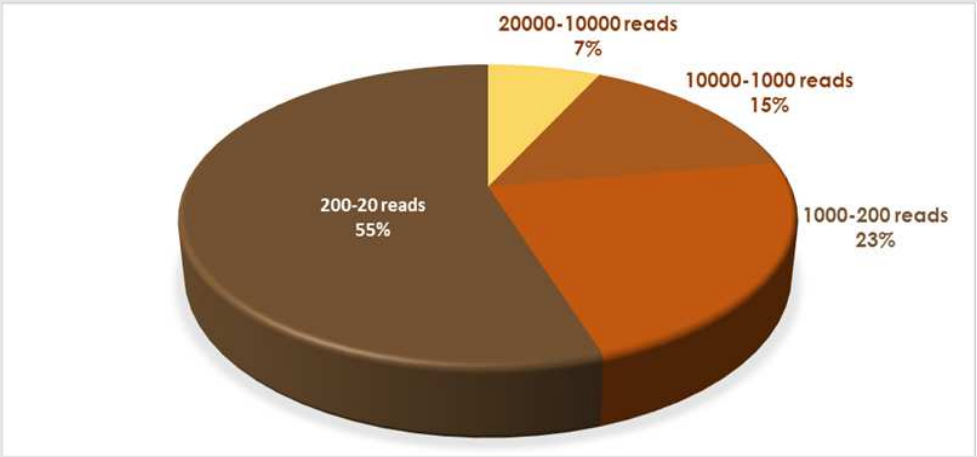

Figure 25: Distribution of the reads among already known miRNAs in T1DM. *Number of miRNAs according with their reads are expressed as percentage of total miRNAs*

Figure 26 shows the most expressed circulating miRNAs in plasma samples from T1DM: miR-16-5p collected more than 150000 reads/sample, followed by miRNAs with under half of counted reads, such as miR-486-5p with almost 60000 reads/sample

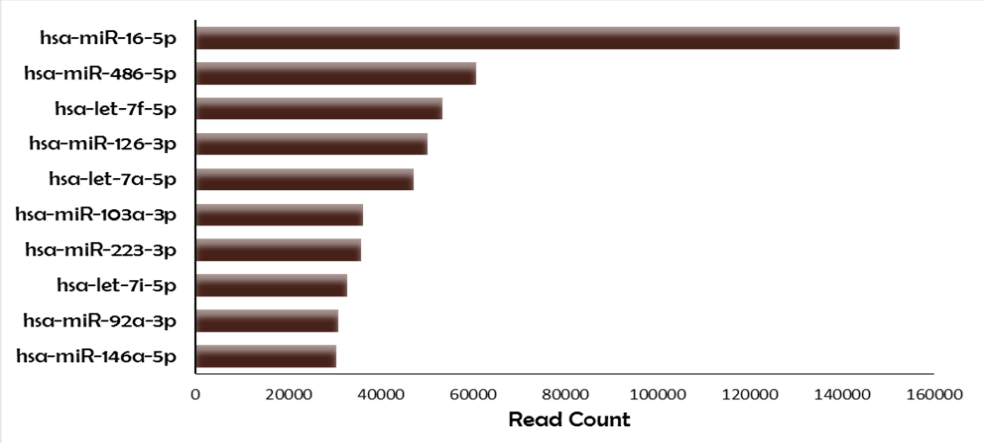

Figure 26: The most abundant circulating miRNAs in T1DM. *the top ten of the highest expressed miRNAs among the 51 samples*

- ***piRNAs quantification***

piRNAs were the second most abundant class of sncRNAs found in our samples. Figure 27 show the distribution of the reads mapped to each piRNAs in the annotation model. Only 7% of piRNAs were high expressed among the samples collecting up to 50000 reads/sample, while 20% of piRNAs counted more than 200 reads/sample and 80% of piRNAs were low expressed (200-20 reads per sample).

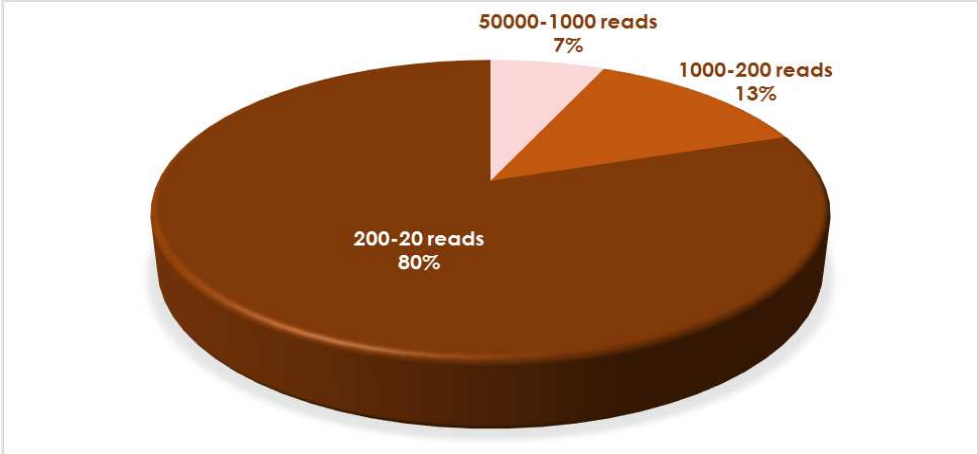

Figure 27: Distribution of the reads among piRNAs in T1DM. *The number of piRNAs according with their reads are expressed as percentage of total piRNAs*

Among the most expressed circulating piRNAs in T1DM, only piR-hsa-23209 and piR-hsa-32159 collected more than 25000 reads/sample, directly followed by piRNAs low expressed with less than 2000 reads/sample (fig. 28).

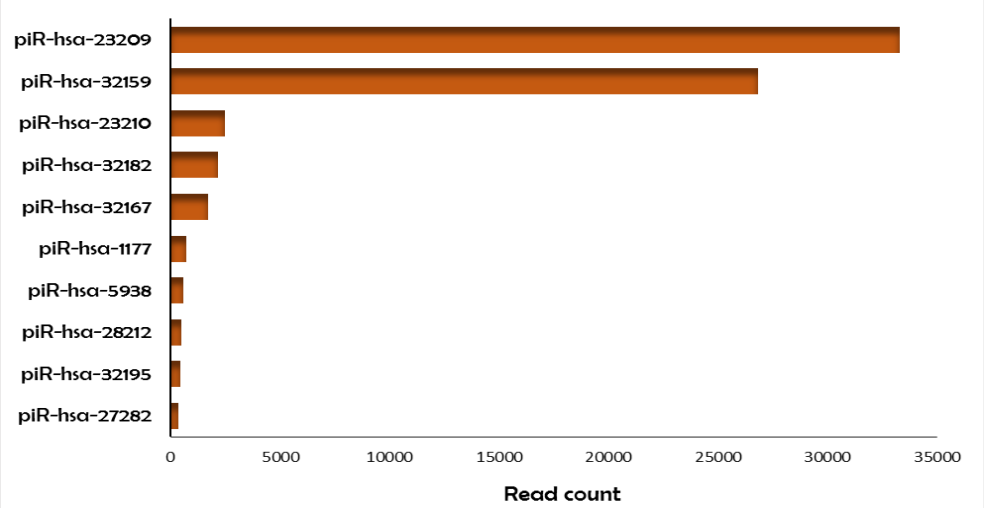

Figure 28: The most abundant circulating piRNAs in T1DM. *The top ten of the highest expressed piRNAs among the 51 samples*

- ***tsRNAs quantification***

tsRNAs were the lowest expressed class of sncRNAs in our samples. Figure 29 show the distribution of the reads mapped for each tsRNAs in the annotation model. 63% of tsRNAs are barely detectable (20-50 reads per sample) while 32% are low expressed with no more than 200 reads/sample. Only 7% are higher expressed among the samples collecting up to 1000 reads/sample.

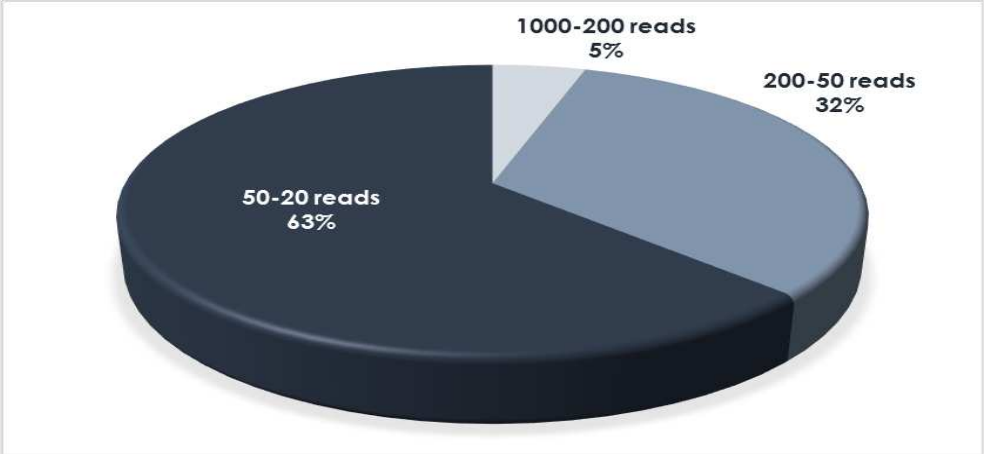

Figure 29: Distribution of the reads among tsRNAs in T1DM. *The number of tsRNAs according with their reads are expressed as percentage of total tsRNAs*

Among the most expressed circulating tsRNAs in T1DM, only trnaMT_MetCAT_MT_+_4402_4469 collected more than 500 reads/sample, followed by tsRNAs low expressed with less than 300 reads/sample (fig. 30).

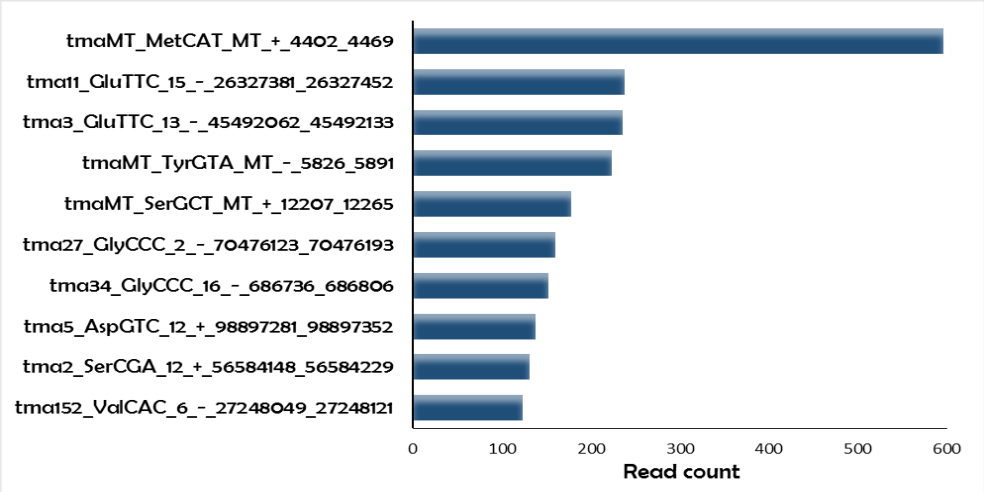

Figure 30: The most abundant circulating tsRNAs in T1DM. *The top ten of the highest expressed tsRNAs among the 51 samples*

4.1.4 Data filtering

Next, we filtered our reads setting a cut off 20 to retain sncRNAs in the next analysis to eliminate the source of systematic error, which may influence the normalization and differential expression. From a result of 2632 miRNAs recognized in our samples, only 296 miRNAs with more than 20 reads were considered for the further analysis. As well as, among 3286 piRNAs and 640 tsRNAs found in our samples. Only 76 piRNAs and 83 tsRNA were considered for differential expression analysis.

4.2 Differential Expression Analysis (DE) of sncRNAs

After collecting the data of the quantification of each class of sncRNAs, we performed the differential expression analysis of sncRNAs in our samples to determine the presence of a potential biomarker able to discriminate the type of atherosclerotic plaque.

As previously described, this is a critical step of the analysis and there is no a gold standard method for normalization of the data. Therefore, we compared the statistical analysis of sncRNA differentially expressed from two different bioinformatics platforms Partek and ClC Genomics, which use different normalization methods.

4.2.1 miRNAs differential expression:

First, we performed the normalization of the data using two different methods: the TMM method provided by CLC Genomics and DeSeq2 provided by Partek. Subsequently, a differential expression analysis of the miRNAs was assessed between T1 DM patients with carotid fibrous plaque (CFP; n =25) and with Carotid calcified plaque (CCP; n =26).

- ***TMM normalization with CLC Genomics statistical analysis (GLM model)***

The differential expression analysis was executed using the general linear model (GLM) for two-group comparisons.

The volcano plot in Figure 31 shows the results obtained from CLC platform performing the analysis using TMM as normalization method to compare CFP Vs CCP

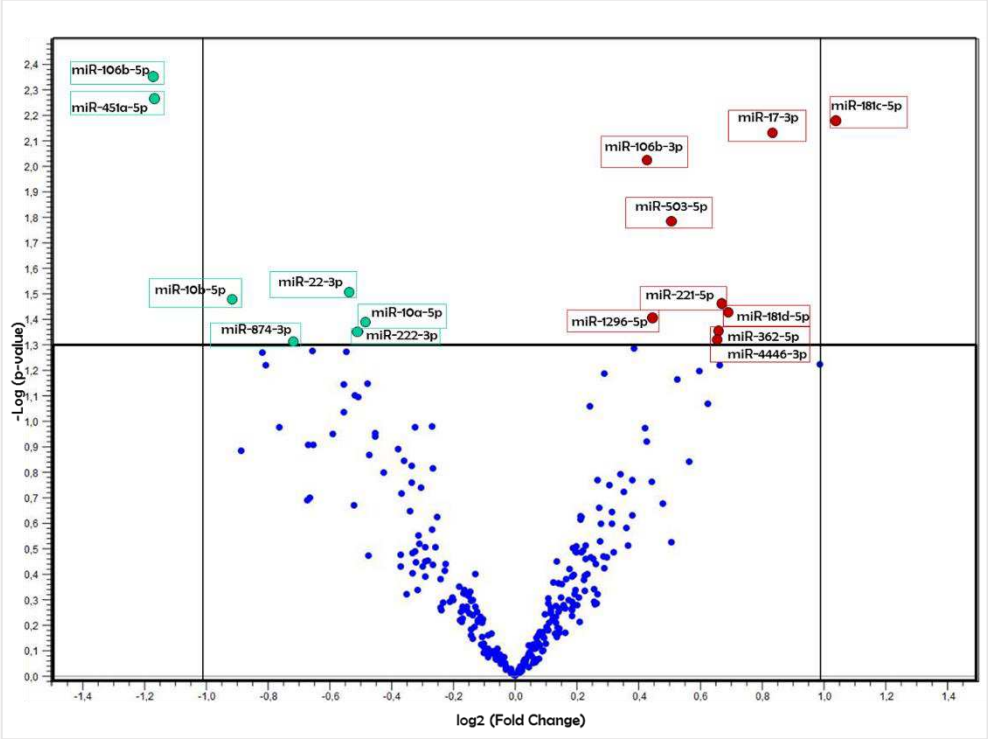

Figure 31: Volcano plot of the expression of circulating miRNAs in CCP Vs CFP according to CLC Workbench using TMM and GLM model. *The differential expression of miRNA between the two groups is expressed as log_2 (Fold change), and the statistical significance as –Log(p-value). Circulating miRNAs significant downregulated (light blue dots) and up-regulated (red dots) are highlighted.*

Nine miRNAs were significantly up regulated in patients T1DM with CCP compared to CFP: miR-181c-5p, miR-17-3p and miR-106b-3p ($p<0,01$), miR-503-5p, miR-221-3p, miR-181d-5p, miR-1296-5p, miR-362-5p and miR-4446-3p ($p<0.05$). Seven miRNAs were downregulated in T1DM patients with CCP compared with patients with CFP: miR-106b-5p and miR-

451a-5p ($p<0.01$), miR-22-3p, miR-10b-5p, miR-10a-5p, miR-222-3p and miR-874-3p ($p<0.05$). The results are summarized in the table 2.

miRNA	Fold change	P-value	miRNA	Fold change	P-value
Up-regulated (CFP Vs CCP)			Down-regulated (CFP Vs CCP)		
miR-181c-5p	2,05	0,006	miR-106b-5p	-2,26	0,004
miR-17-3p	1,79	0,007	miR-451a-5p	-2,25	0,005
miR-106b-3p	1,35	0,009	miR-22-3p	-1,45	0,016
miR-503-5p	1,43	0,016	miR-10b-5p	-1,88	0,033
miR-221-3p	1,60	0,035	miR-10a-5p	-1,40	0,041
miR-181d-5p	1,62	0,037	miR-222-3p	-1,42	0,044
miR-1296-5p	1,36	0,039	miR-874-3p	-1,64	0,049
miR-362-5p	1,58	0,044			
miR-4446-3p	1,57	0,048			

Table 2: Circulating miRNAs significant differential expressed in CCP Vs CFP according to CLC Workbench using TMM and GLM model. *The differential expression of miRNA between the two groups is expressed as Fold change and p-value.*

The heatmap visualization for the expression of miRNAs obtained by differential expression analysis across samples is shown in Figure 32.

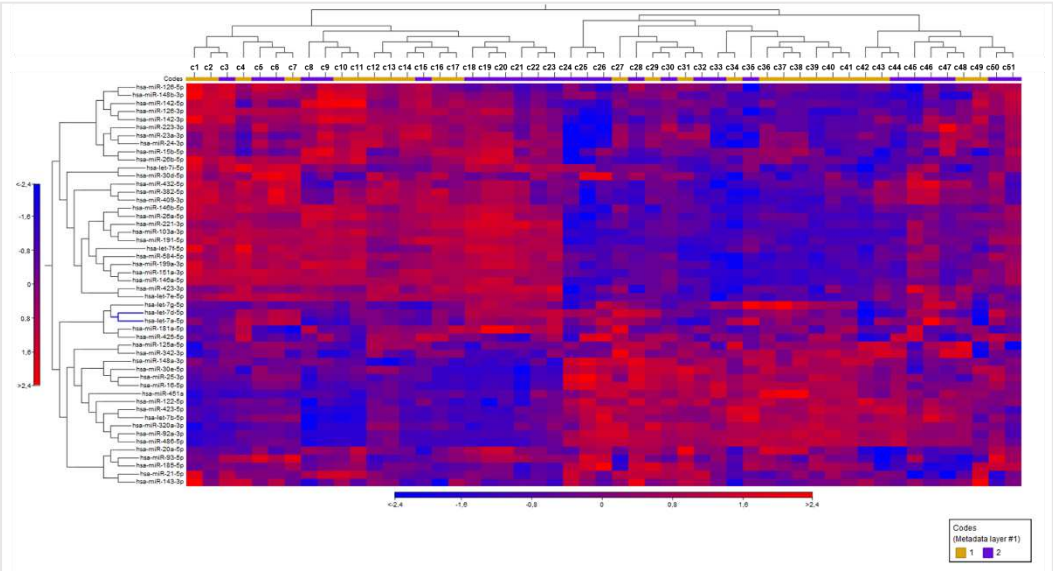

Figure 32: Heatmap and a hierarchical clustering of differential expression of miRNAs. *In the Heatmap, dark-blue color corresponds to lower expression, and dark-red color corresponds to high expression in log scale. Code 1 corresponds to T1DM with fibrous plaque; Code 2 corresponds to T1DM with calcified plaque.miRNAs are displayed in the vertical axis while the samples in horizontal axis.*

- ***TMM normalization with Partek statistical analysis (GSA model)***

The volcano plot in Figure 33 shows the results obtained from Partek platform performing the analysis using TMM as normalization method and GSA model to compare the expression of miRNAs in the two groups of patients (CFP Vs CCP)

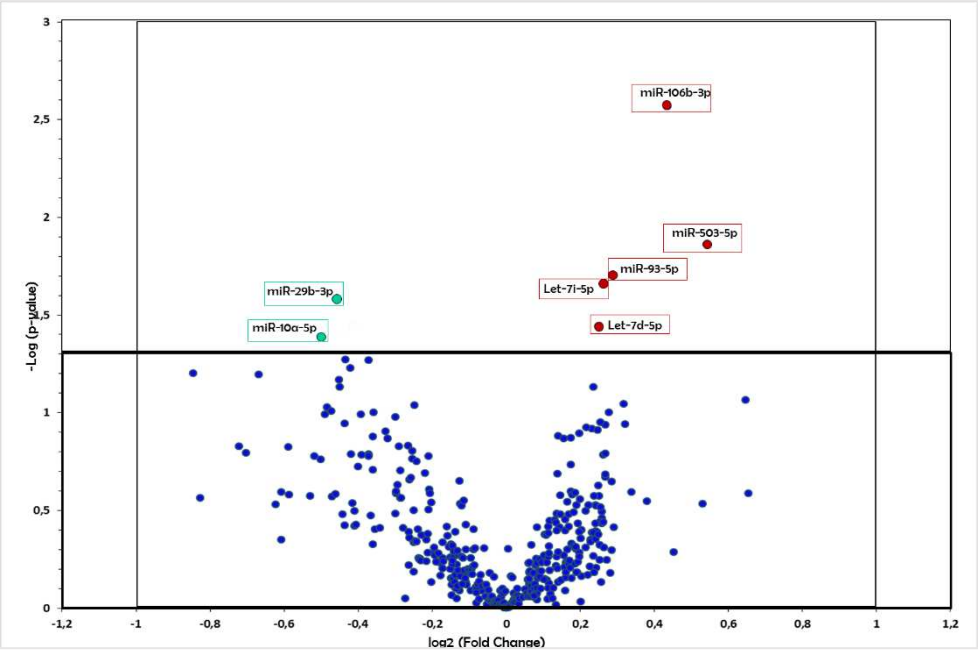

Figure 33: Volcano plot of the expression of circulating miRNAs in CCP Vs CFP according to Partek Flow using TMM and GSA model. *The differential expression of miRNA between the two groups is expressed as log_2 (Fold change), and –Log(p-value). Circulating miRNAs significant downregulated (light blue dots) and up-regulated (red dots) are highlighted.*

Five miRNAs were significantly up regulated in patients T1DM with CCP compared to CFP: miR-106b-3p ($p<0,01$), miR-503-5p, miR-93-5p, let-7i-5p and let-7d-5p ($p<0.05$). Two miRNAs were significantly downregulated in T1DM patients with CCP compared with patients with CFP: miR-29b-5p and miR-10a-5p ($p<0.05$). The results are summarized in the table 3.

miRNA	Fold change	P-value
Up-regulated (CFP Vs CCP)		
miR-106b-3p	1,35	0,002
miR-503-5p	1,46	0,013
miR-93-5p	1,50	0,019
let-7i-5p	1,20	0,021
let-7d-5p	1,19	0,036

miRNA	Fold change	P-value
Down-regulated (CFP Vs CCP)		
miR-29b-3p	-1,42	0,040
miR-10a-5p	-1,36	0,041

Table 3: Circulating miRNAs significant differential expressed in CCP Vs CFP according to Partek Flow using TMM and GSA model. *The differential expression of miRNA between the two groups is expressed as Fold change and the statistical significance as p-value.*

- ***DESeq2 statistical analysis***

The volcano plot in Figure 34 shows the results obtained from Partek platform performing the analysis using DESeq2 to compare CFP Vs CCP

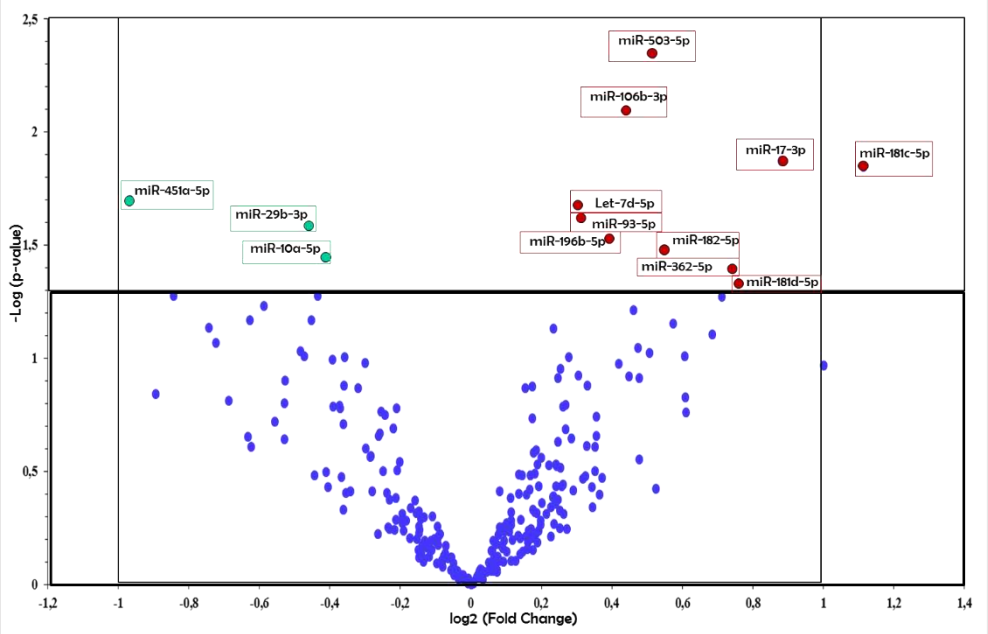

Figure 34: Volcano plot of the expression of circulating miRNAs in CCP Vs CFP according to Partek Flow using DeSeq2. *The differential expression of miRNA between the two groups is expressed as log_2 (Fold change), and –Log (p-value). Circulating miRNAs significant downregulated (light blue dots) and up-regulated (red dots) are highlighted.*

Ten miRNAs were significantly up regulated in patients T1DM with CCP compared to CFP: miR-503-5p and miR-106b-3p ($p<0.01$), miR-17-3p, miR-181c-5p, let-7d-5p, miR-93-5p, miR-196b-5p, miR-182-5p, miR-362-5p and miR-181d-5p ($p<0.05$). Three miRNAs were significantly downregulated in T1DM patients with CCP compared with patients with CFP: miR-451a-5p, miR-29b-3p and miR-10a-5p ($p<0.05$). The results are summarized in the table 4.

miRNA	Fold change	P-value
Up-regulated (CFP Vs CCP)		
miR-503-5p	1,43	0,004
miR-106b-3p	1,36	0,008
miR-17-3p	1,84	0,013
miR-181c-5p	2,16	0,014
Let-7d-5p	1,23	0,021
miR-93-5p	1,24	0,023
miR-196b-5p	1,31	0,029
miR-182-5p	1,46	0,033
miR-362-5p	1,67	0,040
miR-181d-5p	1,69	0,046

miRNA	Fold change	P-value
Down-regulated (CFP Vs CCP)		
miR-451a-5p	-1,95	0,020
miR-29b-3p	-1,38	0,026
miR-10a-5p	-1,33	0,035

Table 4: Circulating miRNAs significant differential expressed in CCP Vs CFP according to Partek Flow using Deseq2. *The differential expression of miRNA between the two groups is expressed as Fold change and p-value.*

- ***Comparative Analysis***

From the comparative analysis of the results obtained from these methods we selected the microRNAs significantly differential expressed between the two groups showed in Venn diagram. (fig. 35)

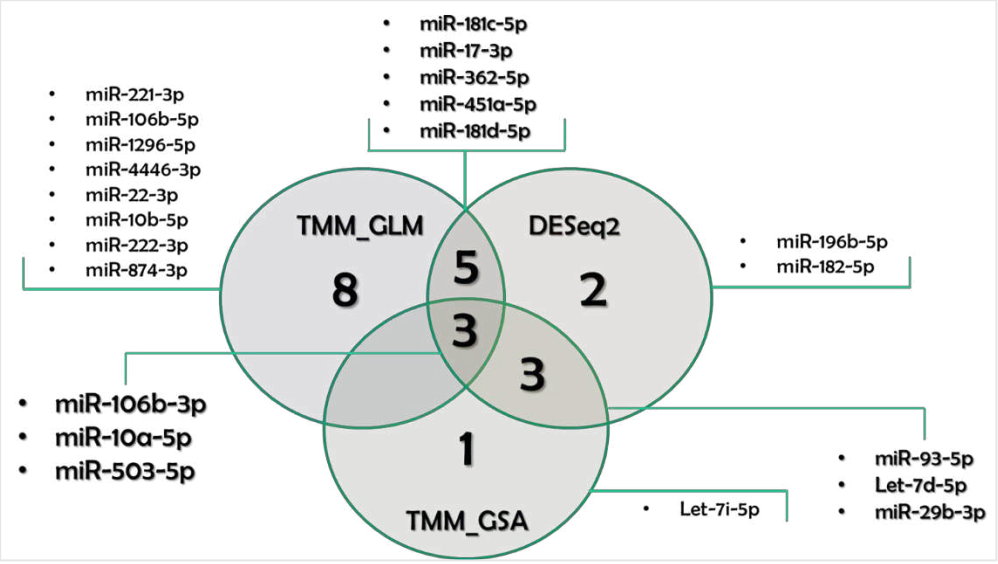

Figure 35: Venn diagram of the significant circulating miRNAs in CCP Vs CFP. *The Venn diagram was used to identify overlapping and non-overlapping miRNAs in the analysis of CLC Genomics and Partek bioinformatics tools.*

Eleven miRNAs were significantly differential expressed in CCP compared to CFP for at least two of the three differential expression analysis: miR-106b-3p, miR-503-5p, let-7d-5p, miR-93-5p, miR-181c-5p, miR-181d-5p miR-17-3p, and miR-362-5p that are upregulated in CCP compared to CFP; miR-10a-5p, miR-29b-3p and miR-451a-5p that are downregulated in in CCP compared to CFP.

4.2.2 Post sequencing quality control

Since the gold standard method for microRNAs expression analysis is the qPCR system, we evaluated the correlation between the reads obtained by NGS and the values of Cq (threshold cycle) obtained by qPCR. We analysed three miRNAs: miR-122-5p with high number of reads, miR-431-5p with very low reads and miR-93-5p that is differential expressed between the two groups. miR-122-5p and miR-93-5p displayed a good curve of amplification during qPCR analysis (respectively, Cq_{mean} 21±0.4 and $reads_{mean}$ 22814±5766; Cq_{mean} 19±0.6 and $reads_{mean}$ 34164±2424) while miR-431-5p did not amplified in all the samples ($reads_{mean}$ 150±100).

Fig.XX shows the correlation of the values of Cq and the number of reads of miR-122-5p and miR-93-5p. We confirmed the high sensitivity of NGS showing a strong correlation (r= 0.80; p=0.0001) (fig. 36).

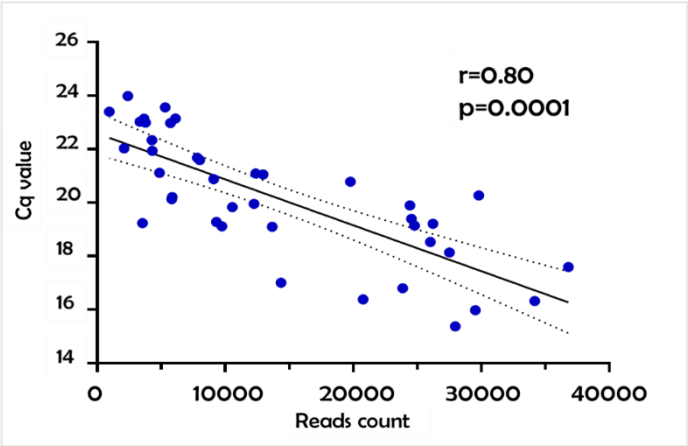

Figure 36: Correlation between Cq values of miRNAs from qPCR and number of reads of miRNAs from NGS.

From these results, we decided to consider for further analysis only miRNAs with $reads_{mean}$ > 150 expected to be dectectable by PCR analysis. For this aim, we retain these miRNA: miR-106b-3p, miR-503-5p, let-7d-5p, miR-93-5p, miR-10a-5p, miR-29b-3p and miR-451a-5p.

4.2.3 Target Gene Network Analysis

To gain insight into the functional role of these miRNAs in vascular calcification, we analyzed their potential targets using MirWalk 3.0, a suite of 13 existing miRNA-target prediction programs. We selected gene targets for atherosclerosis, vascular calcification, and diabetes networks, through the gene ontology functional analysis and the gene ontology biological process.

Using Cytoscape, we created a biological network showing the match of predictive targets for these miRNAs involved in diabetes and cardiovascular complication pathways (fig. 37)

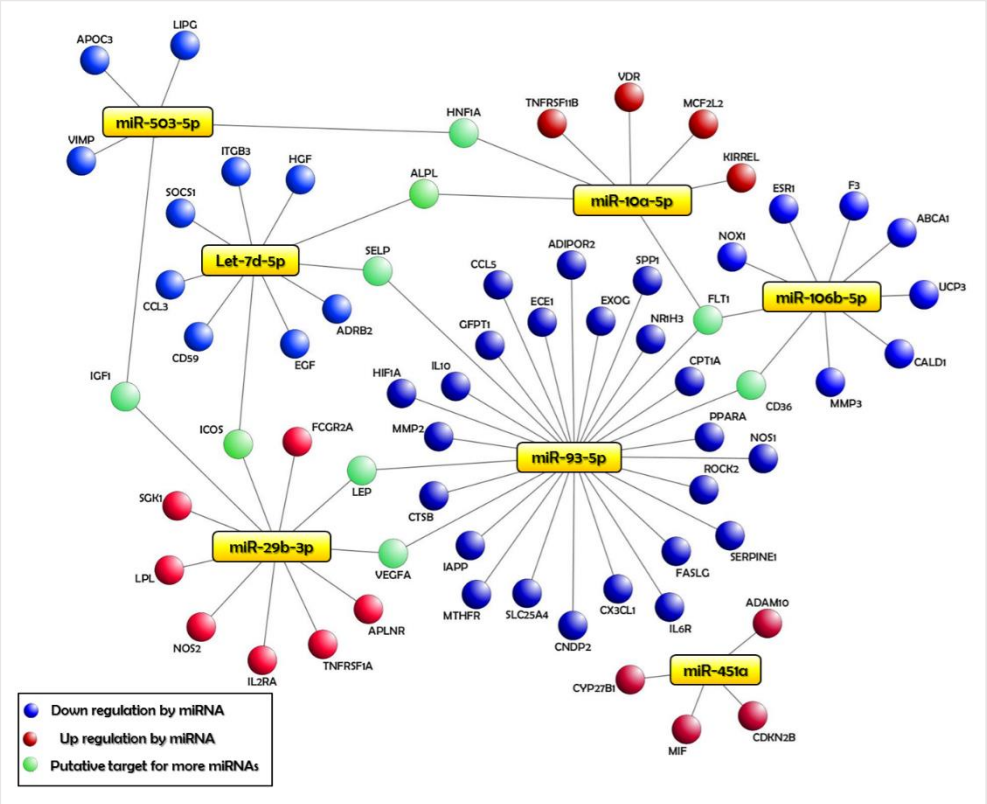

Figure 37: Network of significantly differential expressed miRNAs in fibrous or calcified plaque composition and their putative gene targets involved in cardiovascular complication of diabetes through the gene ontology (GO) functional analysis and the gene ontology biological process (GOBP). *Blue dots indicate putative target gene downregulated by miRNAs, Red dots indicate putative target gene upregulated by miRNAs; green dots indicate putative target gene for more miRNAs.*

Table 5 shows that a large proportion of gene targets of these miRNAs are implicated in vascular remodeling, glucose, lipid metabolism, and inflammation.

miRNAs	KEGGs Pathway	P-value
miR-503-5p miR-451a miR-93-5p miR-106b-5p miR-10a-5p Let-7d-5p miR-29b-3p	Insulin signaling pathway	0,0001
	mTOR signaling pathway	0,0001
	T cell receptor signaling pathway	0,0001
	Adherens junction	0,0002
	Wnt signaling pathway	0,0003
	MAPK signaling pathway	0,0005
	Calcium signaling pathway	0,0007
	Endocytosis	0,0010
	Focal adhesion	0,0013
	Axon guidance	0,0018
	diabetes mellitus	0,0019

miRNAs	KEGGs Pathway	P-value
miR-93-5p; miR-503-5p; let-7d-5p; miR-10a-5p; miR-106b-5p; miR-29b-3p	Apoptosis	0,0001
miR-93-5p; miR-503-5p; let-7d-5p; miR-451a; miR-106b-5p; miR-29b-3p	Gap junction	0,018
miR-93-5p; miR-503-5p; miR-10a-5p; miR-106b-5p; miR-29b-3p	Adipocytokine signaling pathway	0,0001
	p53 signaling pathway	0,0008
miR-93-5p; miR-503-5p; let-7d-5p; miR-10a-5p; miR-106b-5p	Regulation of sodium reabsorption	0,008
	VEGF signaling pathway	0,012

Table 5: KEGGs Pathways of significantly differential expressed miRNAs in fibrous or calcified plaque composition. *Common pathways for all the miRNAs (left); common pathways for 6 or 5 miRNAs with the strongest statistical support for enrichment.*

4.2.4 piRNAs differential expression

The volcano plot shows the results obtained performing the analysis of piRNAs in CFP Vs CCP (fig. 38).

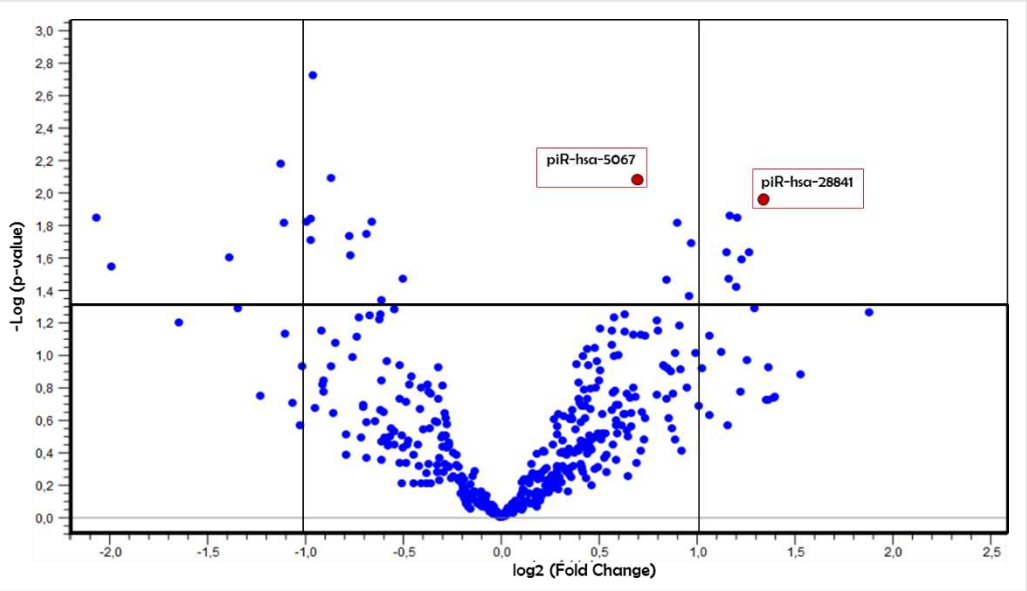

Figure 38: Volcano plot of the expression of circulating piRNAs in CCP Vs CFP according to CLC Genomics and Partek Flow. *The differential expression of piRNA between the two groups is expressed as log_2 (Fold change), and –Log(p-value)according to CLC Workbench.. After matching the results with Partek flow systems, the significant circulating piRNAs are highlighted as up-regulated (red dots).*

From the comparative analysis of the results obtained from CLC Workbench and Partek flow systems, we selected the piRNAs that are significantly differential expressed between the two groups. Two piRNAs are upregulated in CCP compared to CFP: piR-hsa-5067 (p=0.008; fold change 1.63) and piR-hsa-28841 (p=0.02; fold change 2.23).

The heatmap visualization for the expression of piRNAs obtained by differential expression analysis across samples is shown in Figure 39.

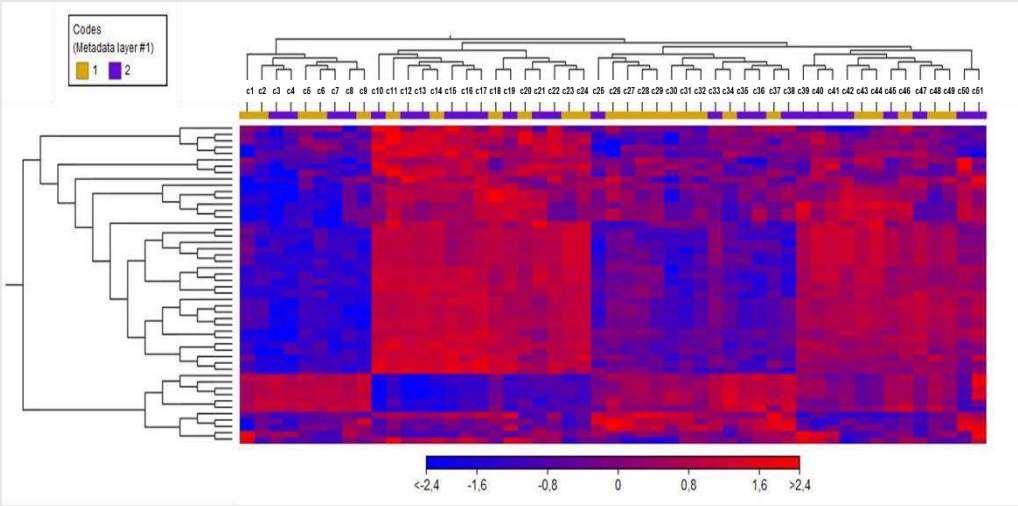

Figure 39: Heatmap and a hierarchical clustering of differential expression of piRNAs. *In the Heatmap, dark-blue color corresponds to lower expression, and dark-red color corresponds to high expression in log scale. Code 1 corresponds to T1DM with fibrous plaque; Code 2 corresponds to T1DM with calcified plaque. piRNAs are displayed in the vertical axis while the samples in horizontal axis.*

4.2.5 tsRNAs differential expression:

The volcano plot shows the results obtained performing the analysis of tsRNAs in CFP Vs CCP (fig. 40)

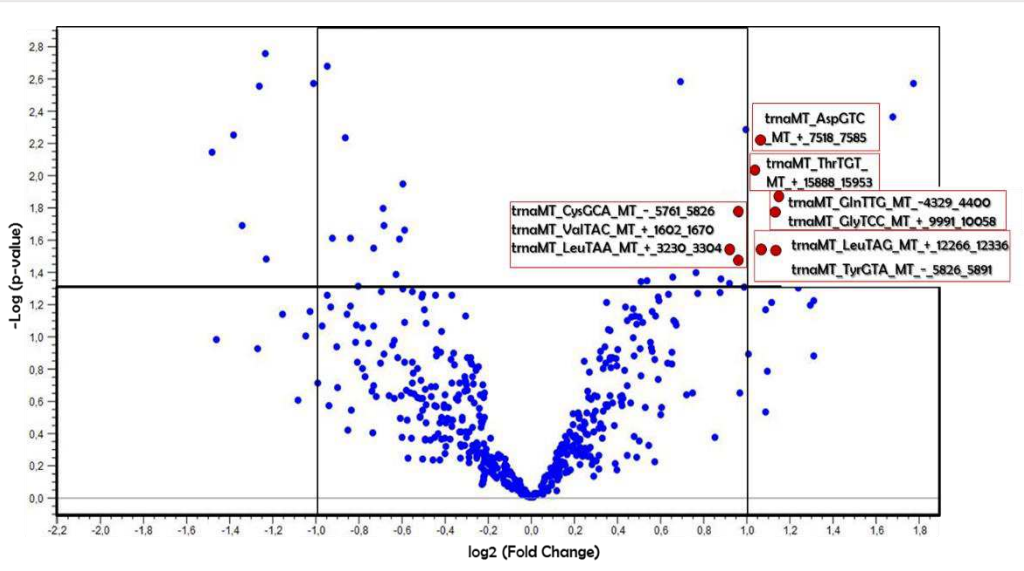

Figure 40: Volcano plot of the expression of circulating tsRNAs in CCP Vs CFP according to CLC Genomics and Partek Flow. *The differential expression of tsRNAs between the two groups is expressed as log_2 (Fold change), and –Log (p-value) according to CLC Workbench. After matching the results with Partek flow systems, the significant circulating tsRNAs are highlighted as up-regulated (red dots).*

Following the same method previously described for tsRNAs we found out that 10 tsRNAs were up regulated in patients T1DM with CCP compared to CFP. The results are summarized in the Table 6.

miRNA	Fold change	P-value
Up-regulated (CFP Vs CCP)		
trnaMT_AspGTC_MT_+_7518_7585	2	0,005
trnaMT_ThrTGT_MT_+_15888_15953	2,09	0,006
trnaMT_GlnTTG_MT_-_4329_4400	2,22	0,01
trnaMT_GlyTCC_MT_+_9991_10058	2,25	0,01
trnaMT_CysGCA_MT_-_5761_5826	1,88	0,01
trnalookalike2_GlnTTG_1_-_564879_564950	2,2	0,02
trnaMT_LeuTAG_MT_+_12266_12336	2,2	0,02
trnaMT_TyrGTA_MT_-_5826_5891	2,09	0,03
trnaMT_ValTAC_MT_+_1602_1670	1,79	0,03
trnaMT_LeuTAA_MT_+_3230_3304	1,94	0,03

Table 6: Circulating tsRNAs significant differential expressed in CCP Vs CFP according to CLC Genomics and Partek Flow. *The differential expression of tsRNA between the two groups is expressed as Fold change and p-value.*

The heatmap visualization for the expression of tsRNAs obtained by differential expression analysis across samples is shown in Figure 41.

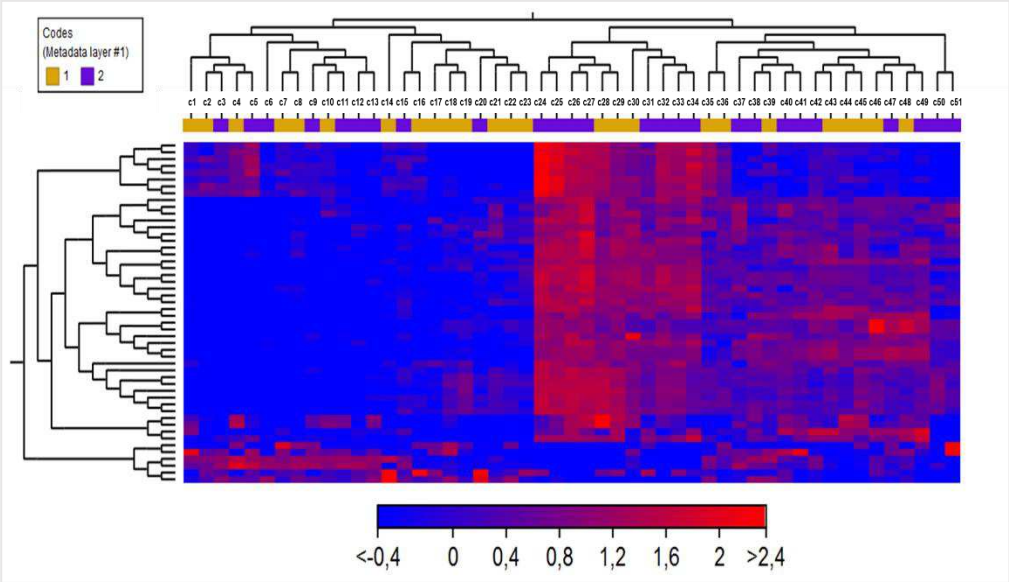

Figure 41: Heatmap and a hierarchical clustering of differential expression of tsRNAs. *In the Heatmap, dark-blue color corresponds to lower expression, and dark-red color corresponds to high expression in log scale. Code 1 corresponds to T1DM with fibrous plaque; Code 2 corresponds to T1DM with calcified plaque. tsRNAs are displayed in the vertical axis while the samples in horizontal axis.*

5. Circulating microparticles characterization from Plasma of T1DM:

MPs were isolated from plasma of 20 T1DM patients with fibrous carotid plaques (CFP) and 20 T1DM patients with calcified carotid plaques (CCP) MPs derived from cell types involved in CV process were characterized and quantified: Endothelial cell-derived MPs (EMP), Platelets derived MPs, (PMP), Leukocyte derived MPs (LMP). Furthermore, MPs derived from staminal compartment (MMP), and Smooth muscle cell-derived MPs (SMP) were assessed. Apoptotic fraction of MPs was detected using Annexin V and MPs positive for calcification labelled with ALP (alkaline phosphatase) were quantified. Images of labelled MPs were also captured using fluorescence microscopy (fig. 42).

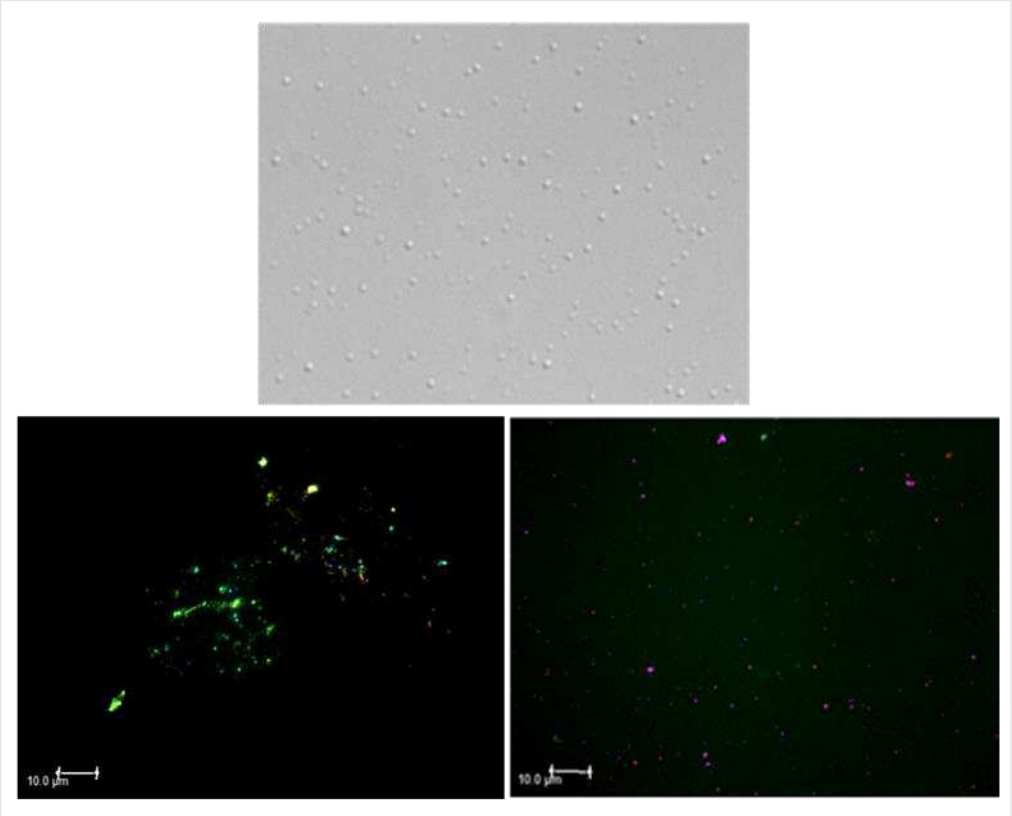

Figure 42: Circulating MPs derived from T1DM. *Images of fixed MP aggregates positive for several markers: (Up panel) bright field ; (Down panel) Annexin V+ MPs, CD45+ MPs, ALP+ MPs are shown in green, red and blue channels; MPs double-positive for Ann V and CD45 are shown in yellow(left); MPs double-positive for CD45 and ALP are showed in violet (right); captured using fluorescence microscopy (x100/1.4)*

Our results show that MPs released from endothelial cells ($p<0.05$) and Platelets ($p<0.01$) were significantly enhanced in T1DM with vascular

calcification (CCP) in comparison to T1DM with fibrous plaque (CFP); (tablexx). Interestingly, a population of MPs derived from a niche of cells positive for CD34 and SMA were also increased in CCP ($p<0.05$). The fraction of apoptotic MPs derived from endothelial cells and platelets were increased in patients with vascular calcification ($p<0.05$).

Furthermore, sub-population of MPs positive for calcification marker was significantly enhanced in patients with CCP in comparison to CFP patients ($p<0.05$) with the main contribution given by MMP ($p<0.01$), EMP and PMP ($p<0.05$) (table 7).

Variable	T1DM (n=40)	Fibrous Plaque CFP (n=20)	Calcified Plaque CCP (n=20)	P-value
EMP (CD62E+)	275,22 ± 184,99	204,17 ± 81,42	346,27 ± 230,35	0,020*
EMP/AnnV+	108,52 ± 73,38	75,07 ± 49,79	141,97 ± 78,93	0,004**
EMP/ALP+	129,56 ± 94,54	94,93 ± 55,46	164,20 ± 112,98	0,024*
PMP (CD62P+)	217,35 ± 112,91	169,50 ± 73,40	265,20 ±126,44	0,008**
PMP/AnnV+	83,32 ± 50,37	58,96 ± 39,77	107,68 ± 48,79	0,002**
PMP/ALP+	146,12 ± 87,08	110,56 ± 54,50	181,68 ± 99,73	0,011*
LMP (CD45+)	242,81 ± 140,12	202,61 ± 68,10	282,99 ±179,61	0,073
LMP/AnnV+	106,69 ± 51,84	89,77 ± 39,55	123,61 ±57,87	0,058
LMP/ALP+	49,19 ± 29,12	36,97 ± 15,08	61,42 ±34,91	0,056
MMP (CD34+)	589,75 ± 479,16	444,34 ± 185,94	735,16 ±625,25	0,059
MMP/AnnV+	134,57 ± 58,33	117,58 ± 54,89	153,45 ±57,62	0,058
MMP/ALP+	53,49 ± 29,97	40,98 ± 21,98	66,01 ±32,13	0,009**
SMP (αSMA+)	589,60 ± 249,12	596,65 ± 307,50	609,55 ±178,87	0,619
SMP/AnnV+	192,93 ± 186,67	179,30 ± 222,20	206,56 ±147,52	0,651
SMP/ALPV+	93,68 ± 70,70	81,09 ± 65,50	106,27 ±75,08	0,266
MP CD34+/αSMA+	63,58 ± 39,63	49,09 ± 21,11	78,05 ±48,32	0,021*
MP_TF+ (CD142+)	390,35 ± 163,91	395,78 ± 122,78	384,92 ±200,03	0,837
MP_Calcein +	4610,88 ± 3970,99	4178,97 ± 4325,94	5042,78 ±3641,56	0,499
MP_AnnV+	3223,82 ± 2321,34	2811,12 ± 2873,16	3636,51 ±1564,35	0,268
MP_ALP+	555,40 ± 209,52	363,96 ± 193,18	488,49 ±126,66	0,013*
MP_ALP+/AnnV+	154,07 ± 96,81	77,80 ± 40,21	218,30 ±82,65	0,0001**

Table 7: Circulating MPs in T1DM significant differential expressed in CCP Vs CFP. *The differential level of characterized MPs between the two groups is expressed as mean ± DS; EMP (Endothelial cell derived MPs); PMP (Platelets derived MPs);LMP (Leucocyte derived MPs);MMP (Mesenchymal/staminal marker+ cell derived MPs); SMP (Smooth Muscle cell derived MPs); AnnV (Annexin V);TF (Tissue Factor); ALP (Alkaline Phosphatase)*

5.1 Endothelial cell derived MPs (EMP)

MPs released from endothelial cells were enhanced in T1DM with vascular calcification (CCP) compare to T1DM with fibrous plaque (CFP) (346,27 ± 230,35 Vs 204,17 ± 81,42; p=0,02). Furthermore, their apoptotic was also increased in patients with vascular calcification (141,97 ± 78,93 Vs 75,07 ± 49,79; p=0.004). EMP response to calcification marker, ALP, was also significant increased (164,20 ± 112,98 Vs 94,93 ± 55,46; p=0.024) as shown in Figure 43

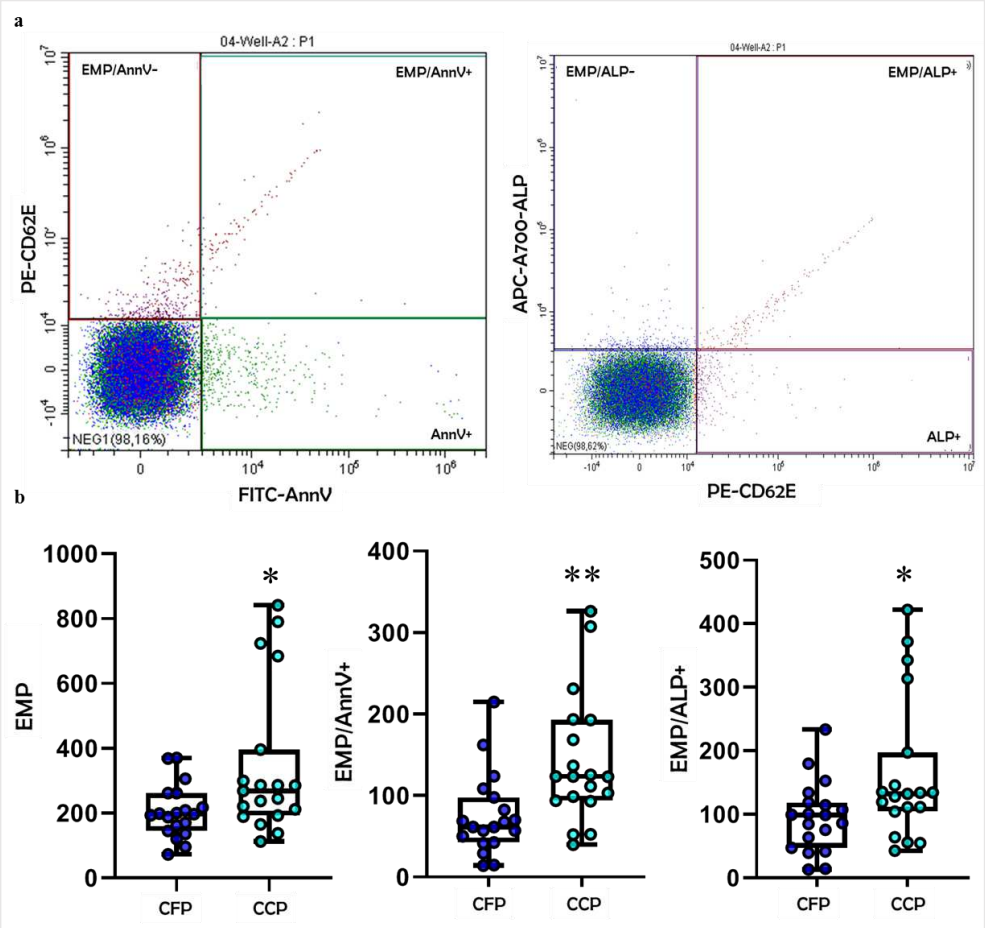

Figure 43: Circulating EMPs derived from T1DM. a) *representative scatter plot of MP labelled with CD62E (EMP), AnnexinV (AnnV) and ALP; double positive MPs are shown (EMP/AnnV+; EMP/ALP+);* ***b)*** *Dot plot of EMP, EMP/AnnV+ and EMP/ALP+ quantification (MPs/µl) in CFP Vs CCP; *p<0.05;**p<0.01*

5.2 Platelets derived MPs (PMP)

MPs released from platelets were increased in T1DM with vascular calcification (CCP) compare to T1DM with fibrous plaque (CFP) (265,20 ±126,44 Vs 169,50 ± 73,40; p=0,008). Furthermore, the release of their apoptotic fraction was also enhanced in patients with vascular calcification (107,68 ± 48,79 Vs 58,96 ± 39,77; p=0.002). PMP response to calcification marker (ALP) was also significant increased (181,68 ± 99,73Vs 110,56 ± 54,50; p=0.011) (fig. 44)

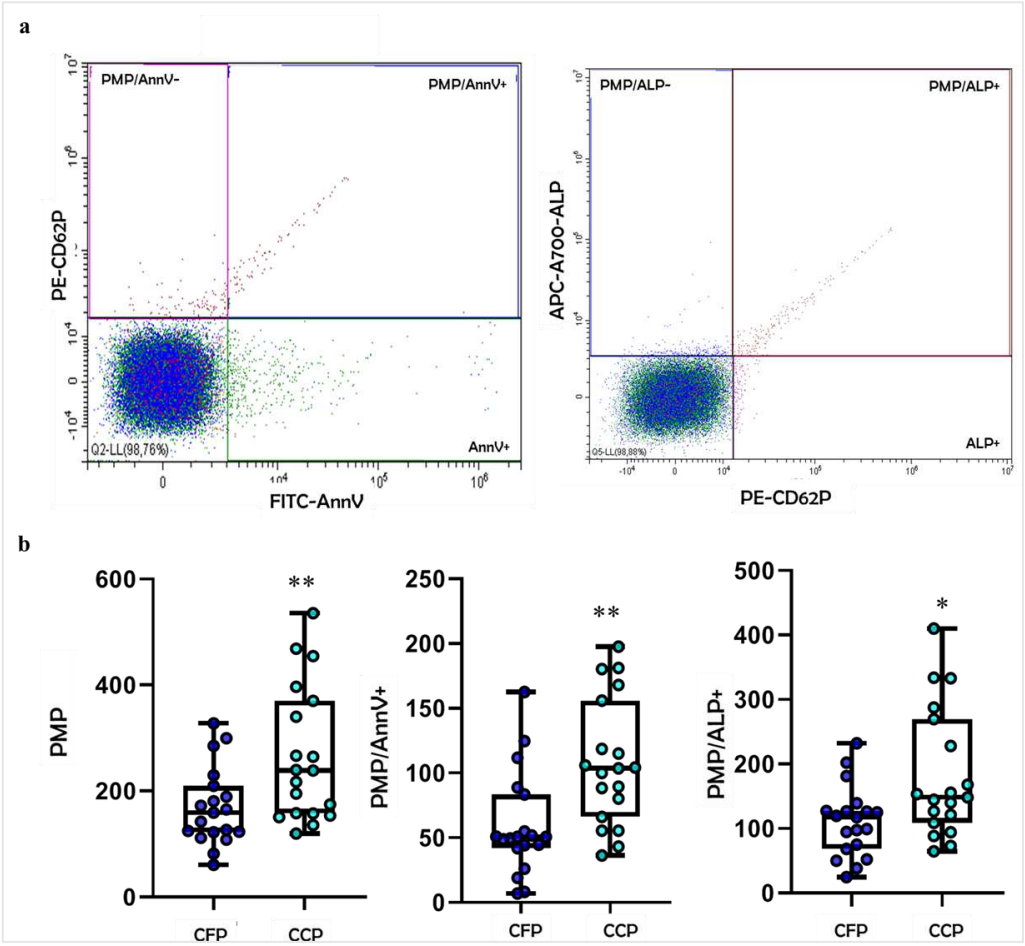

Figure 44: Circulating PMPs derived from T1DM. a) *representative scatter plot of MP labelled with CD62P (PMP), AnnexinV (AnnV) and ALP; double positive MPs are shown (PMP/AnnV+; PMP/ALP+);* ***b)*** *Dot plot of PMP, PMP/AnnV+ and PMP/ALP+ quantification (MPs/µl) in CFP Vs CCP; *p<0.05;**p<0.01*

5.3 MPs derived from staminal compartment (MMPs) and Smooth muscle cells (SMP)

Interestingly, although MPs released from staminal compartment or mesenchymal cells CD34+ were not significant increased per se in T1DM with vascular calcification (CCP) compare to T1DM with fibrous plaque (CFP) the release of their fraction positive for the calcification marker ALP was enhanced in patients with vascular calcification (66,01 ±32,13 Vs 40,98 ± 21,98; p=0.009). Furthermore, a sub-population of MPs double positive for CD34+ and for αSMA (Marker for SMP) was also significantly increased in patients with CCP in comparison to CFP patients (78,05 ±48,32 Vs 49,09 ± 21,11; p=0.021) (fig 45)

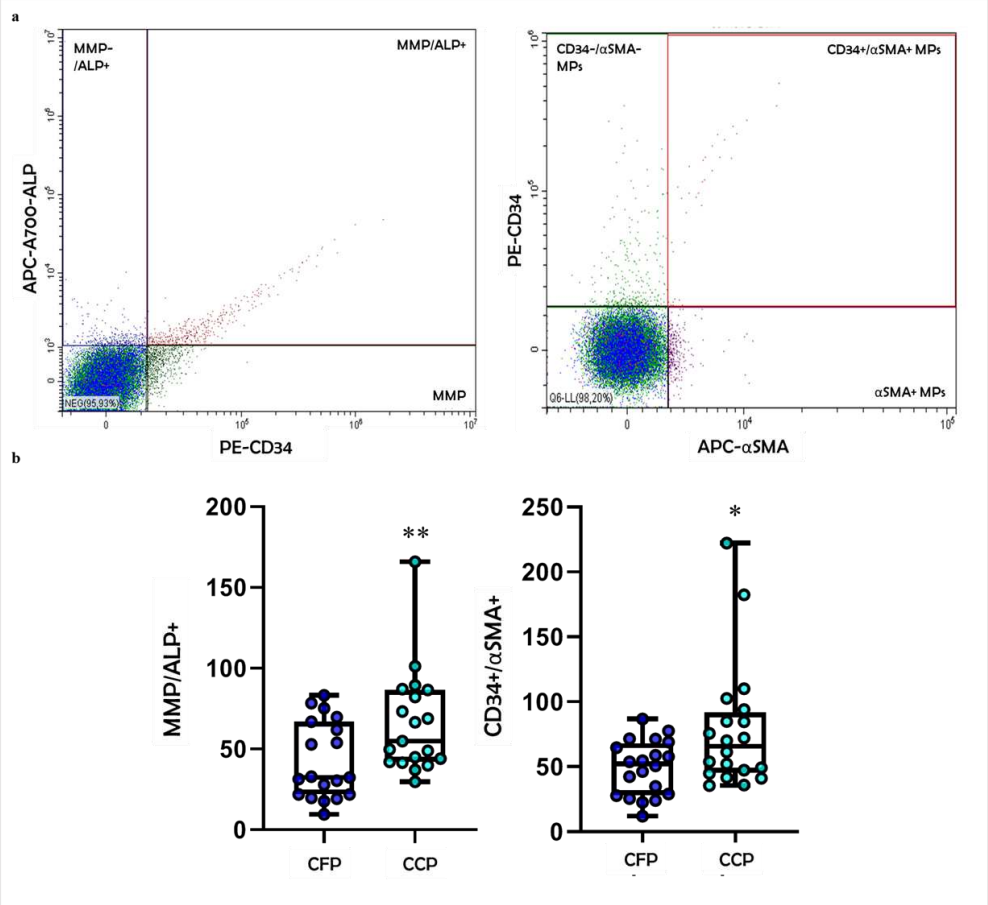

Figure 45: Circulating MPs derived from staminal compartment (MMPs) and Smooth muscle cell derived MPs (SMP) in T1DM. a) *Representative scatter plot of MP labelled with CD34 (MMP), αSMA (SMP), and ALP; double positive MPs are shown (MMP/ALP+; CD34+/αSMA+);* ***b)*** *Dot plot of MMP/ALP+ and CD34+/αSMA+ MP quantification (MPs/µl) in CFP Vs CCP; *p<0.05;**p<0.01*

5.4 Alkaline Phosphatase positive MPs and their apoptotic fraction

Finally, a significant enhanced release of circulating MPs positive for Alkaline Phosphatase (ALP) was found in plasma of T1DM with vascular calcification (CCP) compare to T1DM with fibrous plaque (CFP) (488,49 ±126,66 Vs 363,96 ± 193,18; p=0.013). Furthermore, their apoptotic fraction was also significantly increased in patients with CCP compared to CFP patients (218,30 ±82,65 Vs 77,80 ± 40,21; p=0.0001) (fig. 46)

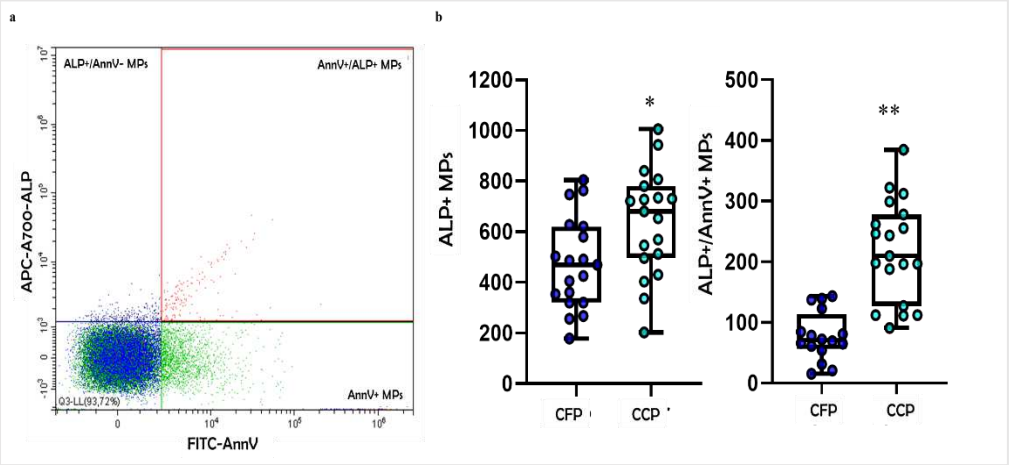

Figure 46: Circulating MPs positive for calcification marker ALP derived from T1DM. a) *representative scatter plot of MP labelled with Alkaline Phosphatase (ALP) and AnnexinV(AnnV); double positive MPs are shown (ALP+/AnnV+);* ***b)*** *Dot plot of ALP+MPs and ALP+/AnnV+MPs quantification (MPs/µl) in CFP Vs CCP; *p<0.05;**p<0.01*

5.5 The size of MPs as indicator of plaque composition

With the constant development of cytofluorimetry, it is possible to further analysed sub- population of MPs according to their size within the main class of MPs: *Big MPs* (900-500 nm); *Small MPs* (500-200 nm) and *Nano MPs* (200-100 nm).

This represents a completely new and unchartered frontier of research in MPs that we are able to explore thank to the high sensitivity of the new generation instrument for cytofluorimetry.

We found out that in T1DM with calcific plaque the sub population of Small MPs was decreased compare with patients with fibrous plaque (p<0.05), On the contrary an increase of the sub-population Nano MPs was

observed in patients with CCP compared to CFP patients ($p<0.005$). No difference were seen for Big MPs in the two groups (table 8 and fig. 47).

Variable	T1DM (n=40)	Fibrous Plaque CFP (n=20)	Calcified Plaque CCP (n=20)	P-value
Big MP (900-500 nm)	454,11 ± 344,15	519,28 ± 440,06	388,93 ± 201,28	0,239
Small MP (500-200 nm)	8580,12 ± 2224,73	9451,81 ± 2331,51	7708,44 ± 1770,24	0,014*
Nano MP (200-100 nm)	30007,85 ± 5897,79	27246,10 ± 5963,64	32769,60 ± 4447,04	0,001**

Table 8: Circulating sub-population of MPs according to their size in T1DM. *The differential level of the three size sub-population of MPs between the two groups is expressed as mean ± DS;*

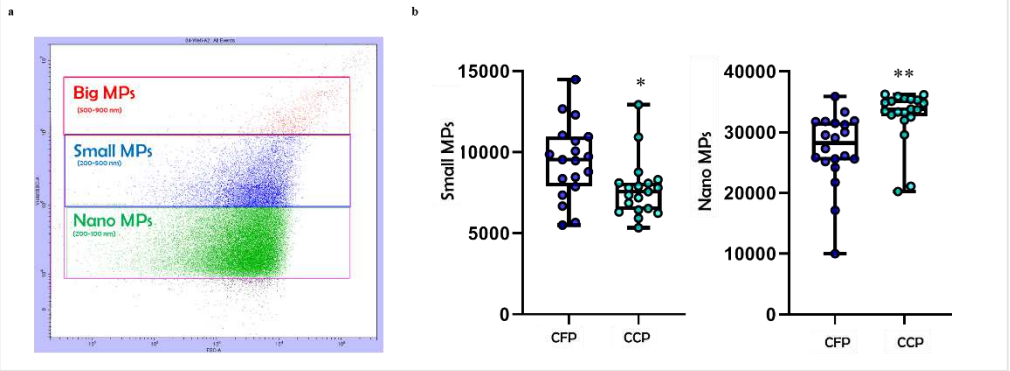

Figure 47: Circulating sub-population of MPs according to their size in T1DM. a) *representative scatter plot of MP gates setting for size in violet-SSC and FSC;* ***b)*** *Dot plot of small and Nano MPs quantification (MPs/µl) in CFP Vs CCP; *p<0.05;**p<0.01*

.

DISCUSSION and CONCLUSIONS

The first aim of this study is to set up a protocol for small RNA-seq data analysis and provide the first comprehensively analysis of all known circulating sncRNAs, as biomolecular markers and potential mediators of the progression of atherosclerotic plaque according to its composition (fibrous or calcified), in type 1 diabetes.

Using high-throughput sequencing technologies, we determined in plasma the presence of three important class of small non coding RNAs, in particular we obtained 2632 miRNAs, 3286 piRNAs and 640 tsRNA and a significant percentage of reads remain unmapped and uncharacterized. Usually, unmapped reads are discarded from the analysis process, but significant biological information and insights can be uncovered from these data that we are going to investigate in future studies.

Study of the association between the circulating sncRNA level and disease represents an active spot in this field. However, the study on sncRNAs as a biomarker for disease diagnosis is still at a preliminary stage, and more clinical and experimental evidence is needed for clinical translation. A possible explanation of this tendency is the difficult to obtain a consistent validation step of the clinical significance of candidate biomarker sncRNAs obtained. In fact, several features of smallRNA-seq data influence the results, from vast discrepancies in the detection methodology, from the biological variability but mainly due to the normalization method used for the analysis. Several study suggest that it is apparent that the differences in the final results depend on the normalization method and not on the model chosen to assess for differential expression.

Normalization is an essential step with considerable impact on high-throughput sncRNAs sequencing data analysis to minimize the technical variation of the samples and sequencing errors and to reduce false-positive

results. Although there are numerous methods for read count normalization, it remains a challenge to choose an optimal method due to multiple factors contributing to read count variability that affects the overall sensitivity and specificity.

To gain insight into this issue we decide to compare the results of differential expression analysis of miRNAs that we obtained from two different bioinformatic tools: CLC Genomics and Partek flow. These platforms provide different method of normalization and differential expression (DE) statistical analysis.

CLC Genomics generate a Ready-to-use pipeline for smallRNA-seq analysis which applies the TMM method of normalization, while the second tool (Partek Flow) allows to customize the normalization method choosing between trimmed mean of M values (TMM) and DeSeq2. Although DeSEq2 is the recommended analysis method for sncRNAs data according to Partek, since it provides an algorithm with internal normalization, both the methods are widely used and give better performance compared to others such as TC (total counts), UQ (Upper Quartile), Median, quantile and RPKM. In fact, in a simulated data study, only DESeq and TMM were successful in achieving a low false positive rate and high power. The authors conclude that DESeq and TMM are the methods of choice based on their ability to perform in the presence of different library sizes and composition.(99,100)

In the first analysis, using TMM normalization and CLC Genomics DE statistical analysis algorithm, nine microRNA were upregulated and seven microRNAs were downregulated in plasma from T1DM with carotid calcified plaque compare with patients with a fibrous type of carotid plaque. In the second analysis, using the same method normalization (TMM) and Partek Flow DE statistical analysis algorithm, five microRNAs were upregulated and two microRNAs were downregulated.

Finally, when we used DeSeq2 in the second bioinformatic tool, 10 microRNAs were upregulated and three microRNAs were downregulated.

These different findings suggest that the statistical model and platform also affect the final results obtained from smallRNA-seq data.

Then, we compared the results of differential expression analysis of miRNAs provided by these three different packages to determine which microRNAs are overlapped and to decide which miRNAs will be consider for further analysis.

Using a filtering method in accordance with preliminary results obtained with qPCR, we retain seven microRNAs significantly differential expressed between the two groups: four miRNAs are upregulated (miR-106b-3p, miR-503-5p, let-7d-5p and miR93-5p), and three were downregulated (miR-10a-5p, miR-29b-3p and miR-451a-5p) in T1DM patients with calcified plaque in comparison to fibrous plaque.

Bioinformatic analysis showed that these seven candidate miRNAs target the expression of many genes that may impact KEGG pathways. In particular, some of these pathways had the highest statistical support for enrichment in vascular remodeling, glucose and lipid metabolism and inflammation. For instance, all of the miRNAs are involved in *Axon guidance signaling pathway*. Furthermore, growing evidence indicates that gene involved in axon guidance signaling pathway have distinct biological activities, which are not only limited to the nervous system but also in other pathophysiological processes, including inflammation, immune response, angiogenesis, and especially atherogenesis. Several evidence reported that genes encoding this pathway were upregulated in endothelial cells under hyperglycemic state suggesting a potential role in the complications of diabetes (107) .

Another pathway in which all of the miRNAs are involved is the *Wnt (Wingless) signaling pathway*. It plays a crucial role in organ formation during embriogenesis, in cell proliferation, polarity migration and differentiation. The WNT family of proteins consists of 19 secreted lipid-modified glicoprotein that bind to the frizzled receptor family. Once Wnt binds to frizzled receptor the signal is transduced into cytoplasm by G-protein dipendent mechanism promoting Ca2+ mobilization. In fact, Wnt signaling plays a key role in atherosclerosis and in particular in vascular calcification. Wnt signaling activation is mediated by several pathogenic stimuli such as tumor necrosis factor, oxidized lipids, and hyperglycemia. Recent evidences demonstrated that Wnt signaling play a role in calcification predisposing vessels to pathological calcification by monocyte adhesion and by the release of proinflammatory factors (108).

Another important example of enriched KEGG pathway we obtained is *mTOR signaling pathway*. It regulates many cellular processes and it is implicated in an increasing number of pathological conditions, including obesity, diabetes and atherosclerosis. For instance, pharmacological interventions with class of macrolide immunosuppressive drugs effect this pathway. The inhibition of mTOR pathway prevent the development of atherosclerotic plaque by decreasing monocyte migration and the release of chemokines. Furthermore, mTOR inhibition blunts the expression of hypoxia-inducible factor 1-alpha (HIF-1alpha) which is a protein associated with rupture-prone atherosclerotic plaque and its downstream target vascular endothelial growth factor (VEGF). Recently, mTOR inhibition was found to prevent the osteoblastic differentiation of isolated human VSMC(109).

The molecular mechanisms of increasing or decreasing circulating miRNA levels during the progression of atherosclerosis in type 1 diabetes are still largely unknown.. The main features of atherosclerosis are endothelial

dysfunction, inflammation and vascular calcification. The development and the progression of atherosclerosis results in tissue and vessel damage or in change of cellular phenotype involvement different type of cells: endothelial cell, macrophages and VSMC. This damage or cellular remodelling of vasculature may result in secretion or leakage of the miRNA or other small non coding RNAs into circulation that then communicate with distant cell target and targeted genes or proteins pathways. Although we could not determine whether the putative microRNAs identified in our study were secreted from certain cells or if they are derived from damaged cells, circulating microRNAs profiles can be useful to better understand the progression of atherosclerosis in type 1 diabetes from fibrous plaque to calcified plaque. Furthermore, these results can be useful to identify novel therapeutics targets to prevent or treat diabetes complications such as atherosclerosis.

In this study, other two classes of small non coding RNA were investigated.

piRNAs are a type of non-coding RNA that interact with PIWI proteins which are members of the Argonaute family. Originally described in the germline, piRNAs are also expressed in human somatic cells in a tissue-specific manner. piRNAs are involved in spermatogenesis, germ stem-cell maintainance, silencing of trasposon, epigenetic and genomic regulation and rearrangement. Furthermore, piRNAs have been reported to be present in human body fluids, including the serum and plasma in a marked stable form. In this study, we found that piRNAs family is the second most abundant sncRNAs class present in human plasma and that the expression of two piRNAs are markedly elevated in T1DM patients with calcified plaque in comparison to T1DM patients with fibrous plaque. Although their pathophysiological role in the progression of atherosclerosis and in the

differentiation of the type of plaque is unknown, the detection of piRNAs circulating in blood plasma is particularly interesting and could have an impact on liquid biopsy-based diagnosis. (54)

Abnormal levels of tsRNAs have been observed in a variety of human diseases, including cancer, neurodegenerative diseases, acquired metabolic diseases, and infectious diseases. There are some evidences that support the exploration of tsRNAs, as new biomarkers and for novel therapeutic strategies, for the detection, monitoring, and treatment of human diseases.(62)

However, the molecular mechanisms and by which these tsRNAs may contribute to disease pathogenesis is still largely unknown. Our results shown that 10 tsRNAs are upregulated in plasma from T1DM patients with calcified plaque in comparison to patients with fibrous plaque. The underlying mechanisms by which tsRNA affect specific cellular processes should be evaluated.

The second aim of this study is characterized circulating microparticles derived from T1DM patients with calcified or fibrous plaques. Our results show that MPs released from endothelial cells and platelets are significantly higher in T1DM patients with calcified plaque in comparison to patients with fibrous plaque.

It is well known that the release of circulating MPs from tissue injury contribute to cardiovascular disorders, promoting inflammation, thrombosis and vascular dysfunction. (89)

Our findings show a different profiling of circulating MPs in relation to the progression of atherosclerosis from fibrous to calcified plaque. Several factors, such as vascular remodeling or the mineralization process into the arterial wall can contribute to an increase of the MPs release. Pathological

conditions that alter mineral metabolism, modify calcification regulators or modulate cell phenotype can have important consequences in vascular structures and release several factors such as cytokines, chemokines and MPs to propagate these signals. Taken together, these studies support the link between release of MPS and the progression and the severity of vascular calcification.

Accordingly, in our study we found that circulating MPs are enriched of a well know calcified marker alkaline phosphatase. This founding suggests that MPs strongly contributed in these processes amplifying signals and participating to cell-to-cell communication.

Furthermore, we found an increase of MPS positive for CD34 and alfa-SMA in T1DM patients with calcified plaque. We speculate that the release of these MPs is due to a niche of staminal mesenchymal cell, resident into the wall, called pericytes, recently discovered to be involved in vascular remodeling and osteogenic transdifferentiation of vascular smooth muscle cells.

Our funding suggest for the first time a potential contribution of these cells in the development of atherosclerotic plaque and its composition towards a calcified type

Finally, we investigated the size of MPS as indicator of vascular calcification. We found that the Small MPs are reduced in calcified plaque while the fraction of Nano MPs are increased in fibrous plaque from T1DM patients, suggesting a different cargo in association to different composition of atherosclerotic plaque.

In the future study, we are planning to measure the content of sncRNAs into MPs and verify the hypothesis that MPs give the main contribution to the expression of circulating sncRNAs involved in the process of atherosclerosis in T1DM. In vitro, the manipulation of the content in

sncRNAs of MPs, as specific carrier of these molecules, may represent a potential tool for a translational approach in therapy.

In conclusion, our results demonstrate the power of NGS technology to identify a huge amount of circulating sncRNAs and to discover different RNA molecules present in human plasma. Furthermore, we demonstrate that microvesicles exhibit differential markers in the presence of vascular calcification suggesting a potential role as carrier of small molecules to amplify their signal.

The identification of new molecular biomarkers with this ultra-high throughput and sensitive technique (NGS) together to identification of MPS , as carriers, will help to go further insight specific pathophysiological processes, such as atherosclerotic plaque composition in diabetes, allowing a potentially more targeted therapeutic approach.

REFERENCES

1. Todd JA. Etiology of Type 1 Diabetes. Immunity. 2010;32:457–67.
2. Leslie RD. Predicting adult-onset autoimmune diabetes clarity from complexity. Diabetes. 2010;59:330–1.
3. Tuomi T. Type 1 and type 2 diabetes: What do they have in common? Diabetes. 2005;54(40–45).
4. 2. Classification and diagnosis of diabetes. Diabetes Care. 2015;38:s8–16.
5. Lind M, Svensson AM, Kosiborod M, Gudbjörnsdottir S, Pivodic A, Wedel H, et al. Glycemic control and excess mortality in type 1 diabetes. N Engl J Med. 2014;371:1972–82.
6. Lachin JM, Genuth S, Nathan DM, Zinman B, Rutledge BN. Effect of glycemic exposure on the risk of microvascular complications in the diabetes control and complications trial-revisited. Diabetes. 2008;57:995–1001.
7. Nathan DM. The diabetes control and complications trial/epidemiology of diabetes interventions and complications study at 30 years: overview. Diabetes Care. 2014;37(1):9–16.
8. Gerstein HC. Diabetes: Dysglycaemia as a cause of cardiovascular outcomes. Nat Rev Endocrinol. 2015 Sep;11(9):508–10.
9. Katsarou A, Gudbjornsdottir S, Rawshani A, Dabelea D, Bonifacio E, Anderson BJ, et al. Type 1 diabetes mellitus. Nat Rev Dis Prim. 2017 Mar;3:17016.
10. Anderzen J, Samuelsson U, Gudbjornsdottir S, Hanberger L, Akesson K. Teenagers with poor metabolic control already have a higher risk of

microvascular complications as young adults. J Diabetes Complications. 2016 Apr;30(3):533–6.

11. Frank RN. Diabetic retinopathy. N Engl J Med. 2004 Jan;350(1):48–58.
12. Tuttle KR, Bakris GL, Bilous RW, Chiang JL, de Boer IH, Goldstein-Fuchs J, et al. Diabetic kidney disease: a report from an ADA Consensus Conference. Diabetes Care. 2014 Oct;37(10):2864–83.
13. Perkins BA, Ficociello LH, Silva KH, Finkelstein DM, Warram JH, Krolewski AS. Regression of microalbuminuria in type 1 diabetes. N Engl J Med. 2003 Jun;348(23):2285–93.
14. Pop-Busui R, Boulton AJM, Feldman EL, Bril V, Freeman R, Malik RA, et al. Diabetic Neuropathy: A Position Statement by the American Diabetes Association. Diabetes Care. 2017 Jan;40(1):136–54.
15. Stephenson JM, Kempler P, Perin PC, Fuller JH. Is autonomic neuropathy a risk factor for severe hypoglycaemia? The EURODIAB IDDM Complications Study. Diabetologia. 1996 Nov;39(11):1372–6.
16. Moreno PR, Murcia AM, Palacios IF, Leon MN, Bernardi VH, Fuster V, et al. Coronary composition and macrophage infiltration in atherectomy specimens from patients with diabetes mellitus. Circulation. 2000 Oct;102(18):2180–4.
17. de Ferranti S, Mozaffarian D. The perfect storm: obesity, adipocyte dysfunction, and metabolic consequences. Clin Chem. 2008 Jun;54(6):945–55.
18. Tabas I. Macrophage death and defective inflammation resolution in atherosclerosis. Nat Rev Immunol. 2010 Jan;10(1):36–46.
19. Geng Y-J, Libby P. Progression of atheroma: a struggle between death and procreation. Arterioscler Thromb Vasc Biol. 2002 Sep;22(9):1370–80.

20. Yahagi K, Kolodgie FD, Lutter C, Mori H, Romero ME, Finn A V, et al. Pathology of Human Coronary and Carotid Artery Atherosclerosis and Vascular Calcification in Diabetes Mellitus. Arterioscler Thromb Vasc Biol. 2017 Feb;37(2):191–204.

21. Wright RJ, Newby DE, Stirling D, Ludlam CA, Macdonald IA, Frier BM. Effects of acute insulin-induced hypoglycemia on indices of inflammation: putative mechanism for aggravating vascular disease in diabetes. Diabetes Care. 2010 Jul;33(7):1591–7.

22. 10. Cardiovascular Disease and Risk Management: Standards of Medical Care in Diabetes-2019. Diabetes Care. 2019 Jan;42(Suppl 1):S103–23.

23. Orchard TJ, Secrest AM, Miller RG, Costacou T. In the absence of renal disease, 20 year mortality risk in type 1 diabetes is comparable to that of the general population: a report from the Pittsburgh Epidemiology of Diabetes Complications Study. Diabetologia. 2010 Nov;53(11):2312–9.

24. Maahs DM, Kinney GL, Wadwa P, Snell-Bergeon JK, Dabelea D, Hokanson J, et al. Hypertension prevalence, awareness, treatment, and control in an adult type 1 diabetes population and a comparable general population. Diabetes Care. 2005 Feb;28(2):301–6.

25. Evrard S, Delanaye P, Kamel S, Cristol J-P, Cavalier E. Vascular calcification: from pathophysiology to biomarkers. Clin Chim Acta. 2015 Jan;438:401–14.

26. Jean G, Terrat J-C, Vanel T, Hurot J-M, Lorriaux C, Mayor B, et al. High levels of serum fibroblast growth factor (FGF)-23 are associated with increased mortality in long haemodialysis patients. Nephrol Dial Transplant. 2009 Sep;24(9):2792–6.

27. Bacchetta J, Cochat P, Salusky IB. [FGF23 and Klotho: the new

cornerstones of phosphate/calcium metabolism]. Arch Pediatr. 2011 Jun;18(6):686–95.

28. Schurgers LJ, Uitto J, Reutelingsperger CP. Vitamin K-dependent carboxylation of matrix Gla-protein: a crucial switch to control ectopic mineralization. Trends Mol Med. 2013 Apr;19(4):217–26.

29. Collin-Osdoby P, Rothe L, Bekker S, Anderson F, Huang Y, Osdoby P. Basic fibroblast growth factor stimulates osteoclast recruitment, development, and bone pit resorption in association with angiogenesis in vivo on the chick chorioallantoic membrane and activates isolated avian osteoclast resorption in vitro. J Bone Miner Res. 2002 Oct;17(10):1859–71.

30. Scatena M, Liaw L, Giachelli CM. Osteopontin: a multifunctional molecule regulating chronic inflammation and vascular disease. Arterioscler Thromb Vasc Biol. 2007 Nov;27(11):2302–9.

31. Towler DA. Inorganic pyrophosphate: a paracrine regulator of vascular calcification and smooth muscle phenotype. Vol. 25, Arteriosclerosis, thrombosis, and vascular biology. United States; 2005. p. 651–4.

32. Matera AG, Terns RM, Terns MP. Non-coding RNAs: lessons from the small nuclear and small nucleolar RNAs. Vol. 8, Nature reviews. Molecular cell biology. England; 2007. p. 209–20.

33. Rinn JL, Chang HY. Genome regulation by long noncoding RNAs. Annu Rev Biochem. 2012;81:145–66.

34. Cai X, Hagedorn CH, Cullen BR. Human microRNAs are processed from capped, polyadenylated transcripts that can also function as mRNAs. RNA. 2004 Dec;10(12):1957–66.

35. Lee Y, Ahn C, Han J, Choi H, Kim J, Yim J, et al. The nuclear RNase III Drosha initiates microRNA processing. Nature. 2003 Sep;425(6956):415–9.

36. Ha M, Kim VN. Regulation of microRNA biogenesis. Nat Rev Mol Cell Biol [Internet]. 2014 Jul 16;15:509. Available from: https://doi.org/10.1038/nrm3838

37. Tian Y, Simanshu DK, Ma J-B, Park J-E, Heo I, Kim VN, et al. A phosphate-binding pocket within the platform-PAZ-connector helix cassette of human Dicer. Mol Cell. 2014 Feb;53(4):606–16.

38. Lee Y, Hur I, Park S-Y, Kim Y-K, Suh MR, Kim VN. The role of PACT in the RNA silencing pathway. EMBO J. 2006 Feb;25(3):522–32.

39. Elkayam E, Kuhn C-D, Tocilj A, Haase AD, Greene EM, Hannon GJ, et al. The structure of human argonaute-2 in complex with miR-20a. Cell. 2012 Jul;150(1):100–10.

40. Bartel DP. MicroRNAs: genomics, biogenesis, mechanism, and function. Cell. 2004 Jan;116(2):281–97.

41. Gebert LFR, MacRae IJ. Regulation of microRNA function in animals. Nat Rev Mol Cell Biol. 2019 Jan;20(1):21–37.

42. Jonas S, Izaurralde E. Towards a molecular understanding of microRNA-mediated gene silencing. Nat Rev Genet. 2015 Jul;16(7):421–33.

43. Braun JE, Truffault V, Boland A, Huntzinger E, Chang C-T, Haas G, et al. A direct interaction between DCP1 and XRN1 couples mRNA decapping to 5’ exonucleolytic degradation. Nat Struct Mol Biol. 2012 Dec;19(12):1324–31.

44. Meijer HA, Kong YW, Lu WT, Wilczynska A, Spriggs R V, Robinson SW, et al. Translational repression and eIF4A2 activity are critical for microRNA-mediated gene regulation. Science. 2013 Apr;340(6128):82–5.

45. Eichhorn SW, Guo H, McGeary SE, Rodriguez-Mias RA, Shin C,

Baek D, et al. mRNA destabilization is the dominant effect of mammalian microRNAs by the time substantial repression ensues. Mol Cell. 2014 Oct;56(1):104–15.

46. Guo H, Ingolia NT, Weissman JS, Bartel DP. Mammalian microRNAs predominantly act to decrease target mRNA levels. Nature. 2010 Aug;466(7308):835–40.

47. Broderick JA, Salomon WE, Ryder SP, Aronin N, Zamore PD. Argonaute protein identity and pairing geometry determine cooperativity in mammalian RNA silencing. RNA. 2011 Oct;17(10):1858–69.

48. Desvignes T, Batzel P, Berezikov E, Eilbeck K, Eppig JT, McAndrews MS, et al. miRNA Nomenclature: A View Incorporating Genetic Origins, Biosynthetic Pathways, and Sequence Variants. Trends Genet. 2015 Nov;31(11):613–26.

49. Lam JKW, Chow MYT, Zhang Y, Leung SWS. siRNA Versus miRNA as Therapeutics for Gene Silencing. Mol Ther Nucleic Acids. 2015 Sep;4(9):e252.

50. Agrawal N, Dasaradhi PVN, Mohmmed A, Malhotra P, Bhatnagar RK, Mukherjee SK. RNA interference: biology, mechanism, and applications. Microbiol Mol Biol Rev. 2003 Dec;67(4):657–85.

51. Ross RJ, Weiner MM, Lin H. PIWI proteins and PIWI-interacting RNAs in the soma. Nature. 2014 Jan;505(7483):353–9.

52. Boeke JD, Garfinkel DJ, Styles CA, Fink GR. Ty elements transpose through an RNA intermediate. Cell. 1985 Mar;40(3):491–500.

53. Cosby RL, Chang N-C, Feschotte C. Host-transposon interactions: conflict, cooperation, and cooption. Genes Dev. 2019 Sep;33(17–18):1098–116.

54. Ozata DM, Gainetdinov I, Zoch A, O'Carroll D, Zamore PD. PIWI-

interacting RNAs: small RNAs with big functions. Nat Rev Genet [Internet]. 2019 Feb 16;20(2):89–108. Available from: http://www.nature.com/articles/s41576-018-0073-3

55. Saxe JP, Chen M, Zhao H, Lin H. Tdrkh is essential for spermatogenesis and participates in primary piRNA biogenesis in the germline. EMBO J. 2013 Jul;32(13):1869–85.

56. Yamanaka S, Siomi MC, Siomi H. piRNA clusters and open chromatin structure. Mob DNA. 2014;5:22.

57. Gunawardane LS, Saito K, Nishida KM, Miyoshi K, Kawamura Y, Nagami T, et al. A slicer-mediated mechanism for repeat-associated siRNA 5' end formation in Drosophila. Science. 2007 Mar;315(5818):1587–90.

58. Ernst C, Odom DT, Kutter C. The emergence of piRNAs against transposon invasion to preserve mammalian genome integrity. Nat Commun. 2017 Nov;8(1):1411.

59. Esteller M. Non-coding RNAs in human disease. Nat Rev Genet. 2011 Nov;12(12):861–74.

60. Girard A, Sachidanandam R, Hannon GJ, Carmell MA. A germline-specific class of small RNAs binds mammalian Piwi proteins. Nature. 2006 Jul;442(7099):199–202.

61. Wang J, Zhang P, Lu Y, Li Y, Zheng Y, Kan Y, et al. piRBase: a comprehensive database of piRNA sequences. Nucleic Acids Res. 2019 Jan;47(D1):D175–80.

62. Li S, Xu Z, Sheng J. tRNA-Derived Small RNA: A Novel Regulatory Small Non-Coding RNA. Genes (Basel). 2018 May;9(5).

63. Oberbauer V, Schaefer M. tRNA-Derived Small RNAs: Biogenesis, Modification, Function and Potential Impact on Human Disease Development. Genes (Basel) [Internet]. 2018 Dec 5;9(12):607.

Available from: http://www.mdpi.com/2073-4425/9/12/607

64. Watson CN, Belli A, Di Pietro V. Small Non-coding RNAs: New Class of Biomarkers and Potential Therapeutic Targets in Neurodegenerative Disease. Front Genet. 2019;10:364.

65. Yamasaki S, Ivanov P, Hu G-F, Anderson P. Angiogenin cleaves tRNA and promotes stress-induced translational repression. J Cell Biol. 2009 Apr;185(1):35–42.

66. Semenov D V, Kuligina E V, Shevyrina ON, Richter VA, Vlassov V V. Extracellular ribonucleic acids of human milk. Ann N Y Acad Sci. 2004 Jun;1022:190–4.

67. Dhahbi JM, Spindler SR, Atamna H, Yamakawa A, Boffelli D, Mote P, et al. 5' tRNA halves are present as abundant complexes in serum, concentrated in blood cells, and modulated by aging and calorie restriction. BMC Genomics. 2013 May;14:298.

68. Sharma U, Conine CC, Shea JM, Boskovic A, Derr AG, Bing XY, et al. Biogenesis and function of tRNA fragments during sperm maturation and fertilization in mammals. Science. 2016 Jan;351(6271):391–6.

69. Saikia M, Jobava R, Parisien M, Putnam A, Krokowski D, Gao X-H, et al. Angiogenin-cleaved tRNA halves interact with cytochrome c, protecting cells from apoptosis during osmotic stress. Mol Cell Biol. 2014 Jul;34(13):2450–63.

70. Zhang Y, Zhang X, Shi J, Tuorto F, Li X, Liu Y, et al. Dnmt2 mediates intergenerational transmission of paternally acquired metabolic disorders through sperm small non-coding RNAs. Nat Cell Biol. 2018 May;20(5):535–40.

71. Chen Q, Yan W, Duan E. Epigenetic inheritance of acquired traits through sperm RNAs and sperm RNA modifications. Nat Rev Genet.

2016 Dec;17(12):733–43.

72. Lyons SM, Fay MM, Ivanov P. The role of RNA modifications in the regulation of tRNA cleavage. FEBS Lett. 2018 Sep;592(17):2828–44.

73. Buratti E, Baralle D. Novel roles of U1 snRNP in alternative splicing regulation. RNA Biol. 2010;7(4):412–9.

74. Yanaizu M, Sakai K, Tosaki Y, Kino Y, Satoh J-I. Small nuclear RNA-mediated modulation of splicing reveals a therapeutic strategy for a TREM2 mutation and its post-transcriptional regulation. Sci Rep. 2018 May;8(1):6937.

75. Viereck J, Thum T. Circulating Noncoding RNAs as Biomarkers of Cardiovascular Disease and Injury. Circ Res. 2017 Jan;120(2):381–99.

76. Garcia-Contreras M, Shah SH, Tamayo A, Robbins PD, Golberg RB, Mendez AJ, et al. Plasma-derived exosome characterization reveals a distinct microRNA signature in long duration Type 1 diabetes. Sci Rep. 2017 Jul;7(1):5998.

77. Giannella A, Radu CM, Franco L, Campello E, Simioni P, Avogaro A, et al. Circulating levels and characterization of microparticles in patients with different degrees of glucose tolerance. Cardiovasc Diabetol. 2017;33:121.

78. Jansen F, Yang X, Hoelscher M, Cattelan A, Schmitz T, Proebsting S, et al. Endothelial microparticle-mediated transfer of microRNA-126 promotes vascular endothelial cell repair via spred1 and is abrogated in glucose-damaged endothelial microparticles. Circulation. 2013;

79. Olivieri F, Spazzafumo L, Bonafe M, Recchioni R, Prattichizzo F, Marcheselli F, et al. MiR-21-5p and miR-126a-3p levels in plasma and circulating angiogenic cells: relationship with type 2 diabetes complications. Oncotarget. 2015 Nov;6(34):35372–82.

80. Peng H, Zhong M, Zhao W, Wang C, Zhang J, Liu X, et al. Urinary

miR-29 correlates with albuminuria and carotid intima-media thickness in type 2 diabetes patients. PLoS One. 2013;8(12):e82607.

81. Alkagiet S, Tziomalos K. Vascular calcification: the role of microRNAs. Biomol Concepts. 2017 May;8(2):119–23.

82. Sudo R, Sato F, Azechi T, Wachi H. MiR-29-mediated elastin down-regulation contributes to inorganic phosphorus-induced osteoblastic differentiation in vascular smooth muscle cells. Genes Cells. 2015 Dec;20(12):1077–87.

83. Rangrez AY, M'Baya-Moutoula E, Metzinger-Le Meuth V, Henaut L, Djelouat MS el I, Benchitrit J, et al. Inorganic phosphate accelerates the migration of vascular smooth muscle cells: evidence for the involvement of miR-223. PLoS One. 2012;7(10):e47807.

84. Ceolotto G, Giannella A, Albiero M, Kuppusamy M, Radu C, Simioni P, et al. MiR-30c-5p regulates macrophage-mediated inflammation and pro-atherosclerosis pathways. Cardiovasc Res. 2017;

85. Kim Y-K, Kook H. Diverse roles of noncoding RNAs in vascular calcification. Arch Pharm Res. 2019 Mar;42(3):244–51.

86. Henaoui IS, Jacovetti C, Guerra Mollet I, Guay C, Sobel J, Eliasson L, et al. PIWI-interacting RNAs as novel regulators of pancreatic beta cell function. Diabetologia. 2017 Oct;60(10):1977–86.

87. Zhou Z, Sun B, Huang S, Jia W, Yu D. The tRNA-associated dysregulation in diabetes mellitus. Metabolism. 2019 May;94:9–17.

88. La Marca V, Fierabracci A. Insights into the Diagnostic Potential of Extracellular Vesicles and Their miRNA Signature from Liquid Biopsy as Early Biomarkers of Diabetic Micro/Macrovascular Complications. Int J Mol Sci. 2017 Sep;18(9).

89. Krohn JB, Hutcheson JD, Martínez-Martínez E, Aikawa E. Extracellular vesicles in cardiovascular calcification: expanding

current paradigms. J Physiol. 2016 Jun;594(11):2895–903.

90. Schurgers LJ, Akbulut AC, Kaczor DM, Halder M, Koenen RR, Kramann R. Initiation and Propagation of Vascular Calcification Is Regulated by a Concert of Platelet- and Smooth Muscle Cell-Derived Extracellular Vesicles. Front Cardiovasc Med [Internet]. 2018 Apr 6;5:36. Available from: http://journal.frontiersin.org/article/10.3389/fcvm.2018.00036/full

91. Randriamboavonjy V, Fleming I. Platelet communication with the vascular wall: role of platelet-derived microparticles and non-coding RNAs. Clin Sci (Lond). 2018 Sep;132(17):1875–88.

92. Bakhshian Nik A, Hutcheson JD, Aikawa E. Extracellular Vesicles As Mediators of Cardiovascular Calcification. Front Cardiovasc Med. 2017;4:78.

93. Yang W, Zou B, Hou Y, Yan W, Chen T, Qu S. Extracellular vesicles in vascular calcification. Clin Chim Acta. 2019 Sep;499:118–22.

94. Passman JN, Dong XR, Wu S-P, Maguire CT, Hogan KA, Bautch VL, et al. A sonic hedgehog signaling domain in the arterial adventitia supports resident Sca1+ smooth muscle progenitor cells. Proc Natl Acad Sci U S A. 2008 Jul;105(27):9349–54.

95. Castelblanco E, Betriu À, Hernández M, Granado-Casas M, Ortega E, Soldevila B, et al. Ultrasound Tissue Characterization of Carotid Plaques Differs Between Patients with Type 1 Diabetes and Subjects without Diabetes. J Clin Med. 2019 Mar;8(4).

96. Touboul P-J, Hennerici MG, Meairs S, Adams H, Amarenco P, Bornstein N, et al. Mannheim carotid intima-media thickness and plaque consensus (2004-2006-2011). An update on behalf of the advisory board of the 3rd, 4th and 5th watching the risk symposia, at the 13th, 15th and 20th European Stroke Conferences, Mannheim,

Germany, 2004, B. Cerebrovasc Dis. 2012;34(4):290–6.

97. Ludwig M, Zielinski T, Schremmer D, Stumpe KO. Reproducibility of 3-dimensional ultrasound readings of volume of carotid atherosclerotic plaque. Cardiovasc Ultrasound. 2008 Aug;6:42.

98. Ewing B, Green P. Base-calling of automated sequencer traces using phred. II. Error probabilities. Genome Res. 1998 Mar;8(3):186–94.

99. Robinson MD, Oshlack A. A scaling normalization method for differential expression analysis of RNA-seq data. Genome Biol. 2010;11(3):R25.

100. Love MI, Huber W, Anders S. Moderated estimation of fold change and dispersion for RNA-seq data with DESeq2. Genome Biol. 2014;15(12):550.

101. Langmead B, Trapnell C, Pop M, Salzberg SL. Ultrafast and memory-efficient alignment of short DNA sequences to the human genome. Genome Biol. 2009;10(3):R25.

102. Kozomara A, Birgaoanu M, Griffiths-Jones S. miRBase: from microRNA sequences to function. Nucleic Acids Res. 2019 Jan;47(D1):D155–62.

103. Pliatsika V, Loher P, Telonis AG, Rigoutsos I. MINTbase: a framework for the interactive exploration of mitochondrial and nuclear tRNA fragments. Bioinformatics. 2016 Aug;32(16):2481–9.

104. Dillies M-A, Rau A, Aubert J, Hennequet-Antier C, Jeanmougin M, Servant N, et al. A comprehensive evaluation of normalization methods for Illumina high-throughput RNA sequencing data analysis. Brief Bioinform. 2013 Nov;14(6):671–83.

105. Teng M, Love MI, Davis CA, Djebali S, Dobin A, Graveley BR, et al. A benchmark for RNA-seq quantification pipelines. Genome Biol. 2016 Apr;17:74.

106. Kok MGM, de Ronde MWJ, Moerland PD, Ruijter JM, Creemers EE, Pinto-Sietsma SJ. Small sample sizes in high-throughput miRNA screens: A common pitfall for the identification of miRNA biomarkers. Biomol Detect Quantif. 2018 May;15:1–5.

107. Aggarwal PK, Veron D, Thomas DB, Siegel D, Moeckel G, Kashgarian M, et al. Semaphorin3a promotes advanced diabetic nephropathy. Diabetes. 2015 May;64(5):1743–59.

108. Albanese I, Khan K, Barratt B, Al-Kindi H, Schwertani A. Atherosclerotic Calcification: Wnt Is the Hint. J Am Heart Assoc. 2018 Feb;7(4).

109. Cai Z, He Y, Chen Y. Role of Mammalian Target of Rapamycin in Atherosclerosis. Curr Mol Med. 2018;18(4):216–32.